Angefertigt am
Fachbereich 08-Biologie und Chemie
in Zusammenarbeit mit dem
Institut für Medizinische Virologie
der Justus-Liebig-Universität Gießen

Uptake mechanism of Hepatitis B Virus into susceptible primary hepatocyte cultures

---

Aufnahmemechanismus des Hepatitis B Virus in suszeptible primäre Hepatozyten Kulturen

Inauguraldissertation
zur Erlangung des akademischen Grades
d o c t o r r e r u m n a t u r a l i u m
(Dr. rer. nat.)
des Fachbereichs 08-Biologie und Chemie
der Justus-Liebig-Universität Gießen

vorgelegt von
Dipl.-Biol. Nicole Kott

Gießen 2010

Dekan: **Prof. Dr. Volkmar Wolters**

Gutachter: **Prof. Dr. Michael Martin**
Prof. Dr. Dr. h. c. Wolfram Gerlich

Tag der Disputation: 14.01.2011

Index

Abbreviations

A

ad	fill up to
Ad2/3/5	Adenovirus type 2/3/5
AP	adaptor protein
Arf1/6	ADP-ribosylation factor 1/6
ASHV	Arctic Squirrel Hepatitis Virus

B

BafA1	Bafilomycin A1
bp	basepair
BFA	Brefeldin A
BSA	bovine serum albumin

C

cav-1/2/3	caveolin-1/2/3
cccDNA	covalently closed circular DNA
CCP	clathrin-coated pit
CCV	clathrin-coated vesicle
Cdc42	cell division control protein 42 homolog
CD59	complement regulatory protein
CHBV	Crane Hepatitis B Virus
ChHBV	Chimpanzee Hepatitis B Virus
CI	clathrin-independent
CLIC	clathrin-independent carriers
CME	clathrin-mediated endocytosis
C-terminus	carboxy terminus
CtxB	Cholera Toxin B
CytoD	Cytochalasin D

D

d	distilled
Da	Dalton
DHBV	Duck Hepatitis B Virus
DMEM	Dulbecco´s Modified Eagle Medium
DMSO	Dimethyl sulfoxide
dn	dominant negative
DNA	Desoxyribonucleotide acid
DR1/2	direct repeat 1/2

E

ε	encapsidation signal
E. coli	Escherichia coli
EE	early endosome
EIPA	(5-[N-ethyl-N-isopropyl] amiloride)
EM	electron microscopy
Enh	enhancer
Eps15	epidermal growth factor receptor substrate 15
ER	endoplasmic reticulum
ERAD	ER-associated protein degradation-machinery

F

FCS	fetal calf serum
Fig	figure

G

g	multiples of gravitational acceleration on earth
GE	genome equivalents
GEEC	GPI-AP enriched endosomal compartment
GiHBV	Gibbon Hepatitis B Virus
GoHBV	Gorilla Hepatitis B Virus
GPI-AP	glycosyl phosphatidyl--inositol-anchored protein

GRAF-1	GTPase regulator associated with focal adhesion kinase-1
GRE	glucocorticoid-responsive element
GSHV	Ground Squirrel Hepatitis Virus

H

h	hour
HA	hemagglutination assay
HBcAg	Hepatitis B core antigen
HBeAg	Hepatitis B e antigen
HBsAg	Hepatitis B surface antigen
HBxAg	Hepatitis B x antigen
HBV	Hepatitis B Virus
HCC	Hepatocellular carcinoma
HGM	hepatocyte growth medium
HHBV	Heron Hepatitis B Virus
HIV-1	Human Immunodefiency Virus 1
HN	hemagglutitin-neuraminidase
HPV-16	Human Papilloma Virus 16
HRP	horseradish peroxidase
HSPGs	heparan sulfate proteoglycans
HSV-1	Herpes Simplex Virus 1

I

ID	internal identification number
IL-2R-β	β-chain of the interleukin-2 receptor
IFN	interferon

J

Jas	Jasplakinolide

K

k	kilo

L

l	liter
L	lysosome
LB medium	Luria Broth medium
LHBs	Large Hepatitis B surface protein

M

µ	micro
m	milli/meter
M	molar
MßCD	methyl-beta-cyclodextrin
MHBs	Middle Hepatitis B surface protein
MHC-1	major histocompatibility complex 1
min	minutes
MLV	Murine Leukemia Virus
MOI	multiplicity of infection
mRNA	messenger ribonucleic acid
MT	microtubule
MTOC	microtubule organizing center
MVBs	multivesicular bodies
MW	molecular weight

N

n	nano
NLS	nuclear localization signal
Noco	Nocodazole
NPC	nuclear pore complex
NRE	negative regulating element
nt	nucleotide
N-terminus	amino terminus

O

OuHBV	Orang-Utan Hepatitis B Virus
ORF	open reading frame

P

PBS	phosphate buffered saline
PCR	polymerase chain reaction
PDH	primary duck hepatocytes
PEG	polyethylene glycol
PFA	paraformaldehyde
PFU	plaque forming units
pg	pregenomic
PHH	primary human hepatocytes
p.i.	post infection
PM	plasma membrane
pol	polymerase
pr	primer domain
PRE	posttranscriptional regulatory element
preS1/2	preSurface 1/2
PTH	primary *Tupaia* hepatocytes

R

Rac1	Ras-related C3 botulinum toxin substrate 1
rcDNA	relaxed circular DNA
RE	recycling endosome
RFP	red fluorescent protein
RhoA	Ras homolog gene family member A
RNA	ribonucleic acid
rpm	rounds per minute
RT	reverse transcription

S

sec	second
S	surface
SARS	severe acute respiratory syndrome
SeV	Sendai Virus
SFV	Semliki Forest Virus
SHBs	Small Hepatitis B surface protein
SV40	Simian Virus 40

T

TEMs	tetraspanin-enriched microdomains
TGN	trans Golgi network
TNE	Tris-Natrium(sodium)-EDTA

V

VacA	*Helicobacter pylori* vacuolating toxin A
v-ATPases	vacuolar-type ATPases
VSV	Vesicular Stomatitis Virus

W

WHO	World Health Organization
WHV	Woodchuck Hepatitis B Virus
WMHBV	Wolly Monkey Hepatitis B Virus

Other

#	Number

Summary

Hepatitis B virus (HBV) can infect only a few cell types including primary *Tupaia* hepatocytes (PTH) which were used in this work. The aim of the study was to characterize the early steps of HBV infection using pharmacological inhibitors and confocal microscopy. The distinction between endocytosis in general and direct fusion with the plasma membrane was made by using hypertonic sucrose concentrations. The fusion of Sendai virus (SeV) with the plasma membrane and its infectivity was not affected, whereas the infection of control viruses known to be taken up via endocytosis, e.g. Semliki Forest virus (SFV) and Simian virus 40 (SV40), was impeded. The HBV infection was inhibited in a dose-dependent manner, suggesting an endocytic uptake. The dynamin inhibitor Dynasore completely inhibited the entry of SFV (clathrin-mediated endocytosis) and SV40 (caveolin-mediated endocytosis), but had no effect on HBV suggesting a dynamin-independent internalization. Furthermore, the inhibitor of macropinocytosis EIPA did not impair HBV infection. HBV was also not able to stimulate the macropinocytic activity of PTH. Also phagocytosis could be ruled out as an entry mechanism. The actin inhibitors Jasplakinolide (actin-stabilisation) or Cytochalasin D (actin-depolymerisation) resulted in a partial inhibition of the early steps of HBV infection. The intracellular transport of HBV could be constrained by utilization of Nocodazole, an inhibitor of microtubule-polymerisation. HBV does not require an acidic pH within the endosomal compartments for the initiation of a productive infection cycle and therefore differs from many other viruses that are internalized via endocytosis (e.g. SFV, which was tested as control virus) and also from the related hepatitis B virus of the duck. No parallels to the retrograde pathway of SV40 were observed, since the HBV infection showed no sensitivity towards inhibitors of specific intracellular transport mechanisms (Brefeldin A), ER protein folding and quality factors (MG-132) and the translocation process to the cytosol (Thapsigargin). Together with previous data it can be concluded that HBV is internalized via a not yet known, possibly virus-induced, endocytic uptake mechanism, which is clathrin-, caveolin-, lipid raft- and dynamin-independent and differs from the process of phagocytosis and macropinocytosis.

Zusammenfassung

Hepatitis B Virus (HBV) kann nur wenige Zelltypen infizieren, u.a. primäre *Tupaia* Hepatozyten (PTH), die hier eingesetzt wurden. Die frühen Schritte der HBV-Infektion sind noch unbekannt und sollten mithilfe von pharmakologischen Inhibitoren und konfokaler Mikroskopie charakterisiert werden. Die Unterscheidung zwischen allen Arten von Endozytosevorgängen und der direkten Fusion von Virushüllen mit der Plasmamembran erfolgte durch Behandlung mit hyperosmolaren Sucrosekonzentrationen. Die Fusion des Sendai Virus (SeV) mit der Plasmamembran und dessen Infektiosität wurden dadurch nicht beeinflusst, während die Infektion endozytisch aufgenommener Kontrollviren, z.B. des Semliki Forest Virus (SFV) sowie des Simian Virus 40 (SV40), unterbunden werden konnte. Auch die Infektion mit HBV wurde dosis-abhängig inhibiert, was auf eine endozytische Aufnahme schließen lässt. Der Dynamin-Inhibitor Dynasore konnte die Eintrittsprozesse von SFV (Clathrin-vermittelte Endozytose) und SV40 (Caveolin-vermittelte Endozytose) vollständig unterbinden, hatte jedoch keinen Einfluss auf die HBV-Infektion, was auf einen Dynamin-unabhängigen Internalisierungsprozess hindeutet. Auch der Inhibitor der Makropinozytose EIPA inhibierte die HBV-Aufnahme nicht. Außerdem stimulierte HBV nicht die Makropinozytose in PTH. Phagozytose konnte als Eintrittsmechanismus ebenfalls ausgeschlossen werden. Die Aktin-Inhibitoren Jasplakinolide (Aktin-Stabilisierung) bzw. Cytochalasin D (Aktin-Depolymerisierung) führten zu einer partiellen Inhibition der frühen Schritte der HBV Infektion. Der intrazelluläre Transport von HBV konnte durch Nocodazol, einem Inhibitor der Mikrotubuli-Polymerisation, behindert werden. HBV benötigt für die Infektion keinen sauren pH innerhalb der endosomalen Kompartimente und unterscheidet sich damit von vielen anderen endozytisch aufgenommenen Viren (u.a. dem Kontrollvirus SFV) und auch vom verwandten Hepatitis B Virus der Ente. Ein retrograder Aufnahmeweg wie bei SV40 liegt bei HBV nicht vor, da entsprechende Inhibitoren bestimmter intrazellulärer Transportprozesse (Brefeldin A), ER-Proteinfaltungs-und Qualitätsfaktoren (MG-132) sowie des Translokationsprozesses ins Zytosol (Thapsigargin) wirkungslos blieben. Zusammen mit früheren Daten kann postuliert werden, dass HBV über einen bislang unbekannten, möglicherweise vom Virus selbst-induzierten, endozytischen Aufnahmemechanismus internalisiert wird, welcher Clathrin-, Caveolin-, lipid raft- und Dynamin-unabhängig ist und sich vom Prozess der Phagozytose und Makropinozytose unterscheidet.

1. Introduction

1.1 Endocytosis

Endocytosis is an internalization process that occurs at the cell surface and has vital physiological roles: Invagination of plasma membrane (PM) regions is used to regulate the protein and lipid content of the cellular surface (maintenance of homeostasis) and thereby controls cell-environmental interactions. Nutrient uptake and modulation of surface receptor signaling are also important roles of endocytic processes and indispensable for cell and tissue function (Doherty and Lundmark 2009; Kumari et al. 2010). It is also required for cell adhesion, cell morphology changes, such as establishment of cellular asymmetry or migration, antigen presentation and mitosis (Doherty and Lundmark 2009; Doherty and McMahon 2009). There is no evidence for an endocytic system in prokaryotes whereas a variety of different processes is found in eukaryotic organisms including protozoans, for example *Trypanosoma*, *Paramecium*, amoebae, certain fungi etc. as well as metazoans, such as plants, invertebrates and vertebrates. Obviously, the different kingdoms have evolved specialized endocytic processes based on environmental adaptations and molecular divergence (Allen et al. 2003; Dacks and Field 2007; Kumari et al. 2010). Over the years, a diversity of endocytic pathways in eukaryotes has been discovered mainly by studies in mammalian cells (Fig. 1).

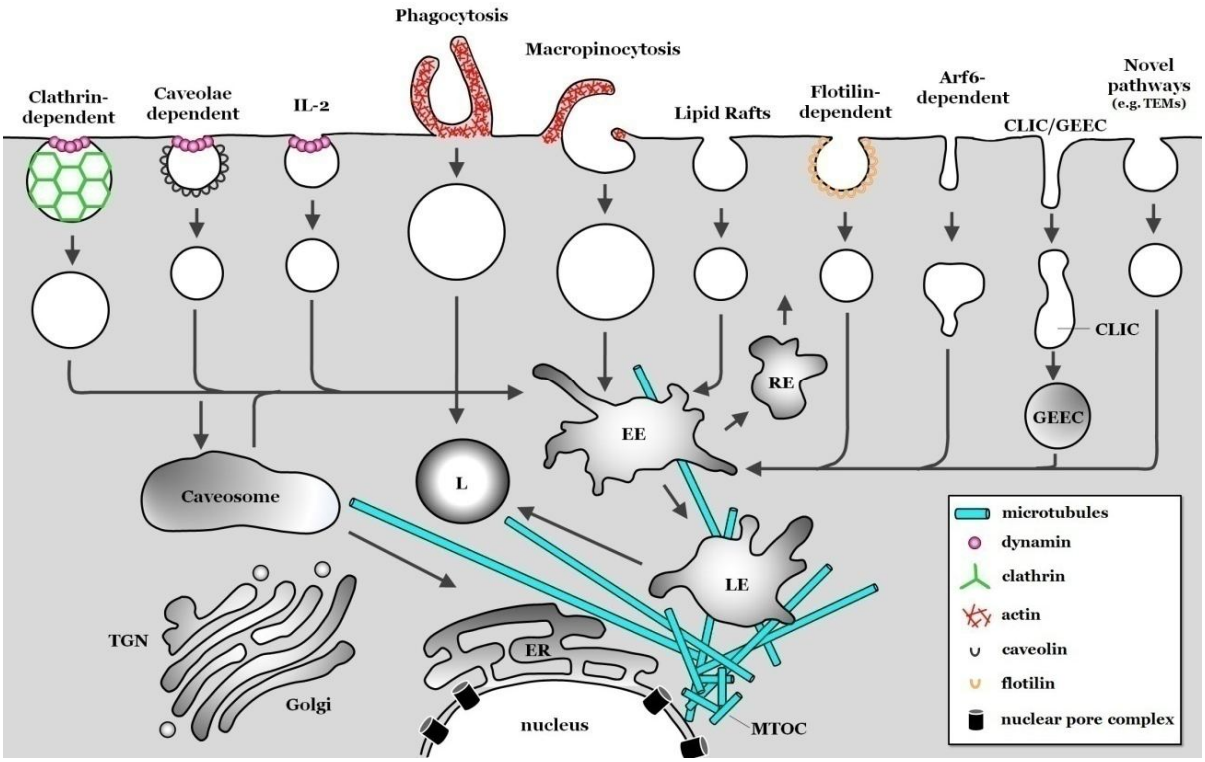

Figure 1: Entry pathways into cells. EE: early endosome, ER: endoplasmic reticulum, MTOC: microtubule organizing centre; L: lysosome; LE: late endosome, RE: recycling endosome; TGN: trans Golgi network. CLIC: clathrin-independent carriers; GEEC: GPI-AP enriched ensosomal compartment.

1.1.1 Entry of pathogens

Viruses are obligatory intracellular parasites and characterized by an extremely simple structure. They lack any metabolic or motile activities therefore being strictly dependent on hosts. In order to invade and infect their host cells, viruses first bind to cell surface structures which can be proteins, lipids or carbohydrates. Some of them merely serve as attachment factors which help to concentrate viruses on the cellular surface. Unlike such relatively unspecific and reversible binding to e.g. carbohydrate structures, binding to high-affinity receptors is usually specific and actively promotes viral entry. In addition to this, many viruses use the cellular signaling pathways to make their presence on the cell surface known. Those signaling activities induce changes in the host cell thereby setting-up specific endocytic mechanisms (Marsh and Helenius 2006). Cells offer a variety of endocytic and trafficking mechanisms that are hijacked by viruses to cross membranes or other barriers and deliver their genomes to their replication site within the cytoplasm or the nucleus (Fig. 1). Some viruses can penetrate into the cytosol directly through the PM (e.g. Herpes simplex virus 1, HSV-1, or Sendai virus, SeV) but most depend on endocytic uptake. One advantage of endocytosis is that endocytic vesicles ferry their “virus-cargo” from the periphery of the cell through the crowded cytoplasm to a more perinuclear area, bypassing barriers, such as the actin cortex, and exploiting molecular motors recruited to the vesicles (Dohner and Sodeik 2005; Mercer et al. 2010). A further advantage of endocytosis whereof viruses benefit, is the condition within maturing endosomes: The pH decrease, the presence of specific proteases and changes in the redox environment provide cues that trigger penetration and uncoating (Smith and Helenius 2004; Mercer et al. 2010). Finally, viruses that penetrate from intracellular organelles avoid leaving viral proteins exposed on the PM therefore causing a delay in immune detection (Smith and Helenius 2004). A risk that viruses must accept when using endocytosis, is the possible delivery to lysosomes which means degradation and a dead-end for most pathogens. That is the reason why viruses have adjusted the threshold pH for activation to match that of early or late endosomes (Smith and Helenius 2004). By utilizing the internalization and trafficking machineries of the host cell, i.e. pleiomorphic endosomal compartments that fuse with one another and thereby promoting trafficking, viruses find the correct replication site for progress of the infectious life cycle (Sieczkarski and Whittaker 2002).

1.2 Pathways of entry into cells

Classification of endocytic mechanisms is rather complicated since many different factors are involved and may be required in more than one route (Fig. 1). In the following, the pathways are classified based on their dependence on the GTPase dynamin. Dynamin is an essential component of vesicle formation during endocytosis, synaptic vesicle recycling and perhaps vesicle trafficking in and out of the Golgi (Hinshaw 2000). To date, three dynamin

genes have been identified in mammalian cells, each expressing at least four different alternatively spliced forms. Dynamin-1 is found specifically in neuronal cells, Dynamin-2 is ubiquitously expressed whereas Dynamin-3 is expressed predominantly in testes but also appears in lung and brain (Hinshaw 2000). There is evidence that the different isoforms and splice variants function at distinct locations within the cell (Cao et al. 1998; Hinshaw 2000). Dynamin self-assembles into higher-ordered structures resembling rings or spirals. This dynamic oligomerization leads to constriction of invaginated membrane areas and budding of a vesicle. However, its exact mechanism of action is still controversially discussed (Mettlen et al. 2009).

1.2.1 Dynamin-dependent endocytosis

1.2.1.1 Clathrin-mediated endocytosis

Clathrin-mediated endocytosis (CME) is the best-studied endocytic pathway. It involves clathrin, which shapes cage-like membrane invaginations (clathrin coated pits, CCPs) on the cytoplasmic face of the PM that pinch off by the action of dynamin and become free clathrin-coated vesicles (CCVs) (Pearse 1976; Marsh and McMahon 1999). Clathrin functions as a trimer of heterodimers, the so-called triskelion, which assembles into a lattice-like structure forming vesicles of different sizes ranging from 100-200 nm in diameter (Pearse 1976; Kumari et al. 2010). Additionally, interaction of clathrin with several accessory proteins like adaptor proteins (e.g. AP-2 or AP-180), amphiphysin, Epsin, Eps15 etc. is required for scaffold formation, local membrane deformation and generation of CCPs/CCVs (Kirchhausen 1999; Marsh and McMahon 1999). CME is a constitutive process responsible for the internalization of PM receptors and also provides a continuous rapid and efficient route for virus entry (Benmerah and Lamaze 2007; Hansen and Nichols 2009). It transports incoming viruses within minutes to early or late endosomes where the acidic pH leads to conformational changes in the particles and triggers fusion of the viral and the endosomal membranes (Marsh and Helenius 2006). Several viruses use this pathway for internalization e.g. Semliki Forest Virus (SFV), Hepatitis C Virus (HCV), SARS Coronavirus, Vesicular Stomatitis Virus (VSV) and many others (Helenius et al. 1980; Sun et al. 2005; Marsh and Helenius 2006; Inoue et al. 2007).

1.2.1.2 Caveolin-mediated uptake

Until the early 1990s there was controversy whether clathrin-independent (CI) endocytosis exists at all (Hansen and Nichols 2009). Studies on the uptake of different types of endogenous and exogenous cargoes showed that pharmaceutical perturbation of CME did not block all kinds of endocytosis (Doherty and McMahon 2009; Hansen and Nichols 2009). Probably the best-characterized dynamin-dependent CI pathway is the caveolin-mediated endocytosis (Mayor and Pagano 2007). It is often equated with lipid rafts which is

not entirely true, since caveolae present only one subset of lipid rafts (Simons and Toomre 2000). Therefore here, the term “caveolae” is used for invaginations of the PM containing caveolin. Caveolae were already recognized in the 1950s by electron microscopy (EM) due to their characteristic flask-shaped morphology (Palade 1953). They are 50-80 nm in diameter and are enriched in caveolins, sphingolipids and cholesterol (Mayor and Pagano 2007).
There are three mammalian caveolin proteins: Caveolin-1 (cav-1) is co-expressed with caveolin-2 (cav-2) in cells with abundant caveolae, such as endothelial cells, adipocytes and fibroblasts, caveolin-3 (cav-3) is muscle-specific (Ikonen et al. 2004; Doherty and McMahon 2009). Caveolae have been implicated in endocytosis, transcytosis and signal transduction but since they are abundant in some cell types (see above) but undetectable in others, e.g. lymphocytes, neurons and hepatocytes, their general cellular function remains unclear (Parton and Richards 2003). Caveolae are relatively stable and immobile in the PM and bud only infrequently suggesting no involvement in constitutive endocytic trafficking (Thomsen et al. 2002). However, it has been shown that dynamin is recruited to caveolae and some pinch off the membrane (Oh et al. 1998; Kirkham et al. 2005). Accordingly, some viruses, certain bacteria as well as bacterial toxins make use of this uptake route, e.g. Simian Virus 40 (SV40), Echo 1 Virus, papilloma viruses, certain E.coli strains, Cholera Toxin B (CtxB) etc. (Oh et al. 1998; Parton and Richards 2003; Smith and Helenius 2004; Kirkham et al. 2005; Marsh and Helenius 2006). The internalized cargoes are either routed to acidic early endosomes or to pH-neutral caveosomes from where they are further transported to reach their penetration or replication site (Marsh and Helenius 2006; Mayor and Pagano 2007).

1.2.1.3 Other pathways

Another dynamin-dependent CI mechanism is responsible for uptake of the β-chain of the interleukin-2 receptor (IL-2R-β), for internalization of other receptors in immune cells and fibroblasts and is possibly used by Rotavirus (Mayor and Pagano 2007; Doherty and McMahon 2009; Mercer et al. 2010). The pathway is dependent on the small G-proteins RhoA and Rac1 (Doherty and McMahon 2009). Particular proteins coating the endocytic vesicles are currently not known and their exact morphology is still unclear (Doherty and McMahon 2009).

1.2.2 Dynamin-independent endocytosis

1.2.2.1 Phagocytosis

Phagocytosis and macropinocytosis (see following chapter 1.2.2.2) belong to a separate class of endocytic processes that involve the uptake of large membrane patches of >1 μm and generation of large, uncoated vacuoles with a diameter of 0.5-10 μm (Mayor and Pagano 2007; Hansen and Nichols 2009; Mercer and Helenius 2009). Phagocytosis is an endocytic

mechanism used by lower organisms for nutrient acquisition (Aderem and Underhill 1999), in metazoa it occurs in specialized cell types including macrophages (e.g. the Kupffer cells of the liver), monocytes and neutrophils and displays a major mechanism for the degradation of large particles, like apoptotic cell debris and pathogens (Aderem and Underhill 1999; Conner and Schmid 2003). In order to discriminate between self and non-self particles, cells have evolved different receptors and types of phagocytic processes (Aderem and Underhill 1999). Internalization by phagocytosis is specific and particle-driven. The attachment of the particle to the PM not only triggers the mechanism but also guides the formation of local actin-protrusions that, in some cases even “zipper up”, to tightly enclose the receptor-coated particle (Anderem and Underhill 1999; Mercer et al. 2010). After internalization, the phagosome undergoes maturation by several fusion and fission events with other endosomal compartments. Thereby gradual acidification takes place which finally leads to particle degradation (Aderem and Underhill 1999). Despite the efficiency of the innate immune system in detecting and destroying pathogens, certain bacteria, such as *Legionella* or *Shigella*, have developed mechanisms to escape degradation and some even persist and replicate inside phagosomes (Kinchen and Ravichandran 2008). Also some large viruses use this pathway to infect host cells as shown with HSV-1 and Mimivirus (Clement et al. 2006; Ghigo et al. 2008).

1.2.2.2 Macropinocytosis

Macropinocytosis has diverse functions ranging from nutrient uptake in amoeba (Koivusalo et al. 2010) to an involvement in cell migration and antigen presentation in some cell types (Ghigo 2010). An important feature of this mechanism is the requirement for extensive reorganization of the actin cytoskeleton (Schelhaas 2010). This rearrangement frequently involves PM protrusions (e.g. lamelipodia, filopodia or blebs) that subsequently either fuse with themselves or back with the PM, resulting in the formation of large, heterogeneous vesicles known as macropinosomes (Sieczkarski and Whittaker 2002; Doherty and McMahon 2009; Mercer et al. 2010). The definite fate of those vesicles is cell type-dependent, but it is known that they can intersect with other organelles of the endolysosomal system during their maturation process, offering possible routes for the entry of diverse pathogens (Sieczkarski and Whittaker 2002; Kerr and Teasdale 2009; Ghigo 2010). In contrast to phagocytosis, macropinocytosis is considered as a nonspecific internalization process of large amounts of fluids and solutes that does not rely on ligand binding to a specific receptor (Sieczkarski and Whittaker 2002). In certain cell types, such as dendritic cells, it is a constitutive process and a major route of entry that does not require stimulation (Sieczkarski and Whittaker 2002; Mercer and Helenius 2009; Kumari et al. 2010). However, in most situations, it is a transient mechanism since macropinosomes are usually not found in resting, unstimulated cells but formed upon growth-factor induced

stimulation of cells (Nichols and Lippincott-Schwartz 2001; Sieczkarski and Whittaker 2002). A variety of particles can induce “membrane ruffling” thus promoting their incidental internalization together with fluid into macropinosomes (Mercer and Helenius 2009). These are for example bacteria like *Shigella* and *Salmonella* (Kumari et al. 2010) and also viruses from different families use macropinocytosis for entry, such as Adenovirus type 3 (Ad3), HIV-1, HSV-1 and Vaccinia Virus (Kumari et al. 2010; Mercer et al. 2010).

1.2.2.3 CLIC-GEEC

Another constitutive dynamin-and clathrin-independent endocytic pathway that is used for the internalization of glycosyl phosphatidylinositol-anchored proteins (GPI-APs) is represented by a mechanism mediated by primary carriers called clathrin-independent carriers (CLICs) which fuse to tubular compartments called GPI-AP enriched endosomal compartments (GEECs) (Sabharanjak et al. 2002; Mayor and Pagano 2007). Beside the role in GPI-AP uptake, the CLIC/GEEC pathway is also responsible for endocytosis of large amounts of extracellular fluid, CtxB, the plant toxin ricin and *Helicobacter pylori* vacuolating toxin (VacA) (Kalia et al. 2006; Mayor and Pagano 2007; Kumari et al. 2010). Endocytosis through this route has been shown to be dependent on the activity of the small GTPases Cdc42 and Arf1 (Kumari and Mayor 2008). Recently, the first specific non-cargo marker of CLIC tubules has been identified: GRAF1 (GTPase regulator associated with focal adhesion kinase-1) localizes predominantly to pleiomorphic tubular structures which are ~40 nm in diameter and is probably used to generate or stabilize membrane curvature (Kumari and Mayor 2008; Lundmark et al. 2008). Until now, no viruses have been shown to use this route as entry pathway but since it has been discovered just recently, further work will determine its biological functions and identify other exogenous cargoes.

1.2.2.4 Other pathways

There is growing evidence that in addition to the established internalization mechanisms (see above) more pathways exist which exhibit differences among each other. They lack detectable coats as seen by EM and are independent of clathrin and caveolin (Mercer et al. 2010). Examples are the ADP-ribosylation factor 6 (Arf6)-dependent pathway, the Flotilin-associated route and the endocytic mechanism via tetraspanin-enriched microdomains (TEMs).

The Arf6-pathway is important for the uptake of MHC-1 (major histocompatibility complex 1), IL-2R-α as well as β1-integrin and it resembles the CLIC/GEEC route since here also tubular structures appear and certain GPI-APs are taken up (Sandvig et al. 2008). However, it is likely that these processes are distinct modes of trafficking since inhibition of GRAF1 does not affect MHC-1 internalization (Sandvig et al. 2008; Kumari et al. 2010).

Flotilin proteins 1 and 2 have a similar topology to cav-1 but are not enriched in caveolae (Doherty and McMahon 2009). They are found oligomerized in distinct microdomains resembling caveolae and can be detected in cav-1-deficient cells (Doherty and McMahon 2009; Hansen and Nichols 2009). Flotilin 1 is necessary for CD59 uptake and a portion of CtxB internalization. Furthermore, it is needed for the uptake of cell surface proteoglycans (Doherty and McMahon 2009; Hansen and Nichols 2009). Until now, no virus has been associated to enter through the Arf6-or flotilin-dependent pathway.
Another form of endocytosis is supported by TEMs. It does not rely on caveolins, flotilins or lipid rafts and is distinct from macropinocytosis and phagocytosis (Mercer et al. 2010). Infectious entry of Human Papilloma Virus 16 (HPV-16), originally proposed to occur via CME, has recently been shown to involve TEMs (Spoden et al. 2008).

1.2.3 pH dependence of viral infection

The intracellular space of eukaryotic cells is compartmentalized into organelles with different properties thus providing diverse local environments for specific functions. A distinctive feature of organelles is e.g. their luminal pH-value which ranges from neutral in the ER to acidic in endosomes or lysosomes. Acidic pH is important for a number of events including protein-processing and degradation, membrane trafficking and dissociation of receptor-ligand complexes after internalization (Jefferies et al. 2008; Lafourcade et al. 2008; Sun-Wada and Wada 2010). Furthermore, the acidic pH within endosomes is also crucial for a productive infection of various viruses, such as SFV, Sindbis and Influenza, and provides cues that trigger penetration and uncoating (Helenius et al. 1980; Glomb-Reinmund and Kielian 1998; Smith and Helenius 2004).

1.2.4 Role of the cytoskeleton for endocytic pathways

The cytoskeleton is essential for the survival of most cells: filaments provide internal mechanical support, force to drive cell motion and tracks for movement of organelles and macromolecules throughout the cytoplasm (Pollard and Cooper 2009). Furthermore, there is evidence that especially actin plays an important role during endocytosis (Smythe and Ayscough 2006; Mercer et al. 2010). Processes like macropinocytosis and phagocytosis involve dramatic membrane remodeling and strictly depend on the formation of actin ruffles for the internalization of extracellular components or particles (Doherty and McMahon 2009). In pinocytic pathways, the cortical actin constitutes a submembranous barrier that is transiently depolymerized upon virus binding which allows endocytosis to proceed (Marsh and Helenius 2006; Doherty and McMahon 2009). The dynamic reassembly of actin might be then required to facilitate vesicle formation and its fission as well as providing a track for subsequent trafficking over short distances (Mayor and Pagano 2007; Doherty and McMahon 2009; Pollard and Cooper 2009). In eukaryotic cells, many

different accessory proteins have been described to be concerned with the actin machinery and a number of those are proteins involved in endocytic processes (Fujimoto et al. 2000; Doherty and McMahon 2008; Polard and Cooper 2009). Although actin is often found associated with some endocytic events, it does not seem to be essential for all pathways since its contribution varies depending on the different cell types or, within the same cell type, under different conditions (Fujimoto et al. 2000; Doherty and McMahon 2008).

1.3 Hepatitis B Virus (HBV)

1.3.1 Taxonomy

HBV belongs to the *Hepadnaviridae*, a family of hepatotropic and highly species-specific DNA viruses that is divided into two genera: the *Orthohepadnavirus* of mammals and the *Avihepadnavirus* of birds. *Orthohepadnaviruses* were discovered in humans (HBV) (Dane et al. 1970), Old World primates such as gorillas (GoHBV) (Grethe et al. 2000), orang-utans (OuHBV) (Warren et al. 1999), chimpanzees (ChHBV) (Vaudin et al. 1988) and gibbons (GiHBV) (Norder et al. 1996) as well as in the woolly monkey (WMHBV), a New World primate (Lanford et al. 1998). Furthermore, several rodents of the *Sciuridae* (squirrels) serve as hosts, e.g. the North American Woodchuck (WHV) (Summers et al. 1978), the California ground squirrel (GSHV) (Marion et al. 1980) and the Arctic Ground squirrel (ASHV) (Testut et al. 1996). *Avihepadnaviruses* are found in various bird species, e.g. Peking ducks (DHBV) (Mason et al. 1980), herons (HHBV) (Sprengel et al. 1988), cranes (CHBV) (Prassolov et al. 2003). HBV is divided into nine genotypes, A to I, based on >8% nucleotide variation over the entire genome (Norder et al. 2004; Yu et al. 2010). The various genotypes reflect a prevalent ethnical distribution (Bartholomeusz and Schaefer 2004).

1.3.2 Transmission and disease

HBV is the causative agent of viral hepatitis type B, an inflammation of the liver which can take an acute or chronic course. Transmission of HBV occurs via blood or other body fluids (i.e. saliva, semen and vaginal fluid) by sexual contact, needle sharing between drug addicts etc. (horizontal transfer). Due to extremely high virus titres of up to $\geq 10^{10}$/ml in the blood of viraemic carriers, very small amounts of serum (1 nl) can be sufficient for infection (Gerlich 2002). In the majority of chronic cases transmission occurs vertically from mothers to their neonates perinatally. Infections via blood transfusions, once a common route of transmission, are negligible in developed countries, since the development of advanced diagnostic tests, broader screening for infection as well as improved production methods (e.g. for virus-inactivated plasma derivates) became standard condition (Lavanchy 2004).

Hepatitis B is a potentially life-shortening liver infection and a major global health problem. According to estimates of the WHO (World Health Organization) two billion people worldwide have been infected with HBV, approx. 370 million are chronic carriers and about 1 million people die each year due to the long term sequelae of the disease. The prevalence of HBV infection varies greatly throughout the world. In western countries, like Europe and North America less than 1% of the population is chronically infected whereas in high endemic countries, like Africa, China and other parts of Asia, 8-10% of the adult population become infected during early childhood (Lavanchy 2005). The course of infection is variable and depends on the infectious dose and fitness of the virus and is also regulated by age, gender and the state of health of the infected person. Wildtype HBV has no direct cytopathic effect, whereas variants of the virus may have an impact on pathogenesis. There is growing consensus that especially the virus-specific T-cell response is the key determinant influencing the pathogenesis of HBV infection (Chisari and Ferrari 1995; Chisari 1997; Baumert et al. 2007). In about 90% of healthy adults low dose-infections lead to a minor viral replication which is eliminated later and results in immunity. Infections with a higher dose predominantly lead to an acute hepatitis B, characterized by general malaise, extreme fatigue, nausea and sometimes jaundice (yellowing of the skin and eyes). The symptoms may last several weeks before the patient recovers and immunity is induced. The most severe form of an acute illness is the fulminant hepatitis B which proceeds in <1% of all cases. It leads to hepatic encephalopathy, failure of the coagulation system and, if left untreated, in 70% of cases to death (Ganem and Prince 2004). The likelihood that a chronic hepatitis emerges from an acute infection depends on the age at which a person becomes infected. Neonates and young children are the most likely to develop a chronic infection. About 25% of adults who become chronically infected during early childhood, later die from the consequences which may be cirrhosis (scarring of the liver) or hepatocellular carcinoma (HCC). Cirrhosis and HCC-incidence has increased worldwide with HCC being the 5th most frequent cancer (Lavanchy 2005).

1.3.3 Prevention and therapy

HBV infection is a preventable disease. A safe and effective vaccine is available since 1982 and is 95% effective in preventing the disease and its consequences (Lavanchy 2004). Currently, SHBs is the only component of the widely used vaccines. Antibodies against this region are neutralizing *in vitro* and *in vivo* and protect infection in most cases, but may fail to protect against naturally occurring escape-mutants (Carman et al. 1993) or mutants selected during antiviral therapy (Kamili et al. 2009). To counteract this problem, the preS1-domain, essential for virus attachment, ought to be included into the vaccine (Bremer et al. in press).

Despite the existence of a vaccine, an estimated 370 million people are chronically infected worldwide implicating the consequences of cirrhosis and HCC. Antiviral treatment is used for preventing liver disease and development of HCC and suppression of virus replication. One option for treatment is interferon alpha (IFNα) which modulates the immune responses against HBV and has antiviral activity (Lavanchy 2004). However, it is associated with side effects such as flu-like symptoms (Tillmann 2007). The different available nucleos(t)ides analogues, e.g. Lamivudine, Adefovir, Entecavir and Tenofovir block the viral reverse transcriptase and thus formation of mature virus, offer the advantage of minimal side effects but lead to selection of HBV mutants and often result in development of resistance during therapy (Tillmann 2007). For this reason, antivirals that target other steps of the viral life cycle, e.g. attachment and entry, rcDNA to cccDNA conversion, assembly or budding, are under development. Myrcludex B is currently the only representative of a novel class of HBV entry inhibitors. It is an acylated peptide corresponding to the preS1-region of the large HBV surface protein and is known to block virus entry *in vitro* and *in vivo* and is currently developed as an antiviral approach (Glebe et al. 2005; Gripon et al. 2005; Petersen et al. 2008).

1.3.4 Morphology

The enveloped HBV has a diameter of 42-47 nm and is therefore one of the smallest animal viruses known (Dane et al. 1970) (Fig. 2). In electron microscopy the virions appear as characteristic double-shelled particles after negative staining (a). The virions contain a core particle which can be released from the lipid envelope by detergent (Almeida et al. 1971). Infected hepatocytes secrete virions and, in a huge excess, noninfectious subviral particles which consist of empty viral enveloped. They form 17-25 nm spheres and filamentous structures variable in length (Robinson 1977) (b). Both the virion and the subviral particles possess in their lipid envelope three different surface proteins: these are the L-(large), M-(middle) and S-(small) hepatitis B surface (HBs) proteins which have a co-terminal carboxy terminus but differ in their N-terminal sequences (Heermann et al. 1984) and glycosylation pattern (Schmitt et al. 1999). The SHBs contains only the S-domain, the MHBs is formed by the S-and preS2-domain and finally the LHBs which consists of the S-, preS2-and preS1-domain. The preS(1+2) domain of LHBs has a dual topology in the particles either lying within the lumen or being outwards exposed (Bruss et al. 1994; Lambert and Prange 2001).
The HBV nucleocapsid (core particle, HBc) has a diameter of 32-36 nm and an icosahedral T3-or T4-symmetry made of 180 subunits (T3) or 240 subunits (T4) of the hepatitis B core antigen (HBcAg) (Crowther et al. 1994; Kenney et al. 1995; Dryden et al. 2006; Seitz et al. 2007). The capsid encloses the HBV genome (Robinson 1974; Summers et al. 1975) with the viral polymerase covalently bound to the DNA (Gerlich and Robinson 1980). The polymerase is a multifunctional enzyme consisting of four subunits: priming domain,

reverse transcriptase domain, RNase H domain and a non-essential spacer domain (Bartenschlager and Schaller 1988; Radziwill et al. 1990; Beck and Nassal 2007). The priming domain is covalently bound to the 5' end of the negative strand and initiates the synthesis which is carried out by the reverse transcriptase (Barthenschlager and Schaller 1988; Weber et al. 1994). The RNase H domain digests selectively RNA from the DNA/RNA hybrid (Radziwill et al. 1990).

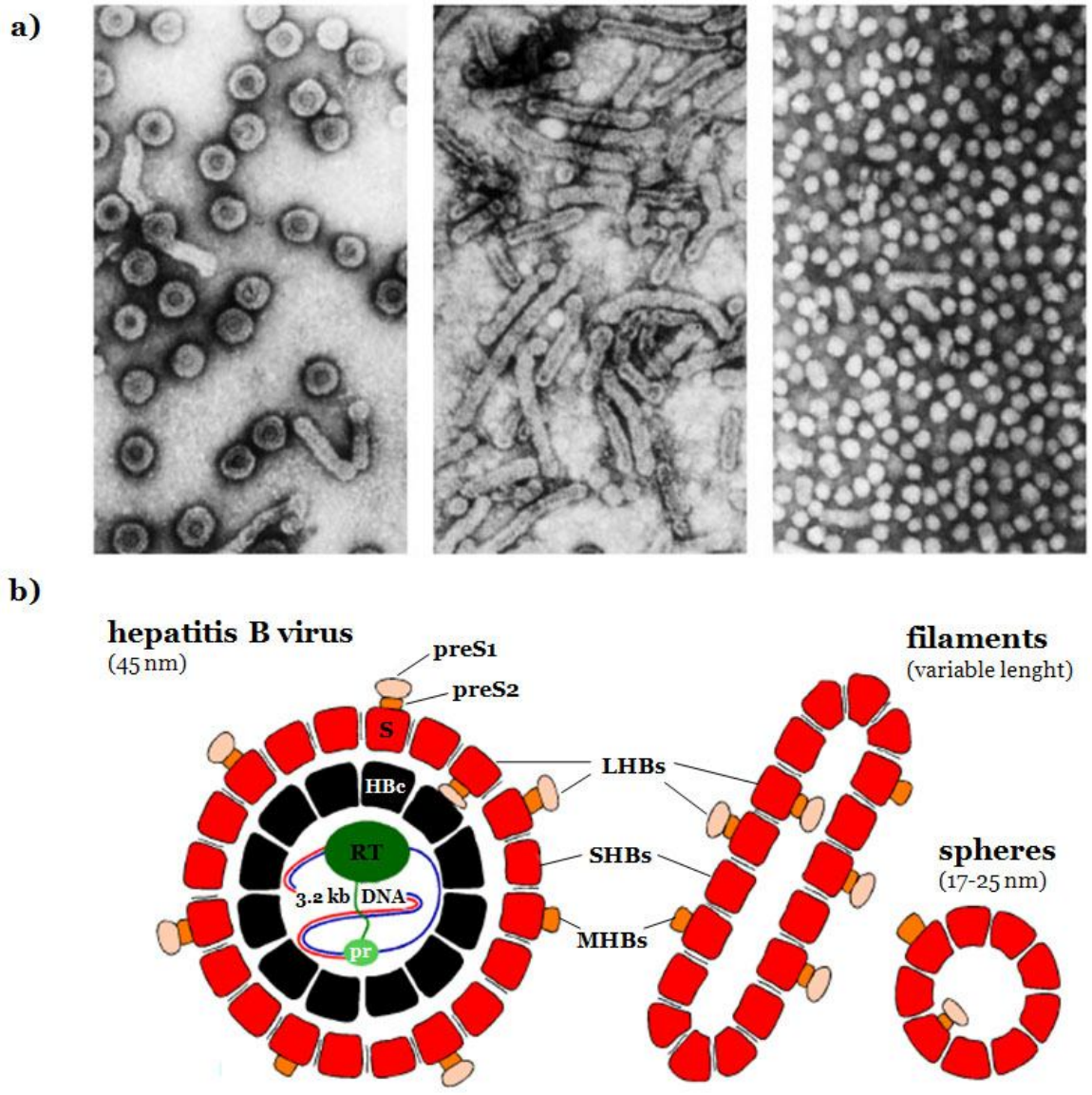

Figure 2: Structure of HBV and subviral particles (filaments and spheres). a) Electron-microscopical photograph of HBV-virions (left), HBsAg-filaments (middle) and HBsAg-spheres (right). b) Model of HBV and subviral particles consisting of the small (SHBs), middle (MHBs) and large (LHBs) proteins. HBs proteins are shown with the S, preS2 and preS1 domain (represented in red, orange and rose). Nucleocapsid (HBc, black). The viral polymerase is depicted with the reverse transcription (RT, dark green) and primer domain (pr, light green) (Kann and Gerlich 2005; modified). Encapsidated cellular proteins (protein kinase and chaperones) are omitted.

1.3.5 Genome

The HBV genome is one of the smallest found so far and consists of a circular, partially double-stranded DNA. The longer, complete strand (negative polarity) comprises the complete coding capacity and is approx. 3.2 kb long depending on the genotype (Summers et al. 1975) (Fig. 3). The ends of this strand are not connected but show an overhang of about 8-10 nt at the 5´end (terminal redundancy) to which the primer domain of the viral polymerase covalently binds (Gerlich and Robinson 1980). This region is also spanned by the complementary plus-strand (Sattler and Robinson 1979) leading to a triplex strand areal (Will et al. 1987). The circularity of the genome does not originate from covalent closure but is rather caused by base pairing between both strands. The positive strand is incomplete with a constant 5' end position and a variable 3' end depending on how far it could be synthesized by the viral polymerase upon secretion (Hruska et al. 1977). The 5' end is associated with an 18 nt long mRNA-like cap-structure (Seeger et al. 1986). The negative strand codes for four conserved, partially overlapping ORFs (Glebe 2006) which encode: 1) the core-protein and a soluble form of it (called HBeAg); 2) the DNA-polymerase with primase, reverse transcriptase and RNase H activity; 3) the surface proteins and 4) the X-protein whose function is still not fully understood. The expression of the ORFs is regulated by several control elements with at least four promoters, two enhancers (Tang et al. 2001), the glucocorticoid-responsive element (GRE) and the negative regulating element (NRE) to which liver-and differentiation-dependent factors bind, leading to a hepatocyte-specific transcription and replication (Glebe 2006). There are additional regulatory elements at the mRNA-level, e.g. the posttranscriptional regulatory element (PRE), which prevents splicing of the transcripts and facilitates their transport into the cytoplasm and utilization (Huang and Liang 1993).

Two identical sequence regions made of 11 nt (DR 1 and DR 2; direct repeats) are located in the genome and play an important role in virus replication (Will et al. 1987).

Termination of transcription is achieved by a certain polyadenylation site resulting in a similar 3´end of all mRNAs (Ganem and Varmus 1987). The ε-signal at the 5´end of the pregenomic RNA participates together with the viral polymerase in the encapsidation process (Junker-Niepmann et al. 1990).

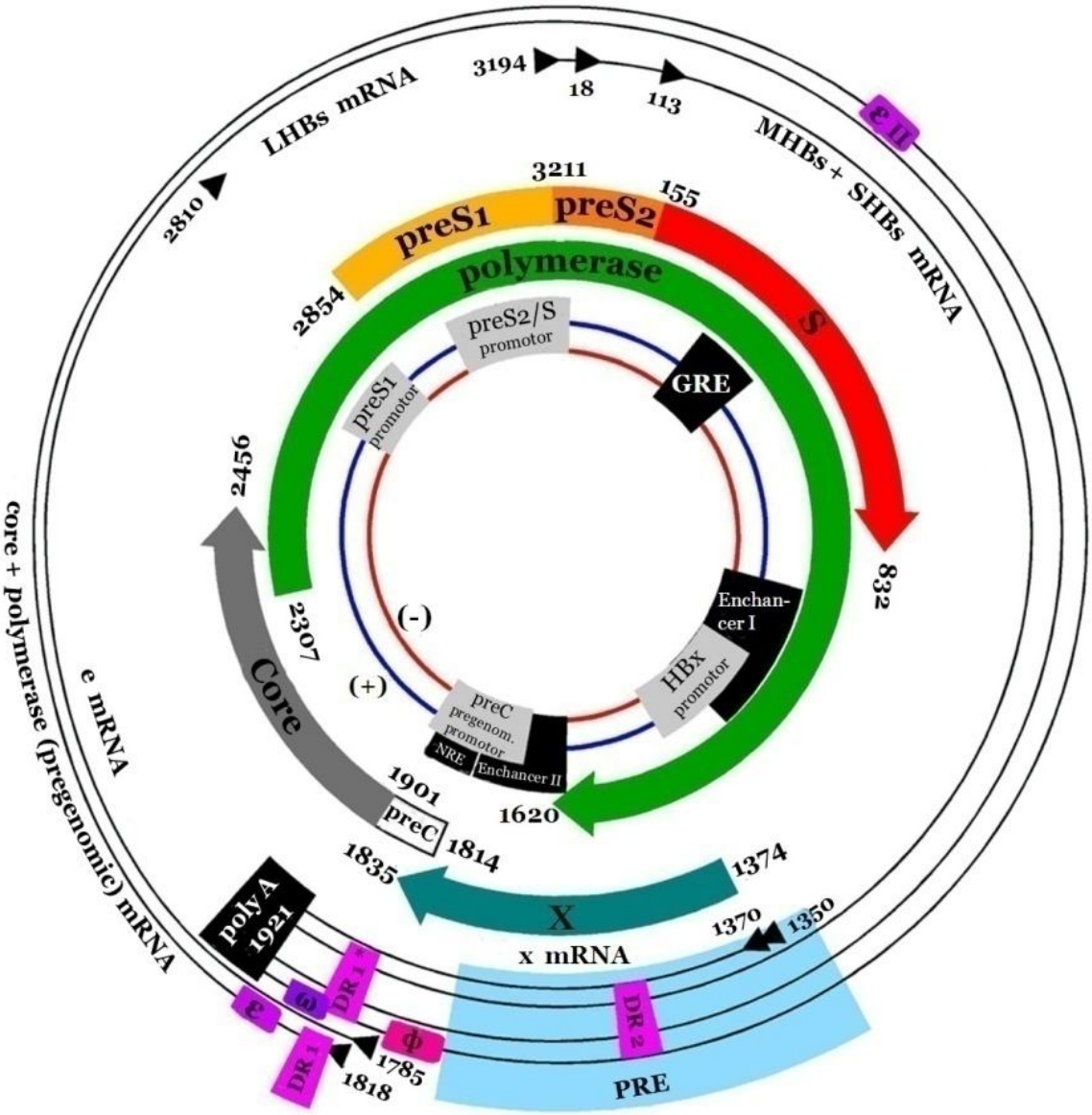

Figure 3: Genome structure of HBV. Inside, the four ORFs of the negative strand of HBV cccDNA are represented with the relevant start and stop codons: S-ORF with preS1-, preS2- and S-domain (red), Pol-ORF (green), C-ORF (dark grey) with preC (white), X-ORF (turquoise) with the respective promoters (light grey).The numbering indicates the base position from the EcoRI restriction site in the genome of HBV-genotype A2 (AJ012207). Transcription start sites (►) in the HBV cccDNA, mRNAs with polyA-tail (black), pregenomic-RNA (outmost circle). GRE: glucocorticoid responsive element; Enh: enhancer I and II; NRE: negative regulating element; PRE: posttranscriptional regulatory element; DR1 and DR2: direct repeats; ε: encapsidation signal; εII, ω and ϕ are sequence elements needed for genome maturation; (+): positive strand; (-): negative strand. (after Schaefer, Glebe and Gerlich, 2009; modified).

1.3.6 Viral life-cycle

Initial attachment of HBV to susceptible hepatocytes occurs via heparan sulfate proteoglycans (HSPGs) that are presumably used to concentrate the virions on the cellular surface (Schulze et al. 2007; Leistner et al. 2008) (Fig. 4). Such primary attachment is relatively unspecific and of low-affinity (Marsh and Helenius 2006; Glebe and Urban 2007). Thereafter, HBV binds via its preS1 domain (amino acids 9-18 and 28-48 respectively) and the N-terminal myristic acid to (a) still unknown high-affinity receptor(s) that is (are) believed to actively promote further entry steps (Neurath et al. 1989; Pontisso et al. 1989; Le Seyec 1999; Glebe et al. 2003; Engelke et al. 2006; Glebe and Urban 2007; Leistner et al. 2008). In addition to the receptor-binding site in the preS1-domain of the LHBs, a determinant of infectivity resides within the S-domain of LHBs possibly needed for fusion (Jaoude and Sureau 2005). It has been assumed that HBV enters the host cells via endocytosis, similar to DHBV, and is taken up into a still unknown cellular compartment (Köck et al. 1996; Glebe and Urban 2007). The exact point in time and site of nucleocapsid release is not fully understood, but for naked core particles, an active transport along microtubules towards the nucleus has been described (Rabe et al. 2006). HBV-capsids contain a NLS (nuclear localization sequence) for targeting the nucleus, where their subsequent import occurs through the nuclear pore complexes (NPCs) in an importin α/β-mediated manner (Kann et al. 1999). NPCs are able to transport particles with a diameter of about 39 nm into the karyoplasm, therefore, HBV capsids can cross the nuclear pore without disassembly (Pante and Kann 2002). Furthermore, it was shown that disintegration of capsids takes place within the nuclear baskets thereby releasing the viral genome (Rabe et al. 2003). Inside the nucleus the relaxed circular DNA (rcDNA) of the virus is converted into the plasmid-like covalently closed circular DNA (cccDNA), the first marker of a productive infection. In the nucleus, the cccDNA molecule is associated with histones and exists as a minichromosome (Bock et al. 1994; Newbold et al. 1995). An integration of the viral DNA into the genome of the host is not part of the life cycle contrary to the retroviruses. However, a random integration of subgenomic DNA fragments can occur. From the cccDNA several genomic (pregenomic (pg) RNA) and subgenomic RNAs are transcribed by cellular RNA polymerase II (Rall et al. 1983). All HBV RNAs are 5´end-capped and contain a PRE (see above) which prevents splicing (Schaller and Fischer 1991; Huang and Yen 1995). After export to the cytoplasm the pgRNA is translated into the polymerase (pol) and core proteins and serves as template for reverse transcription. The pgRNA interacts via its ε-signal with the polymerase and cellular chaperons thereby forming a complex which is encapsidated when sufficient core protein is available (Junker-Niepmann 1990; Bartenschlager and Schaller 1992; Seifer et al. 1993; Hu and Seeger 1996). Within this immature capsid, reverse transcription and subsequent plus strand synthesis take place (Summers and Mason 1982). After completion of the negative strand synthesis,

the now mature capsid either re-migrates to the nucleus to amplificate/refill the intranuclear cccDNA-pool or interacts with HBsAg-containing membranes at the ER (Tuttleman et al. 1986; Wu et al. 1990). The other mRNAs (2.4 kb, 2.1 kb and 0.7 kb) are also transported into the cytoplasm and translated into the LHBs, MHBs, SHBs surface proteins or the HBx protein. Virus budding and secretion occurs via multivesicular bodies (MVBs) (Lambert et al. 2007), whereas the subviral particles leave the cell via the normal secretory pathway through ER and Golgi.

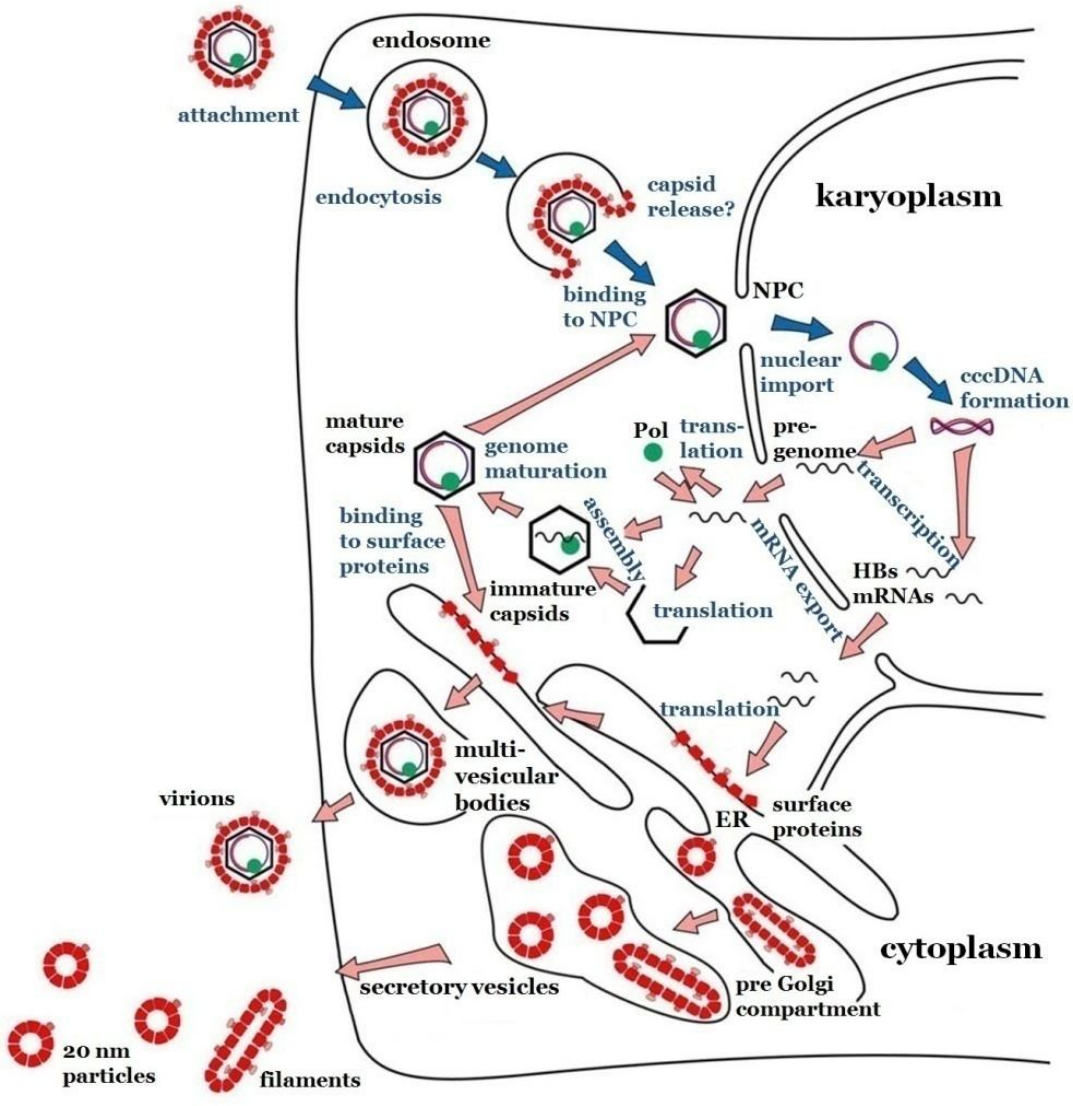

Figure 4: Intracellular life cycle of HBV. ER: endoplasmatic reticulum, NPC: nuclear pore complex, Pol: polymerase. For simplification the synthesis of HBeAg and HBxAg is neglected. (after Kann and Gerlich, 2005; modified).

1.3.7 Model systems for HBV infection

Due to the lack of appropriate animal models or cell lines, studies of the early stages of HBV infection were very difficult for a long time. HBV has a narrow host range and infects only humans or closely related species i.e. higher primates such as chimpanzees (Barker et al. 1973). Therefore, classical laboratory animals, like mice or rats, are not suitable for HBV infection studies. The impropriety of using chimpanzees as model becomes apparent when the ethical as well as economic concerns are considered. Therefore, current *in vivo* models for investigating hepadnaviruses are ducks (DHBV infection) and woodchucks (WHV, GSHV and ASHV infection). Also the *in vitro* infection proves to be difficult because HBV infection does not only depend on the species origin but also on the differentiation state of the cells. Indeed, hepatoma cell lines such as HepG2 have been shown to bind HBV as well as produce virions upon transfection, but fail to support a complete infectious circle (Neurath et al. 1986; Shih et al. 1989; Qiao et al. 1994; De Falco et al. 2001; Rabe et al. 2006). One exception is the HepaRG cell line which is susceptible for HBV infection after several weeks of differentiation with DMSO (Gripon et al. 2002). Primary hepatocyte cultures from ducklings (PDH) or embryonic hepatocytes from fertilized eggs are used to perform *in vitro* infection assays with DHBV (Glebe and Urban 2007). Primary human hepatocytes (PHH) can be infected with HBV but are not easy to handle and need certain growth factors for maintenance of their differentiated state. Furthermore, they are only available after surgical resection and show a heterogeneous quality since the state of health, age and gender of the donor varies (Glebe and Urban 2007). Alternatively, primary hepatocytes of the Southeast Asian tree shrew *Tupaia belangeri* (PTH), which is phylogenetically related to primates (Schmitz et al. 2000), can be used to study HBV infection *in vitro* (Su 1987) and also *in vivo* (Yan et al. 1996). The course of infection is analogous to that in human hepatocytes, but shows less variability and does not need growth or differentiation factors for successful infection (Glebe et al. 2003).

1.4 Aim of this work

To date, neither specific HBV receptors nor the exact mechanism for HBV entry into hepatocytes have been identified. In the present work the uptake mechanism of HBV should be investigated using primary hepatocyte cultures of *Tupaia belangeri* (PTH).

Two main questions should be addressed:

1. Does HBV infect its target cells by direct fusion with the plasma membrane or by an endocytic step?
2. If HBV is taken up by an endocytic step, it should be analyzed which cellular pathway HBV is using for infecting liver-derived naturally susceptible hepatocytes and which organelles and components of the cellular transport machinery are involved.

A comparison is made between the results obtained here with HBV and the entry characteristics of various control viruses with known entry and uptake mechanisms.

2. Material

For the preparation of all solutions, water from an ion exchanger (Millipore) was used.

2.1 Buffer, solutions and media

2.1.1 Buffers

name	components	concentration/amount
Agarose sample buffer (6x)	Glycerin Bromophenol blue ad TAE	60 ml 0.1 g 100 ml
ELISA coating buffer (NaPP); pH 7.4	NaCl Na_2HPO_4 x H_2O KH_2PO_4	83 mM 8.6 mM 2.2 mM
HBSS (without $MgCl_2$ and $CaCl_2$);	+/- EGTA (Sigma)	
Lysis buffer for cccDNA isolation	dH_2O Triton-X-100 (Sigma) $MgCl_2$ TBS (Tris Buffered Saline)	15 ml 750 µl 75 µl 1 tablet
MOPS/SDS-Buffer	Tris MOPS EDTA SDS	1M 1M 20.5 mM 69.3 mM
PBS	NaCl, pH 7.4 KCl Na_2HPO_4 x 2 H_2O KH_2PO_4 ad dH_2O	137 mM 3.4 mM 10 mM 1.8 mM 1 l
TAE (modified: 0.01 mM EDTA); (Millipore)		1x
TFB 1 (Transformation Buffer 1); pH 5.8 (adjust with acetic acid); sterile filtered	10 mM MES (pH 6.2) (Roth) 100 mM RbCl (Sigma) 10 mM $CaCl_2$ x 2 H_2O (Sigma) 50 mM $MnCl_2$ x 4 H_2O (Sigma) ad dH_2O	5 ml (1M) 6.05 g 0.74 g 4.94 g 500 ml
TFB 2 (Transformation Buffer 2); pH 6.5 (adjust with KOH); sterile filtered	10 mM MOPS (Roth) 10 mM RbCl (Sigma) 75 mM $CaCl_2$ x 2 H_2O (Sigma) 87 % Glycerol (v/v) (Merck) ad dH_2O	1 ml (1M) 0.12 g 1.1 g 17.24 100 ml
TNE; pH 7.4	NaCl EDTA Tris-HCl	140 mM 1 mM 20 mM
Wash buffer	DMEM BSA HEPES	 0.1% 20 mM

2.1.2 Solutions

name	components	concentration/amount
Agarose Gel	SeaKem® LE Agarose (Biozym) TAE mod.	2%
Collagenase solution (sterile filtered)	collagenase type IV DMEM	250 mg 100 ml

name	components	concentration/amount
Embedding medium	Mowiol (Sigma) dH_2O Glycerine (87%) (Merck) Tris/Cl, pH 8.5 DABCO (Sigma)	2.4 g 6 ml 6 g 12 ml 100 mg
Fixer (for silverstain)	Photofixer ad dH2O	120 ml 500 ml
Goat serum (5%)	dried goat serum H_2O PBS (1 x) BSA	 1 ml 38 ml 0.4 g
NED-reagent	boric acid (Sigma) dH_2O H_2SO_4 (conc.) NED (Sigma) Brij-35 (10%) (Pierce) ad dH_2O	2.5 g 300 ml 111 ml 300 mg 1.5 ml 500 ml
o-Phtalaldehyde	dH_2O H_2SO_4 (conc.) o-Phtalaldehyde (Sigma) Brij-35 (10%) (Pierce) ad dH_2O	400 ml 37 ml 100 mg 1.5 ml 500 ml
Paraformaldehyde (3%)	PFA (Merck) 3M KOH PBS (10x) H_2O	6 g 200 µl 20 ml 180 ml
Reducer (for silverstain)	Citric acid Formalin 37% ad dH_2O	50 mg 0.7 ml 1000 ml
Silver nitrate solution	Solution A: $AgNO_3$ dH_2O Solution B: NaOH, 1M Ammoniak, 25 % dH_2O add solution A dropwise in solution B. ad dH2O	1.55 g 8 ml 3.8 ml 2.8 ml 38.2 ml 200 ml
Triton-X-100 (0,2 %)	PBS (1x) Triton-X-100	500 ml 1 ml

2.1.3 Media

name	components	concentration/amount
Bactoagar	Agar (BD Biosciences) Kanamycin Ampiciline	2% 50 µg/ml 100 µg/ml
Cell culture medium	DMEM (Gibco) FCS Penicillin/Streptamycin solution; (PAA)	500 ml 1% 5 ml
HepaRG growth medium	Williams E (Gibco) FCS (Biochrom) Hydrocortison (50 µM) (Sigma) Penicillin/Streptamycin solution; (PAA) Insulin (5 µg/ml) (Sigma)	500 ml 50 ml 250 µl 5 ml 250 µl
HepaRG differentiation medium	see "HepaRG growth medium" plus 2.5- 10 ml DMSO (Merck)	 0.5-2%

name	components	concentration/amount
HGM (Hepatocyte Growth Medium) (according to Block et al. 1996, modified)	DMEM	1 l
	ITS Mix; (Invitrogen)	10 ml
	BSA (Sigma)	2 g
	D(+)-Glucose (Merck)	2 g
	D(+)-Galactose (Merck)	2 g
	Ornithine (Sigma)	100 mg
	Proline (Sigma)	30 mg
	Nicotinamide (Sigma)	610 mg
	$ZnCl_2$ (Fluka)	1 ml
	$ZnSO_4$ x 7 H_2O (Sigma)	1 ml
	$CuSO_4$ x 5 H2O (Sigma)	1 ml
	$MnSO_4$ (Sigma)	1 ml
	Glutamax I (5M)*)	10 ml
	Dexamethasone (Sigma)	100 µl
	Gentamycine (50mg/ml); (Invitrogen)	2 ml
	Amphotericin B (250µg/ml); (Invitrogen)	1 ml
Incubation medium (immunostaining)	DMEM (without phenolred)	
	BSA	0.1%
LB medium	Bacto-Trypton	10 g
	Yeast extract	5 g
	NaCl	10 g
	ad dH2O	1 l

2.2 Chemicals

name	company
Antioxidant agent (SDS-PAGE)	Invitrogen
BSA fraktion V	Roth
Casein 1 % (solution in PBS)	Pierce
Chicken eryhrocytes	Labor Dr. Merk+Kollegen (Ochsenhausen)
Collagenase Typ I	Worthington
Collagen Typ I	BD Biosciences
Crystal violet	-
Dako OPD tablets	Dako
EDTA solution	Sigma
Ethidium bromide	Serva
FCS	Invitrogen
FCS plus	Pan
$MgCl_2$ (1 M)	Sigma
Matrigel™ Basement Membrane Matrix	BD Biosciences
Methylcellulose	Fluka
Perhydrol® 30 %	Merck
Peroxidase (from horseradish)	Sigma
SDS solution (10 %)	Sigma
Sucrose	Sigma
Trypan blau solution (0.4 %)	Sigma
TWEEN® 20	Merck

2.3 Inhibitors

2.3.1 Pharmacological inhibitors

name	used concentration	company
Bafilomycin A1	100 nM	Sigma (B1793)
Blebbistatin	100 µM	Sigma (B0560)
Brefeldin A	0.1 µg/ml	Sigma (B7651)
Cytochalasin D	5-100 µM	Sigma (C8273; C2618)
Dynasore	100 µM	Sigma (D7693)
EIPA	100 µM	Sigma (A3085)
Jasplakinolide	0.25-2 µM	Enzo (ALX-350-275-C100)
Methyl-ß-Cyclodextrin	1-10 mM	Sigma (C4555)
MG-132	20 µM	Sigma (C2211)
NH_4Cl	20 mM	Merck (168320)
Nocodazole	5-100 µM	Sigma (M1404)
Sucrose	0.125 M, 0.25 M, 0.5 M	Sigma (S0389)
Thapsigargin	1 µM	Sigma (T9033)

2.3.2 myr preS1-HBV peptide

The peptide was synthesized and purified by S. Urban (Department of Biomolecular Chemistry of the Center for Molecular Biology, Heidelberg).

2.4 Viruses

2.4.1 HBV

The virus preparations used in the present work were isolated from human HBV carrier plasma. All used ID´s were from genotype D:

ID*)	fraction	GE/ml	used GE
326	5	2,10E+10	5,25E+06
323	4	2,00E+10	2,00E+07
309	5	7,30E+12	5,48E+09
*) internal identification number			

2.4.2 HBsAg

ID*)	fraction	mg/ml
323	main fraction	~ 8.8
*) internal identification number		

2.4.3 Control viruses

name	reference address
Semliki Forest Virus (SFV)	kindly provided by Prof. Wengler; Gießen
Sendai virus (strain Z) (SeV)	kindly provided by Prof. S. Pleschka; Gießen
Simian Virus 40 (SV40)	D. Glebe

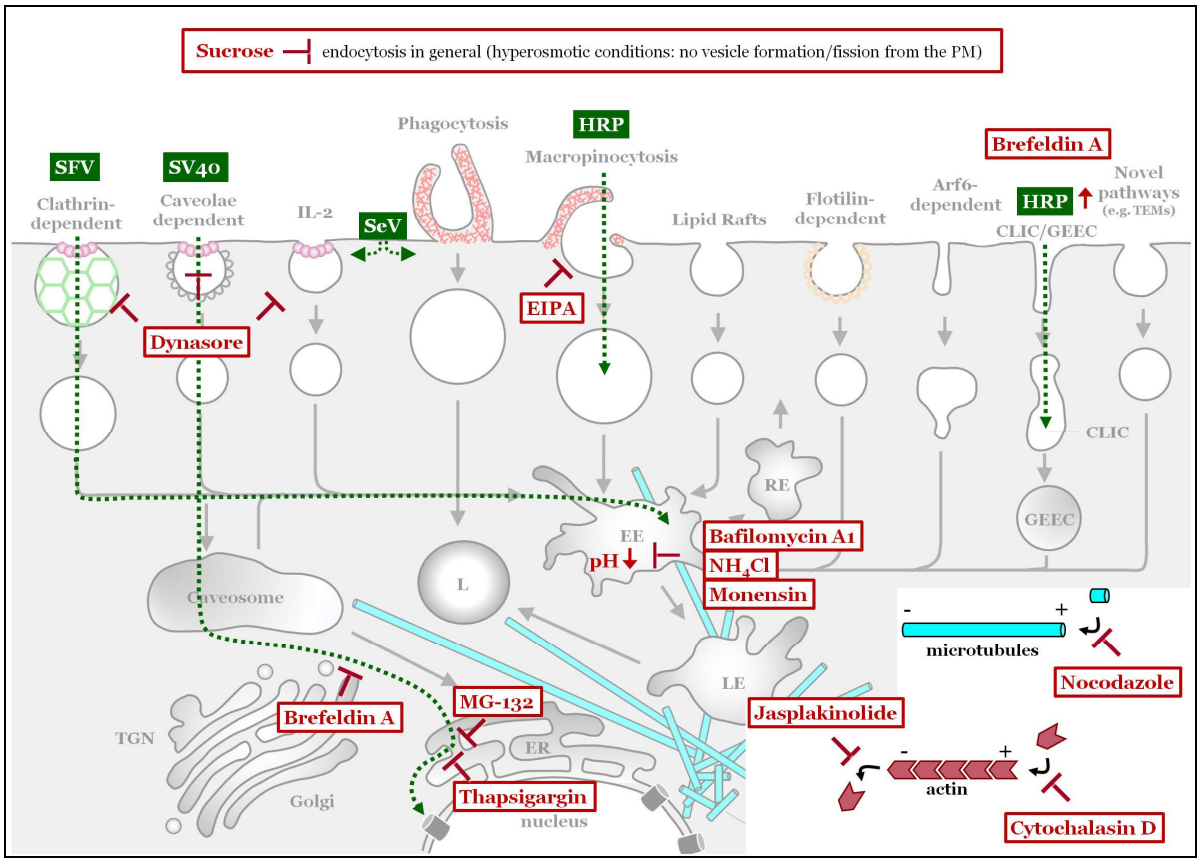

Figure 5: Summary of the control viruses with their respective entry pathways (green) and the pharmacological inhibitors used to block these mechanisms (red). HRP: horseradish peroxidase; PM: plasma membrane; SeV: Sendai Virus; SFV: Semliki Forest Virus; SV40: Simian Virus 40.

2.5 Cell Culture

2.5.1 Cell culture systems

name	company
6-well plates	BD Biosciences
12-well plates	BD Biosciences
24-well plates	BD Biosciences
96-well plates	BD Biosciences
96-well plates (round bottom)	Thermo Scientific
ibidi slides	Ibidi

2.5.2 Cells

2.5.2.1 Primary *Tupaia* hepatocytes (PTH)

For the different infection as well as binding and uptake experiments PTH were freshly isolated. The animals are from the animal breed that is kept by the Institute of Anatomy and Cell Biology at the Justus-Liebig-University in Giessen.

2.5.2.2 HepG2

HepG2 cells were isolated from biopsy material of a human primary liver cancer (Aden et al. 1979). The parenchymal cells are HBV-DNA free and have differentiated liver cell functions.

2.5.2.3 HepaRG

HepaRG cells were isolated from a human primary liver cancer (Gripon et al. 2002). The cells are HBV-DNA free and were obtained from S. Urban (Centre for Molecular Biology, Heidelberg).

2.5.2.4 BHK

BHK21 cells were obtained from the kidneys of one day old hamsters (Macpherson and Stoker, 1961). The cells were purchased from ATCC.

2.5.2.5 CV-1

CV-1 is an epithelial cell line of African green monkey kidney origin (Jensen et al. 1964).

2.5.2.6 Huh-7

Human hepatoma cell line was established from a Japanese isolate (Nakabayashi et al. 1982).

2.5.2.7 HeLa

Cell line originating from a cervical biopsy of Henrietta Lacks whose initial two letters of first and last name were used for nomenclature (Gey 1952).

2.6 Antibodies and –sera

2.6.1 Primary antibodies and –sera

name	epitope	used concentration	reference address
anti-alpha tubulin*)	aa426-450	1:1000	abcam (7291)
anti-caveolin1*)	caveolin-1	1:200	Cell Signalling Technology (#3238)
anti-HBs biotin conjugate (Enzygnost® HBsAg 5.0)		1:100	Dade Behring
anti-HBcAg *)	HBcAg	0.05 mg/ml	Dako
anti-Sendai *)		1:200 [1)]	Prof. Garten; Marburg
anti-SFV **)	E1/E2-protein	1:200 [1)]	Prof. Wengler; Gießen
anti-SHBs (C20/2) **)	HBs-antigen loop (conformational)	1 µg/ml	Prof. Gerlich; Gießen
anti-Strep-POD **)	N-or C-terminal or internal Strep-tag II		IBA
anti-SV40 large T-antigen **)	within aa 83-123 of the large T-antigen	0.5 µg/ml	abcam (ab16879)

*) polyclonal; **) monoclonal; 1) original concentration unknown

2.6.2 Secondary antibodies

name	used concentration	company
Alexa Fluor 488 F(ab')$_2$ fragment of goat anti–mouse IgG	5 mg/ml	Invitrogen (A-11017)
Alexa Fluor 594 F(ab')$_2$ fragment of goat anti–mouse IgG	2.5 mg/ml	Invitrogen (A-11020)
Alexa Fluor 594 F(ab')$_2$ fragment of goat anti–rabbit IgG	2.5 mg/ml	Invitrogen (A-11072)
Streptavidin-POD	2 µg/ml	Dianova

2.7 Fluorescent dyes

name	used concentration	company
Alexa Fluor®647 phalloidin	160 nM	Invitrogen (A-22287)

2.8 DNA-and protein standards

name	company
pUC Mix Marker, 8	Fermentas
1 kb ladder	Invitrogen
Mark12 Protein Marker	Invitrogen

2.9 Plasmids

name	company/reference adress
pmax	Amaxa
pBs HBV 991 T7 Dimer	D.Glebe
pcX	D.Glebe

2.10 Commercial kits

name	company
Endofree Plasmid Maxi Kit	Qiagen
FuGene HD Transfection Reagent	Roche
High Pure Viral Nucleic Acid Kit	Roche
illustra™ MicroSpin™ S-400 HR Columns	GE Healthcare
LightCycler® FastStart DNA Master Hybridization Probes Kit	Roche
LightCycler® FastStart DNA MasterPLUS Hybridization Probes Kit	Roche
LightCycler® Capillaries	Roche
Mach1™ T1 Phage-Resistant (T1R) competent E. coli	Invitrogen
Mouse Hepatocyte Nucleofector Kit	Amaxa
Organelle Lights™ Endosomes-RFP	Invitrogen
pHrodo E.coli BioParticles	Invitrogen
Thermocycler Capillary Mix	Thermo Scientific
TSA™ Kit with HRP–goat anti-mouse IgG and Alexa Fluor® 647	Invitrogen

2.11 PCR

2.11.1 X-PCR

The serum ID259 from a chronic HBV carrier (genotype D) was used as standard (U. Wend, personal communication).

2.11.2 cccDNA-PCR

The used standard plasmid “pBs HBV plasmid 991 T7 Dimer” was generated by cloning a HBV complete genome-dimer from pUC991 (HBV genotype A2) into the pBluescript II SK

vector (Stratagene). It was freshly diluted (10^7-10^0 GE) for each PCR run. Unreactive virion-derived HBV DNA from plasma ID259 (see above) and additionally H_2O served as negative controls.

2.11.3 SV40-PCR

Urine from a BK-virus carrier was used as standard (provided by Ch. Schüttler, Diagnostic Laboratory, Institute of Medical Virology, Giessen).

2.11.4 Primer and Hybridisation probes (Hybprobes)

Primer and Hybprobes for the X-and ccc-PCR were purchased from TIB MOLBIOL, SV40-PCR primer were provided by the Diagnostic Laboratory (Institute of Medical Virology, Giessen).

X-PCR	**primer**		
	X2 sense	5´-gacgtcctttgtytacgtcccgtc	(nt 1413-1436)
	X2 antisense	5´-tgcagagttgaagcgaagtgcaca	(nt 1519- 1601)
	Hybprobes		
	3FL XB Hyprobe	5´-acggggcgcacctctctttacgcgg-FL	(nt 1519- 1543)
	3LC XB Hyprobe	LC Red 640-ctccccgtctgtgccttctcactgc-PH	(nt 1545- 1570)
		Y = C / T	
ccc-PCR	**primer**		
	C1 sense	5'- tgcacttcgcttcacct	(nt 1580- 1596)
	C1 antisense	5'- aggggcatttggtggtc	(nt 2314- 2298)
	Hybprobes		
	3FL CB Hybprobe	5'- caatgtcaacgaccgacctt—FL	(nt 1678- 1697)
	5LC CB Hybprobe	5'- LC Red 640- aggcmtacttcaaagactgtktgt—PH	(nt 1699- 1722)
		m = A / C ; k = G / T	
SV40-PCR	**primer**		
	Pol1 sense	5´-taggccytcaatggttag	
	Pol1 antisense	5´-ggttggggccatcttc	

2.11.5 Mastermixes

Enlisted Mastermix compositions count per test (10 µl in total) and are mixed with 10 µl (11 µl in case of SV40-PCR) purified DNA sample.

X-PCR	3 µl	H_2O
	1 µl (10 pmol/µl)	X2 sense
	1 µl (10 pmol/µl)	X2 antisense
	0.5 µl (8 pmol/µl)	3FL XB Hyprobe
	0.5 µl (8 pmol/µl)	5LC XB Hyprobe
	4 µl	Fast Start Plus Taq Polymerase
ccc-PCR	3.4 µl	H_2O
	1.6 µl	$MgCl_2$
	1 µl (10 pmol/µl)	C1 sense
	1 µl (10 pmol/µl)	C1 antisense
	0.5 µl (8 pmol/µl)	3FL CB Hybprobe
	0.5 µl (8 pmol/µl)	5LC CB Hybprobe
	2 µl	Fast Start Taq Polymerase
SV40-PCR	1 µl	Pol1 sense
	1 µl	Pol1 antisense
	11 µl	Thermo-Fisher Capillary Mix

3. Methods

3.1 Cell culture

3.1.1 Isolation of PTH

For each infection as well as binding and uptake assay PTH were freshly isolated. The isolation was carried out according to the two-step-collagenase-method (Seglen 1976). The animal was aerated for 5 min with CO_2 according to the animal protection guidelines. After a negative eye reflex-test the animal´s death was assured by cervical dislocation. To dispose of coarse dirt particles and microbial contamination of the fur, the animal was shortly put in 70% ethanol. Subsequently, the animal was placed with his back on a polystyrene pad and fixed on all limbs.

After removing the fur from the abdomen and thorax, the abdomen was opened along the linea alba. The chest was removed and the liver including the portal vein (*Vena portae*) was uncovered. The vein was punctuated with a needle (22G, Braunüle, Vasocan) and its plastic tube was fixed with a small hemostat. The liver was perfused via a peristaltic pump with 5 mM EGTA/HBSS for 20 min. The solution was free of calcium ions to destabilize cell-cell contacts and to prevent thrombosis of the hepatic capillaries. Successful perfusion was identified by brightening of the liver lobes. The liver was dissected and placed on a suction filter and further perfused with HBSS without EGTA for 10 min and then with a sterile filtered collagenase solution. With this solution, the liver was perfused in a recirculation system until the liver capsules became porous.

The liver was transferred to a sterile cell culture dish and, after removal of the gall bladder, minced with scalpels. To finalize liver dissection, the tissue pieces were incubated with the collagenase solution in an Erlenmeyer flask (shaking with ~85 rpm) for 10-15 min at 37°C.

For removal of non-perfused liver parts, the suspension was filtered through sterile gauze. The following steps were performed on ice and with ice cold materials. The filtrate was equally divided in four Falcon tubes (BD Biosciences) and then centrifuged (4°C, 40*g*, 6 min), resulting in selective sedimentation of hepatocytes. Supernatants, containing mainly other cell types, were discarded and the pellets were resuspended in 10 ml DMEM, then further 30 ml DMEM were added. This washing step was repeated two times. After the third centrifugation, the hepatocytes were resuspended in 20-40 ml HGM with 10% FCS. To check cell viability a trypan blue-test was performed. 10 µl cell suspension was mixed with 10 µl trypan blue on a glass slide and covered with a coverslip. After a successful isolation the viability of the cells is usually around 90-95%. Depending on the density of the cell suspension 2-3 drops were plated in 12-well cell culture dishes coated with Matrigel, resulting in about 10^5 hepatocytes per well. For binding and uptake assays, the cells were plated on coated coverslips (in 12-well dishes), for cccDNA assays in 6-well plates which were also coated with Matrigel. After 4 h at 37°C (5% CO_2), the cells had attached. In order to achieve optimal re-differentiation of the hepatocytes, the FCS-containing medium was

removed and replaced by HGM (hepatocyte growth medium) without FCS. The cells were stored at 37°C (5% CO_2) until the experiments were performed.

3.1.2 Cultivation of stable cell lines

3.1.2.1 BHK21, CV-1, HeLa, HepG2, Huh-7

All stable cell lines were cultivated in 1-5% FCS/DMEM (37°C, 5% CO_2) and splitted regularly before reaching a confluent state.

3.1.2.2 HepaRG

The hepatocyte precursor cell line HepaRG was differentiated to hepatocyte-/and epithelial-like cells in a two-step process (König 2010). After being confluent, the cells were passaged three times with high cell density and finally seeded on coverslips, where they were cultured for 14 days in 1 ml growth medium with regular medium changes (every 2-3 days). For differentiation, the cells were cultivated in growth medium containing 1-2% DMSO (differentiation medium) for further 2 weeks with regular medium changes.

3.2 Virus preparation

3.2.1 HBV

Isolation and purification of HBV and HBsAg from plasma of chronically infected patients was done as described previously (Glebe et al. 2003; Grün-Bernhard 2008). Briefly, 30 ml HBV-positive plasma was layered on a sucrose cushion consisting of 6 ml 15% sucrose and 2 ml 10% sucrose and ultracentrifuged for 18 h at 25,000 rpm at 10°C (SW 28.38 rotor; Beckman). The pellet, containing viral and subviral particles, was resuspended in 1 ml cold TNE and loaded on a discontinuous sucrose density gradient (15, 25, 35, 45 and 60% [wt/wt]/TNE) and again ultracentrifuged for 15 h (see above). The gradient was fractionated and the sucrose density of each fraction was determined with a refractometer. The concentration of virions was calculated as HBV genome equivalents (GE/ml) in virus-containing fractions (40-45% sucrose) and determined by quantitative real-time PCR (LightCycler, Roche) using primers and hybridization probes against the HBV X-region as described previously (Jursch et al. 2002). Subviral HBsAg particles (fractions containing 35-40% sucrose) were analyzed by SDS-polyacrylamid gelelectrophoresis (SDS-PAGE) and subsequent silver staining.

3.2.2 SFV

SFV was purified from infected cell culture supernatants by S. Broehl.

3.2.3 SV40

CV-1 cells were cultivated in 5% FCS until they formed a confluent monolayer. Infection was done with 150 µl cell culture supernatant-derived SV40 in 1% FCS. When the cells showed first apoptotic signs, the supernantants were collected, viral genomes were purified ("High Pure Viral Nucleic Acid Kit", Roche) and tested via PCR.

3.2.4 SeV

Stock solutions containing activated SeV (strain Z) was kindly provided by Prof. S. Pleschka, Institute of Medical Virology, JLU Giessen.

3.3 Hemagglutination (HA)-assay

SeV has the ability to agglutinate erythrocytes. To determine the SeV-titer a HA-assay was performed in a 96-well microtiter plate (round bottom). With 2 µl virus stock a serial twofold dilution series was made in PBS and applied to an equal volume of a 1% chicken erythrocytes solution (Donald and Isaacs 1954). The plate was stored for 1 h at 4°C. The dilution, at which still a complete agglutination occurred, equates to the HA-titer. The calculated HA-titer of the stock was 640/ml which corresponds to $6.4*10^9$ virions/ml.

3.4 Plaque assay

3.4.1 SFV

To determine the plaque-forming units per milliliter (PFU/ml) of SFV, BHK cells were seeded in a 12-well plate and cultivated for 20 h with 1% FCS/DMEM. The confluent monolayers were inoculated with 150 µl of a serial tenfold dilution of the virus stock (1 µl-0.00001 µl) for 1 h at 37°C. After three washing steps with wash buffer, the cells were overlaid with 1 ml 1% methylcellulose/ 1% FCS/DMEM and incubated 48 h at 37°C. Then, the cellulose medium was removed; the cells were gently washed twice with PBS and finally fixed with 3% PFA (30 min, room temperature). After washing once with H_2O, the cells were stained with 1% crystal violet solution for 5 min, washed again with H_2O and dried at room temperature before the plaques were counted. The PFU/ml was determined using following formula: PFU/ml = number of plaques x dilution factor x conversion to 1 ml. The calculated PFU was $2*10^9$/ml.

3.5 Horseradish peroxidase (HRP)-Assay

HRP was used as control substrate for cellular fluid phase uptake. PTH were preincubated with different pharmaceutical inhibitors (30 min at 37°C) or with HBV (30 min/60 min at 4°C). Afterwards, the cells were replaced on ice, 0.025 mg/ml HRP was added and the cells were shifted again to 37°C for 3 h. Finally, the cells were washed five times (on ice with icecold wash buffer) and scraped off in 0.5 ml 0.1% Triton-X-100/PBS and centrifuged

(4°C, 5000*g*, 10 min). The pellets were discarded, 5 µl of the supernatants was pipetted into a microtiter plate and OPD-substrate (o-phenylenediamine; 100 µl) was added (room temperature, in the dark). After approx. 3 min the colouring reaction was stopped with 50 µl 0.5 M H_2SO_4, the extinction was measured photometrically at 492 nm (reference-wavelenght: 620 nm).

3.6 Competent bacteria

2 ml of an E.coli Mach1 (Invitrogen)-overnight culture were mixed with 40 ml LB-medium and incubated at 37°C (shaking) until the bacterial suspension reached an OD_{550} of approx. 0.45. Afterwards, the culture was stored on ice for 15 min and henceforeward kept at 4°C. The bacteria were centrifuged (2500 rpm, 15 min), the pellet was resolved in 2 ml cold TFB1. 14 ml TFB1 were added, followed by a further incubation on ice (15 min). After another centrifugation (see above), the pellets were resuspended in 1.6 ml cold TFB2, incubated on ice again (15 min) and finally aliquoted and stored at -70°C. The competence of the bacteria for taking up plasmids was tested in a control transformation with the pcx-plasmid conferring resistance against ampicillin.

3.7 Transformation

50 µl of the competent bacteria were thawed on ice, 50-100 ng of the desired plasmid DNA was added and the mixture was incubated for 20 min at 4°C. After heat shock (42°C, 30-45 sec) and incubation (2 min, on ice), 950 µl LB-medium were added (incubation for 1 h at 37°C; shaking). The bacteria were subsequently pipetted on LB-agar plates containing adequate antibiotics and were stored upside down overnight at 37°C.

3.8 Plasmid isolation

Preparation of pmaxGFP-plasmid DNA was performed with the “EndoFree Plasmid Maxi Kit” (Qiagen) according to the manufacturer´s instructions.

3.9 Transfection

3.9.1 FuGene

PTH-transfection was performed 2 days after isolation (see Roche manual) using a 4:2 ratio (FuGene:DNA). The cells were incubated 48 h at 37°C and GFP-expression was checked microscopically.

3.9.2 Amaxa

Freshly isolated PTH (in suspension) were directly transfected with the Nucleofector®Device (courtesy of Prof. Rümenapf, Institute of Virology, Giessen) using the

"Mouse Hepatocyte Nucleofector Kit" (program "T-028") according to the procedure outline. GFP-expression was checked after 48 h.

3.9.3 Baculovirus-mediated transduction

PTH were transduced with the BacMam reagent (Organelle Lights™ Endosomes RFP, Invitrogen) the day after isolation according to the manufacturer´s instructions. Rab5-expression was examined 48 h afterwards.

3.10 Binding and uptake studies

3.10.1 HBsAg

The HBsAg binding and uptake assays in PTH were performed analogous to the infection assays 2-3 days after isolation. PTH were washed icecold and incubated with 8ng purified HBsAg (2 h; 4°C). Afterwards, the cells were washed three times on ice and the different chemical inhibitors were added for 15-30 min. The 4°C- approaches were directly fixed on ice. The other cells were shifted to 37°C for 2 h in the continous presence of the inhibitors, fixed and stained for HBsAg using an anti-SHBs antibody. In some HBsAg-binding samples (4°C) the actin-cytoskeleton was additionally stained using "Alexa Fluor®647-Phalloidin".

3.10.2 Phagocytosis

In order to examine the phagocytic potential of PTH, the cells were incubated with pHrodo E.coli BioParticles (Invitrogen) and HBsAg to examine whether colocalisation occurs. On day 3 after isolation, PTH were washed once and incubated with 40 µg pHrodo particles and ~8 ng purified HBsAg per coverslip for 2 h at 37°C, washed thrice and fixed. pHrodo conjugates are non-fluorescent outside the cell but fluoresce brightly inside acidic cellular compartments (product manual) therefore an extra immunostaining was not necessary. HBsAg was stained similar to the binding and uptake samples.

3.11 Infection assays

3.11.1 HBV

The experimental setup of the infection assays is depicted in Fig. 6. After isolation, PTH were cultivated for 2-3 days in 600 µl HGM. The cells were preincubated with different chemical inhibitors (for 15-30 min at 37°C; see "Material" for the used concentrations). Subsequently, the cells were infected with different amounts of purified HBV virions from sera of chronic patients depending on the ID (see "Material"). The infection was blocked by addition of HBV myr preS1-peptide (100 nM) after 4 h, in case of HBsAg-assay with subsequent ELISA, or after 20 h p.i., when cccDNA of incoming viral particles was examined. The cells were washed three times. For the HBsAg-assay, the infected hepatocytes were cultivated for 14 days with regular medium-changes (600 µl HGM) every

3-4 days. Detection of newly produced HBsAg in the cell culture supernatants was done with an "in-house" sandwich-ELISA (see below). For cccDNA detection, the cells were lysed directly after the infection.

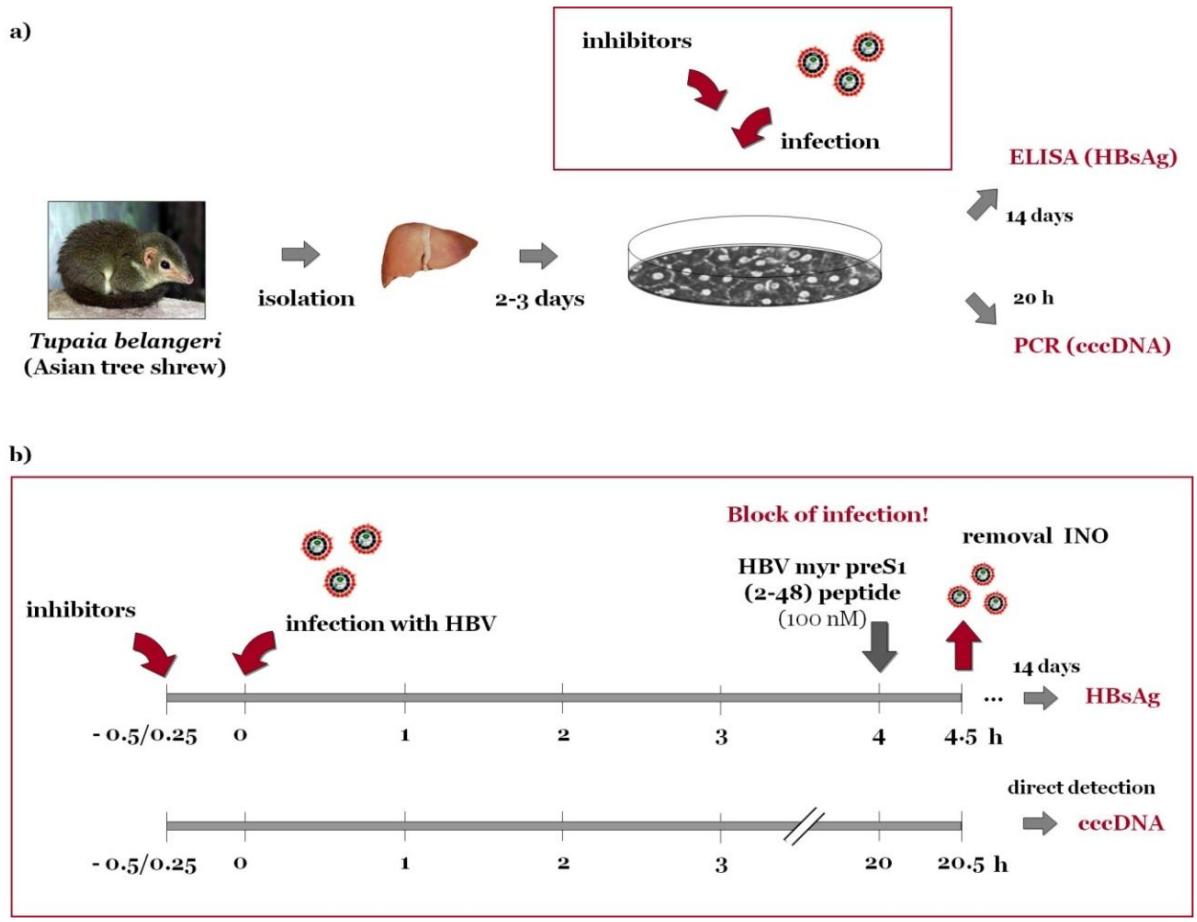

Figure 6: Model system and experimental setup.

a) After isolation of the liver, the hepatocytes were plated and cultivated for 2-3 days. 15-30 min before infection the cells were preincubated with different chemical inhibitors. A resulting infection was determined by detection of secreted HBsAg and cccDNA after 14 days and 20 h respectively. A detailed view of the infection period (red rectangle) is depicted in b).

b) After the preincubation, the cells were infected with HBV for 4 h (HBsAg-assay) or 20 h (cccDNA). The infection was blocked by addition of HBV myr preS1-peptide. The cells were washed and either further incubated for 14 days (HBsAg-assay) or directly lysed for cccDNA detection.

3.11.1.1 cccDNA isolation and Hirt extraction

cccDNA of incoming viruses was isolated from infected PTH. All steps were performed on ice and with icecold materials. PTH were washed twice with PBS scraped off in 1 ml PBS. The cells were pelleted by centrifugation (2000 rpm, 2 min), the supernatants were discarded. 200 µl cell-lysis buffer were added, the tubes were gently vortexed and centrifuged (see above). The supernatants were discarded, the pellets (containing the nuclei) were frozen at -70°C. After thawing the pellets on ice, viral cccDNA was isolated by "Hirt-extraction" (Hirt 1969). 400 µl SDS/EDTA [0.6% (w/v)/10 mM EDTA] were added to the pellets and gently mixed. After 20 min at room temperature, NaCl (5 M; 100 µl) was added (the chromosomal DNA precipitated). The samples were stored for 20 h at 4°C and

then centrifuged (4°C, 14,000 rpm, 4 min). Supernatants comprising the viral cccDNA were additionally purified with the "High Pure Viral Nucleic Acid Kit" (Roche), before being applied in the PCR.

3.11.1.2Urea-Test

As hepatocytes are the only cells producing urea, this organic compound was used to determine the viability of the PTH after each HBV infection assay. PTH-supernatants (100 µl) were pipetted into a microtiter plate and 75 µl o-Phtalaldehyde and 75 µl NED-reagent were added. After 5 min at room temperature, the plate was measured photometrically at 492 nm (reference-wavelenght: 620 nm). The obtained values were allocated with the amount of secreted HBsAg (ELISA).

3.11.2 SFV

BHK cells were seeded on glass coverslips and were grown for 20 h in 1% FCS/DMEM until they reached a confluency of about 70-80%. Similar to HBV infection or HBsAg binding and uptake assays, PTH were infected with SFV 2-3 days after isolation. The cells were washed once with wash buffer, then preincubated with different chemical inhibitors for 15-30 min at 37°C and infected with a MOI of 10 for 1 h (BHK) or with a MOI of 1000 (PTH) for 4 h at 37°C. The cells were washed twice with wash buffer, once with glycin-buffer (pH 2.2) and finally three times with wash buffer. All washing steps were performed on ice and with icecold buffers. After an additional incubation period of 4 h at 37°C the cells were fixed with 3% PFA and subsequently stained for newly synthesized viral E1/E2-protein.

3.11.3 SV40

CV-1 cells were plated on glass coverslips until they were 70-80% confluent after growing 20 h in 1% FCS/DMEM. The cells were washed once (wash buffer) and preincubated with chemical inhibitors (15-30 min; 37°C). Then, the cells were infected with 3.00E+03 GE for 10 h in the continous presence of the inhibitors. The cells were washed three times on ice with icecold wash buffer and then fixed with 3% PFA. For immunostaining, a monoclonal anti-large T- antigen antibody was used.

3.11.4 SeV

CV-1 cells were grown to a confluency of 70-80% with 1% FCS/DMEM, washed once with wash buffer, preincubated with the distinct chemical inhibitors and infected with approx. 10^7 virions for 8 h. The cells were washed thrice with cold wash buffer on ice, fixed and finally immunostained with an anti-SeV antiserum.

3.12 ELISA

96-well microtiter plates were coated with 100µl (1µg/ml) anti-HBs-antibody (C20/2) for 48 h at 4°C. The following and all subsequent washing steps were done with an automatic ELISA washer (Tecan). The used program consisted of four washing steps (2x 0.1% tween/PBS and 2x PBS; 300 µl each). The wells were blocked with 10% FCS/TNE (200 µl/well; 2 h at 37°C, shaking). After washing, 100 µl cell culture supernatants of infected cells were pipetted into the wells. For quantification, purified HBsAg served as standard and was diluted in 1% caseine/PBS (10-0.3 ng/ml HBsAg). The plates were incubated for 20 h at 4°C. Before and after incubation with a biotinylated anti-HBs-antibody (1:100 in 0.1% casein/PBS; 100µl; 1 h at 37°C, shaking) the plates were washed again. Streptavidine-POD was added (1:500 in 0.1% casein/PBS; 100 µl; 0.5 h at 37°C, shaking) the plates were washed and 100 µl OPD-substrate were added (room temperature, in the dark). The reaction was stopped with 50 µl 0.5 M H_2SO_4. Extinction of the colored substrate was measured photometrically at 492 nm (reference-wavelenght: 620 nm).

3.13 Immunostaining

At the end of the infection, binding and uptake studies, the cells were fixed with 3% PFA, permeabilized with 0.2% Triton-x-100 and blocked with 5% goat-serum. All steps were performed at room temperature for 30 min with 1-2 washing steps in between. Primary antibodies were incubated for 1.5 h at 37°C. Before and after the incubation with the secondary antibodies for 1 h at 37°C, the cells were washed five times. For nucleus-staining, the cells were incubated with DAPI for 5 min at room temperature, washed five times and finally mounted on a glass slide using Mowiol.

All immunostained samples were analyzed with a Leica TCS SP5 confocal microscope.

3.14 PCR

Viral DNA was purified with the "High Pure Viral Nuceleic Acid Kit" (Roche) according to the manufacturer´s manual and then applied in the PCRs.

3.14.1 X-PCR

Table 1: LightCyler program for the X-PCR:

	Activation	Amplification			Meltingcurve			Cooling
Cycles	1	45			1			1
Type	Regular	Quantification			Melting Curve			Regular
Target Temp. (°C)	95	95	62	72	95	50	95	40
Incubation Time	10 min.	10"	15"	13"	10"	15"	0"	30"
Temp. Transition Rate (°C)	20	20	20	5	20	20	0,1	20
Second Target Temp. (°C)			50°					
Step Size			1					
Step Delay			1					
Acquisition Mode	none	none	single	none	none	none	cont.	

3.14.2 cccDNA-PCR

The used PCR specifically discriminates between cccDNA and genomic DNA due to primer that bind before and after the nick-and-gap structure and an optimized protocol with rapid temperature changes (Glebe et al. 2003).

Table 2: LightCycler program for the ccc-PCR:

	Activation	Amplification			Meltingcurve			Cooling
Cycles	1	45			1			1
Type	Regular	Quantification			Melting Curve			Regular
Target Temp. (°C)	95	95	57	72	95	50	95	40
Incubation Time	10 min.	10"	20"	32"	10"	20"	0"	30"
Temp. Transition Rate (°C)	20	20	20	5	20	20	0,1	20
Second Target Temp. (°C)			50°					
Step Size			1					
Step Delay			1					
Acquisition Mode	none	none	single	none	none	none	cont.	

3.14.3 SV40-PCR

Table 3: LightCyler program for the SV40-PCR:

	Activation	Amplification				Meltingcurve			Cooling
Cycles	1	45				1			1
Type	Regular	Quantification				Melting Curve			Regular
Target Temp. (°C)	95	95	63	72	81	95	60	92	40
Incubation Time	15 min.	9"	8"	13"	1"	10"	15"	0"	30"
Temp. Transition Rate (°C)	20	20	20	5	20	20	20	0,1	20
Second Target Temp. (°C)			51°						
Step Size			1						
Step Delay			1						
Acquisition Mode	none	none	none	none	single	none	none	cont.	none

3.14.4 Agarose gel electrophoresis of PCR products

After the PCR runs, the capillary contents were centrifuged into an Eppendorf tube, mixed with 6x SDS-containing Agarose-samplebuffer and loaded on a 2% agarose gel (with ethidium bromide). pUC Mix 8 DNA marker was used for the cccDNA-and the SV40-gel. The separation was carried out at 150V for 30 min.

4. Results

4.1 HBsAg binding and uptake in PTH

To study the early events of HBV infection, the binding and uptake characteristics of purified HBV subviral particles (HBsAg) in PTH were examined at first.

Fig. 7 shows immunostaining of HBsAg after incubation of purified subviral particles with PTH at 4°C. HBsAg strongly bound to cellular membrane protrusions (a, open arrowheads) and, to a lesser extent, to non-protruding structures on the cellular surface. However, not all hepatocytes were equally covered with HBsAg, instead an uneven distribution within the hepatocyte population was observed. In some cases one cell bound HBsAg and its next neighbor not (b and c, open arrowheads). Furthermore, on the single-cell-level the HBsAg-signal showed a distinct staining pattern in certain membrane patches. There was no noticeable attachment of HBsAg to bile canaliculi which are thin tubes formed at the lateral surfaces between adjacent hepatocytes that can be visualized by actin staining (c, grey arrowhead). Besides a binding to PTH, also an uptake into vesicular-like compartments was observed after warming to 37°C (d and e, full arrowheads).

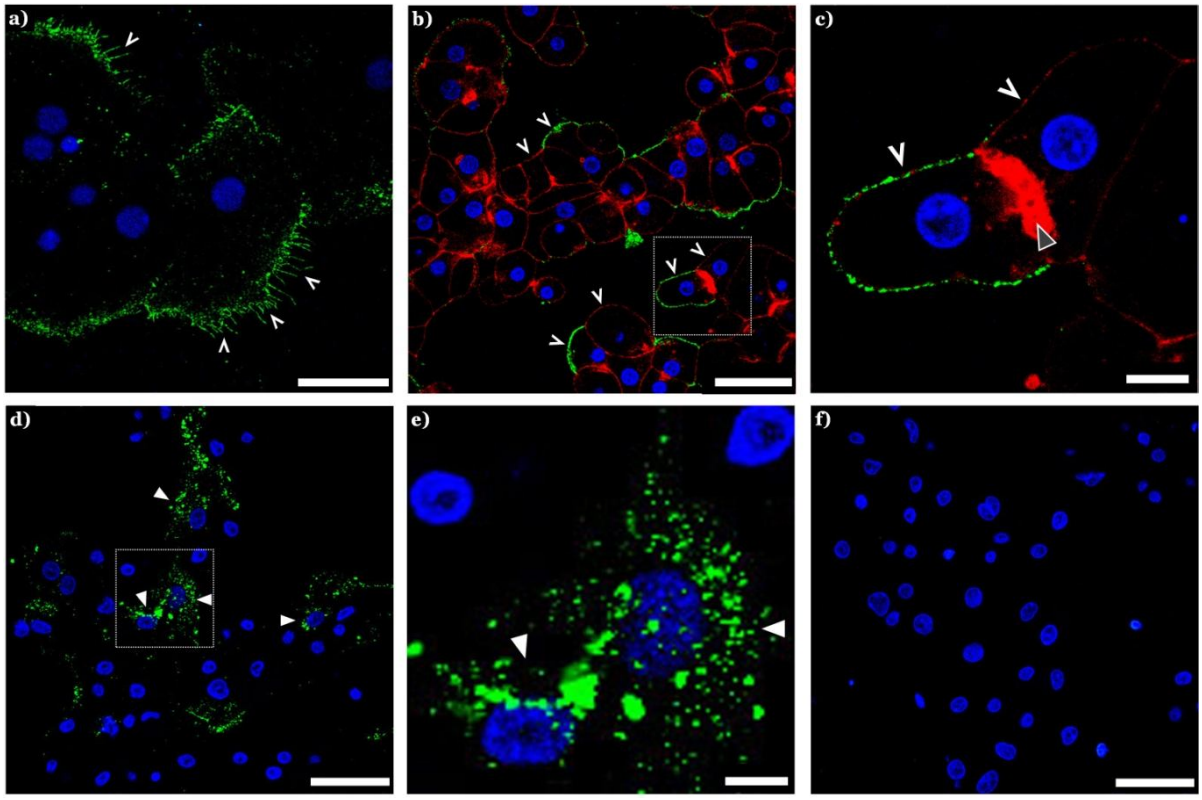

Figure 7: Binding and uptake of HBsAg subviral particles by PTH. The cells were incubated with HBsAg (8ng) at 4°C for 2 h and either fixed directly (4°C, a-c) or shifted to 37°C for 2 h (d+e) before immunostaining for SHBs (green) and actin (red) as well as DAPI-staining of nuclei (blue) was performed. f) negative control without HBsAg. Scale bars: a) 25 µm, b, d, f) 50 µm, c + e) 10 µm.

4.2 Endocytosis vs. plasma membrane fusion of HBV and control viruses

To learn more about the entry of HBV into PTH, certain viruses with different well-known uptake pathways were used as controls. The results from these experiments were compared with HBV.

4.2.1 Semliki Forest Virus (SFV)

SFV, an enveloped *Alphavirus*, is known to be internalized from the cell surface by CME (Helenius et al. 1980; Glomb-Reinmund and Kielian 1998).

SFV infects many different cell types, including PTH (Fig. 8c and d). A striking different staining pattern of newly synthesized viral surface proteins was observed in the two cell types: in BHK (baby hamster kidney) cells the E1/E2-proteins are distributed within the complete cytoplasm with larger accumulations in the vicinity of the nuclei (a and b), whereas in PTH they are mainly located directly below the plasma membrane or in close proximity to the nucleus (d).

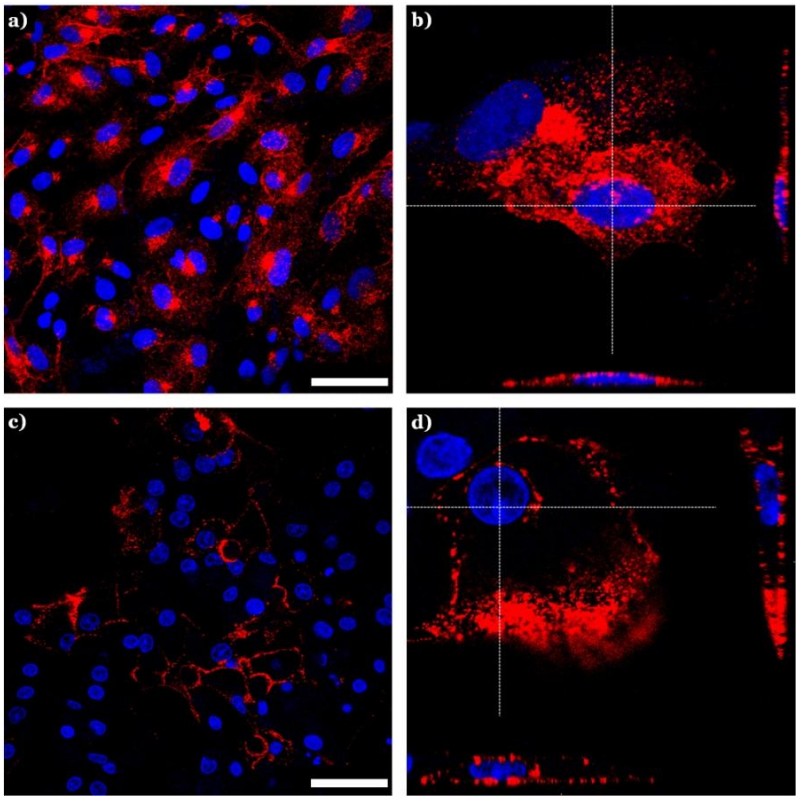

Figure 8: Semliki Forest Virus infects BHK and PTH. Th cells were incubated with MOI 10 (BHK) or MOI 1000 (PTH) and stained for newly produced viral E1/E2-protein (red) after 5 h p.i. (BHK) and 8 h p.i. (PTH) respectively. a) BHK (b: z-stack image), c) PTH (d: z-stack image). Nuclei (blue). Scale bars: 50µm.

4.2.2 Simian Virus 40 (SV40)

The unenveloped SV40 is a well-studied member of the *Polyomaviridae* (Pelkmans et al. 2001). The entry process of SV40 begins with the adsorption of the virion to MHC class I molecules on the cellular surface (Stang et al. 1997; Norkin 1999) before being internalized via caveolar/lipid raft-mediated endocytosis (Anderson et al. 1996; Pelkmans et al. 2001). In cells devoid of cav-1 the virus uses a different, lipid raft-dependent pathway which also leads to a productive infection (Damm et al. 2005). To investigate whether PTH could also be infected with SV40, the cells were inoculated with 3.00E+03 GE (genome equivalents) for 72 h and subsequently immunostained for SV40 early large T-antigen expression. Fig. 9 shows that in contrast to CV-1 cells (a) SV40 infection was not supported by PTH (b). For this reason SV40 could unfortunately not be used as a direct control for e.g. caveolin-mediated entry in PTH. Nevertheless it was utilized at least in CV-1 cells to analyze potential inhibitory effects on the entry of unenveloped viruses and to prove the impact of certain pharmaceutical inhibitors on special cellular entry routes (see chapter “4.7 Retrograde pathway”).

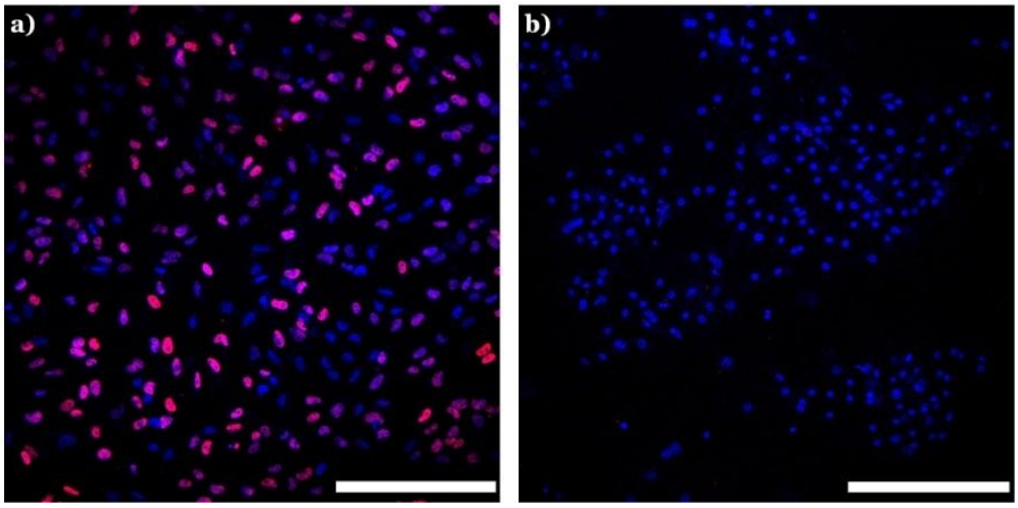

Figure 9: SV40 infects CV-1 cells but not PTH. Cells were infected with 3.00E+03 GE SV40 for 10 h (CV-1) or 72 h (PTH) following detection of early large T-antigen expression (red) by immunostaining. DAPI-staining of nuclei (blue). a) CV-1 cells, b) PTH. Scale bars: 250 µm.

4.2.3 Sendai Virus (SeV)

Fusion of the enveloped SeV (*Paramyxoviridae*, Genus *Respirovirus*) occurs directly at the plasma membrane (PM) at neutral pH (Bossart 2010). SeV is a common pneumotropic pathogen that is endemic in many rodent colonies in the world (Faisca and Desmecht 2007). In natural infections, SeV replicates primarily in the respiratory epithelium but since the viral hemagglutinin-neuraminidase (HN) binds to sialic acid-containing gangliosides, which are ubiquitously expressed on the surface of all eukaryotic cells, other organs are potentially permissive for infection (Ito et al. 1983; Bitzer et al. 1997). Fig. 10 demonstrates that in vitro, besides CV-1 cells, also PTH can be infected with SeV, though with less productivity. In both cases virtually all cells show a cytoplasmic staining of newly synthesized viral proteins.

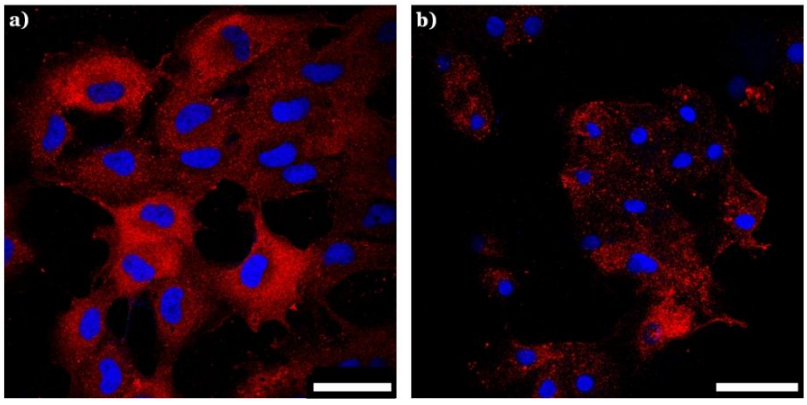

Figure 10: SeV infects CV-1 cells and PTH. Cells were infected with 10^7 virions for 8 h and stained for newly produced SeV proteins using a polyclonal anti-SeV antiserum (red). DAPI-staining of nuclei (blue). a) CV-1 cells, b) PTH. Scale bars: 50 µm.

4.2.4 Inhibitors used to block certain cellular endocytic steps

Medium containing high concentrations of sucrose was used to differentiate between endocytosis and direct fusion with the PM as possible mechanism for HBV entry. The above-mentioned viruses served as controls. Transient treatment with hypertonic sucrose prevents CME due to dispersion of CCPs on the PM (Heuser and Anderson 1989). To test whether this has any effect on SFV infection in BHK and PTH, the cells were preincubated with different sucrose concentrations (0.125 M, 0.25 M and 0.5 M) and subsequently infected with the virus. Fig. 11 and 12 show that in both cell types a dose-dependent inhibition of the SFV infection occurred. It is noteworthy that in PTH, even when no inhibitors are present, only approx. 30% of the cells are infected with SFV.

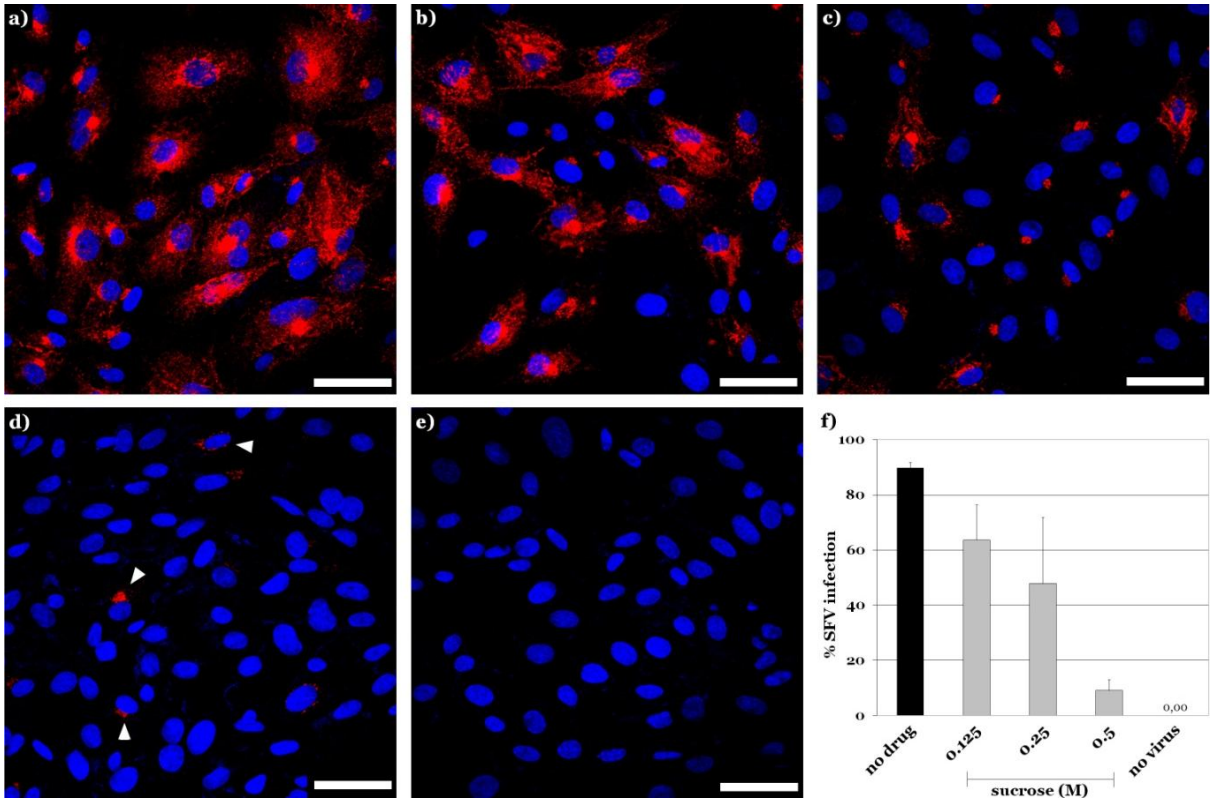

Figure 11: Dose-dependent inhibition of SFV infection of BHK cells by sucrose. The cells were preincubated with different sucrose concentrations (15 min, 37°C) and subsequently infected (MOI 10). The cells were fixed 5 h p.i. and newly synthesized SFV E1/E2-protein (red) and nuclei (blue) were stained. a) untreated cells without inhibitor, b) 0.125 M sucrose, c) 0.25 M sucrose, d) 0.5 M sucrose, e) uninfected control. f) Three randomly chosen fields were analyzed for the amount of E1/E2 positive cells. Data are expressed as percentage ± SD of E1/E2 positive cells in untreated cells. Scale bars: 50µm.

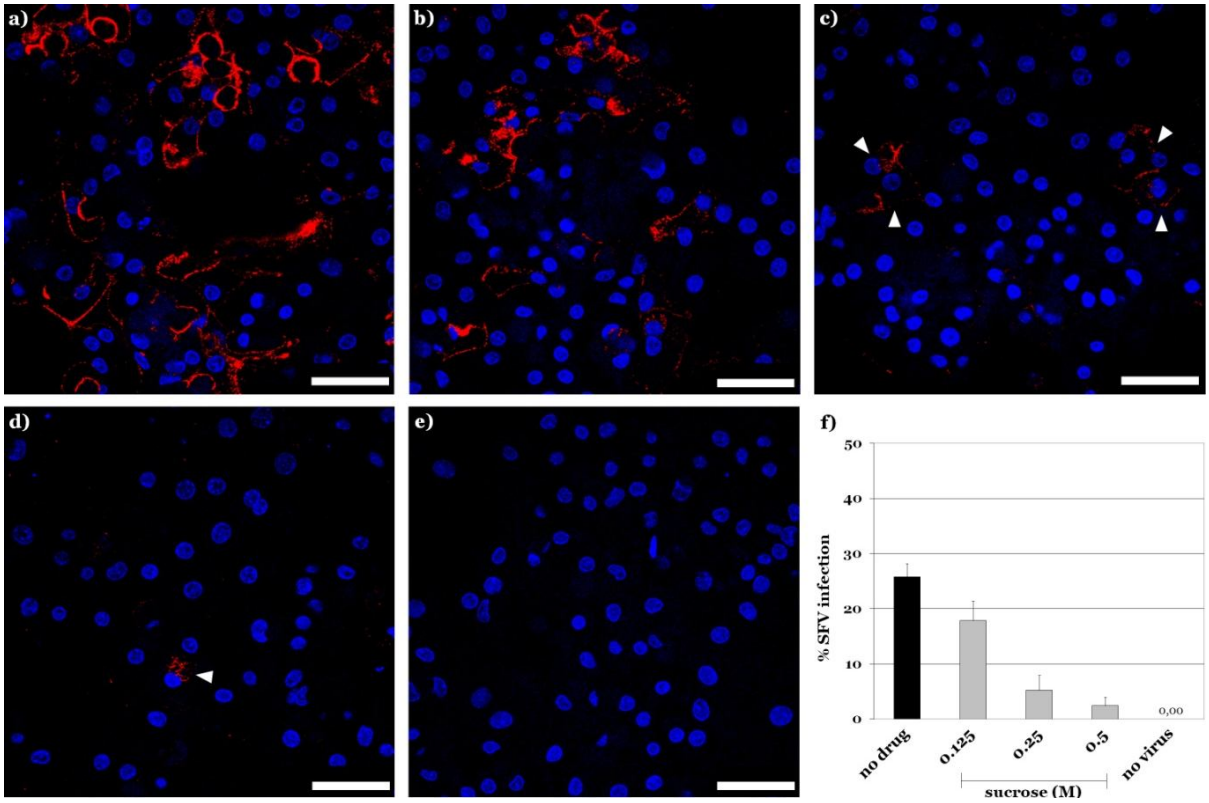

Figure 12: Sucrose inhibits SFV infection of PTH in a dose-dependent manner. The cells were preincubated with different sucrose concentrations (15 min, 37°C) and subsequently infected (MOI 1000). The cells were fixed 8 h p.i. and newly synthesized SFV E1/E2-protein (red) and nuclei (blue) were stained. a) untreated cells without inhibitor, b) 0.125 M sucrose, c) 0.25 M sucrose, d) 0.5 M sucrose, e) uninfected control. f) Three randomly chosen fields were analyzed for the amount of E1/E2 positive cells. Data are expressed as percentage ± SD of E1/E2 positive cells in untreated cells. Scale bars: 50µm.

It is known by now that treatment with sucrose does not constrict CME alone but also affects clathrin-independent (CI)-uptake and endocytosis in general (Nieland et al. 2005; Ivanov 2008). Using similar concentrations of hypertonic sucrose, the SV40 infection was also affected (Fig. 13) with a virtually complete reduction at 0.5 M sucrose (d).

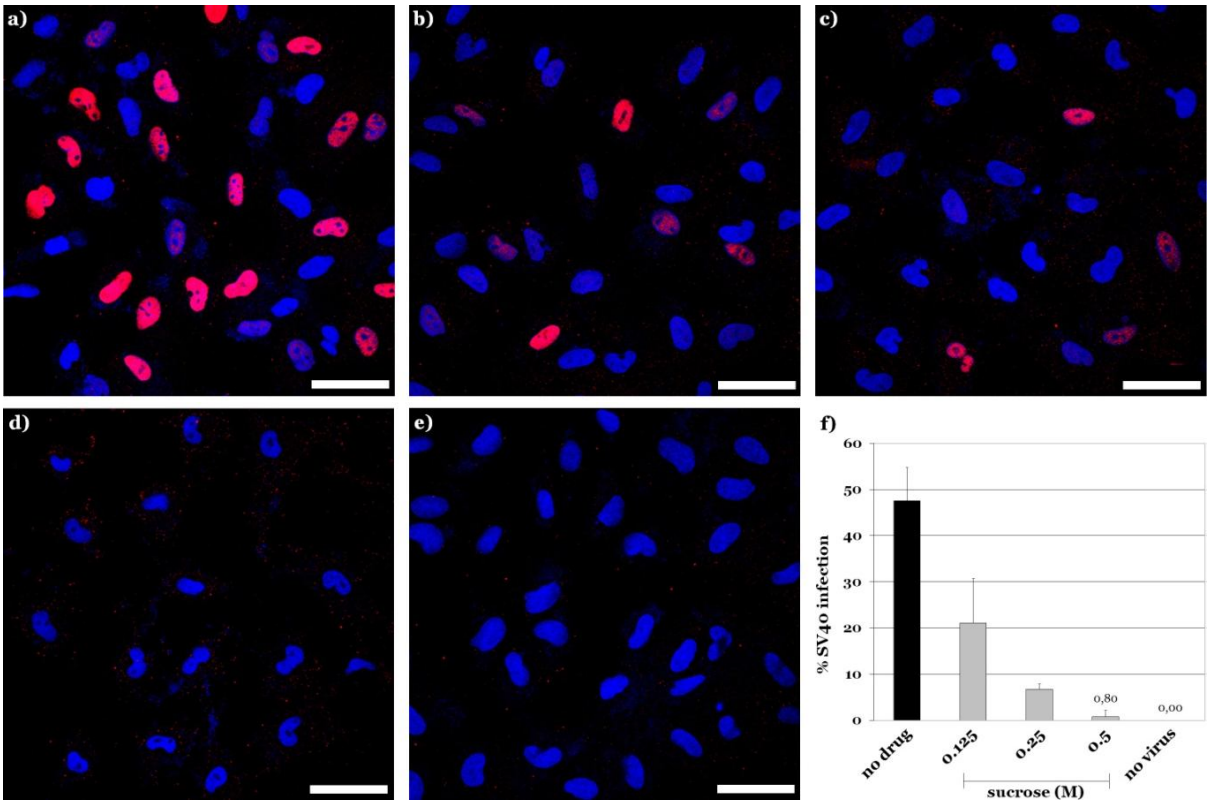

Figure 13: Inhibition of SV40 infection in CV-1 cells by sucrose. Cells were preincubated with different sucrose concentrations (15 min, 37°C), subsequently infected with 3.00E+03 GE SV40 and stained for early large T-antigen expression (red) and nuclei (blue). a) untreated cells without inhibitor, b) 0.125 M sucrose, c) 0.25 M sucrose, d) 0.5 M sucrose, e) uninfected control. f) Five randomly chosen fields were analyzed for the amount of cells expressing large T-antigen. Data were expressed as percentage ± SD of T-antigen expression in untreated cells. Scale bars: 50µm.

In contrast, SeV infection was not impaired in CV-1 cells or in PTH (Fig. 14 and 15). Even at the highest sucrose concentration of 0.5 M all cells are infected to a certain extent. The only visible difference in comparison with the positive control is a more punctuated pattern rather than a smooth staining throughout the complete cytoplasm (Fig. 14d and Fig. 15d).

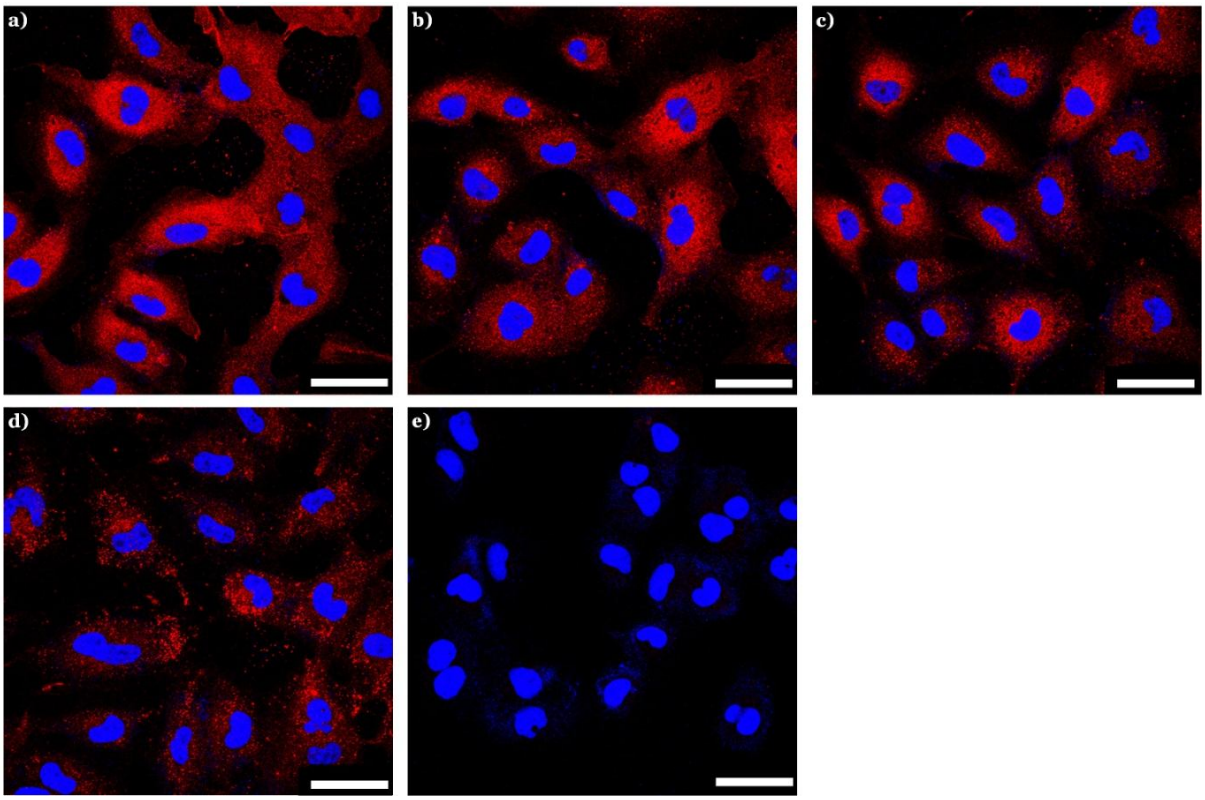

Figure 14: Hypertonic sucrose does not inhibit SeV infection of CV-1 cells. Cells were preincubated with different sucrose concentrations (15 min, 37°C), subsequently infected with 10^7 virions and stained for newly produced SeV proteins (red) and nuclei (blue) 10 h p.i. a) untreated cells without inhibitor, b) 0.125 M sucrose, c) 0.25 M sucrose, d) 0.5 M sucrose, e) uninfected control. Scale bars: 50µm.

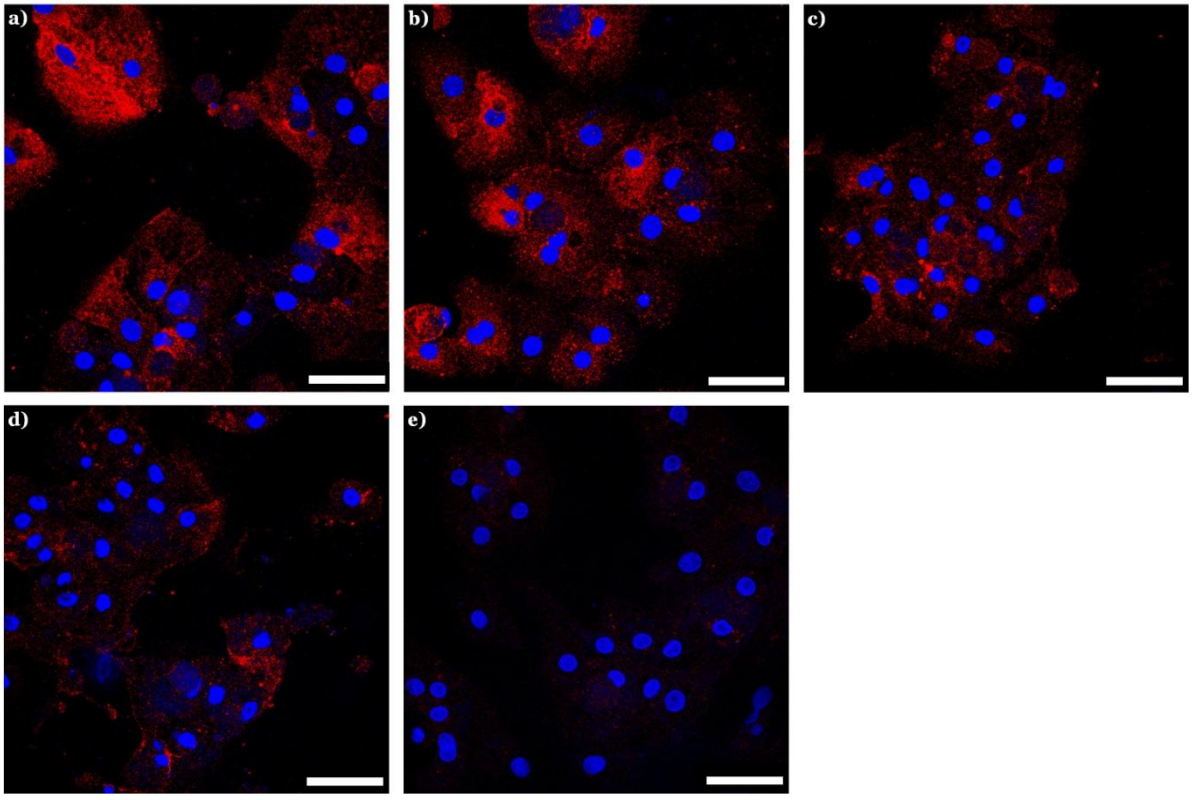

Figure 15: Hypertonic sucrose does not inhibit SeV infection of PTH. Cells were preincubated with different sucrose concentrations (15 min, 37°C), subsequently infected with 10^7 virions and stained for newly produced SeV proteins (red) and nuclei (blue) 10 h p.i. a) untreated cells without inhibitor, b) 0.125 M sucrose, c) 0.25 M sucrose, d) 0.5 M sucrose, e) uninfected control. Scale bars: 50 µm.

Next, the effect of sucrose on uptake of HBsAg was studied by confocal microscopy. PTH with prebound HBsAg (4°C) were exposed to different hypertonic sucrose concentrations and shifted to 37°C for additional 2 h. Afterwards, the cells were fixed and subviral particles were immunostained with an anti-SHBs antibody. Fig. 16 illustrates cut views through z-stack-images of single cells. Even after 2 h at permissive temperature for endocytosis a certain amount of HBsAg still remained bound at the plasma membrane (open arrowheads). However, also vesicular-shaped staining inside the cells could be observed (full arrowheads) the number of which was reduced with increasing sucrose concentrations. Full inhibition of uptake was observed at 0.5 M sucrose. The inhibitory effect of hypertonic sucrose treatment on HBsAg uptake had direct effect on HBV infectivity for PTH. Infection was inhibited with hypertonic medium in a dose-dependent manner (Fig. 17) as determined by detection of cccDNA formation of incoming virus particles after 20 h (a) and newly secreted HBsAg after 14 days (b).

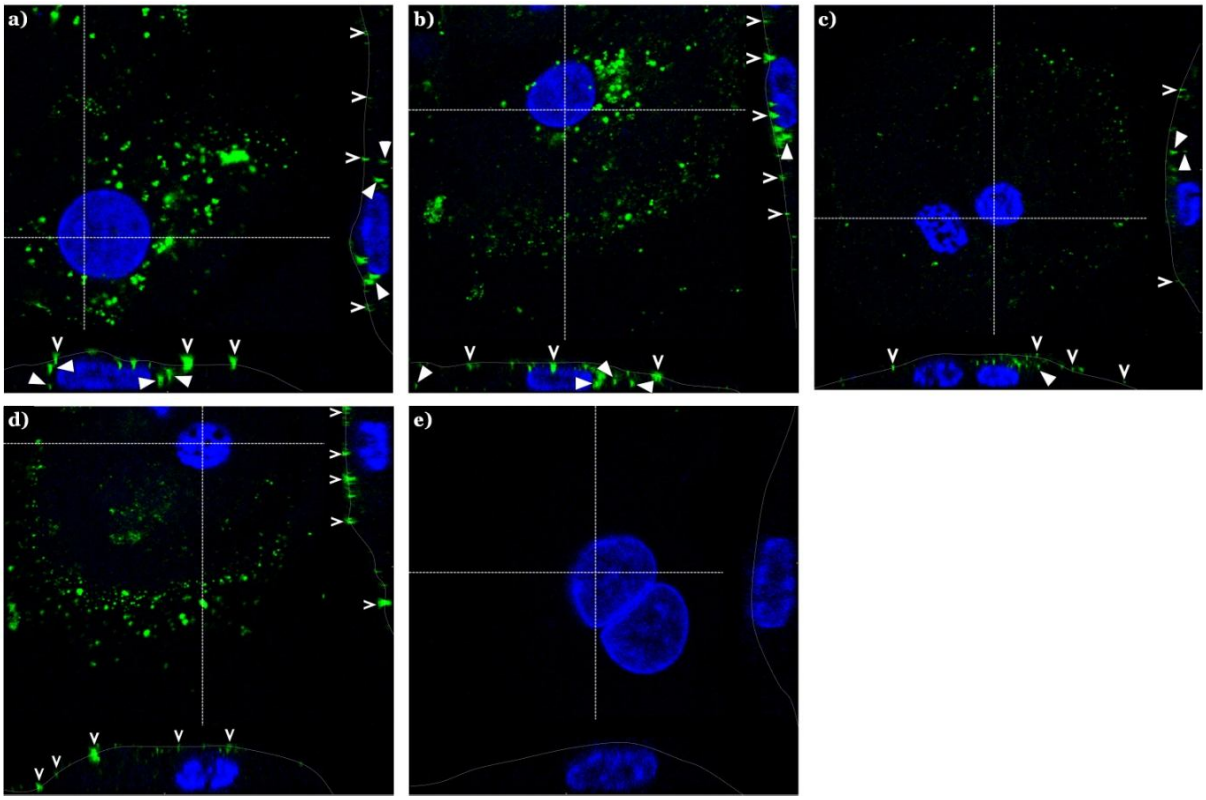

Figure 16: HBsAg uptake in presence of hypertonic sucrose. PTH were preincubated with 8ng HBsAg (4°C, 2 h) before different sucrose concentrations were added and the cells were shifted to 37°C for 2 h. The cells were stained for SHBs (green) and nuclei (blue). a) untreated cells without inhibitor, b) 0.125 M sucrose, c) 0.25 M sucrose, d) 0.5 M sucrose, e) negative control without HBsAg. Confocal images show a cut view through z-stack-images of single cells.

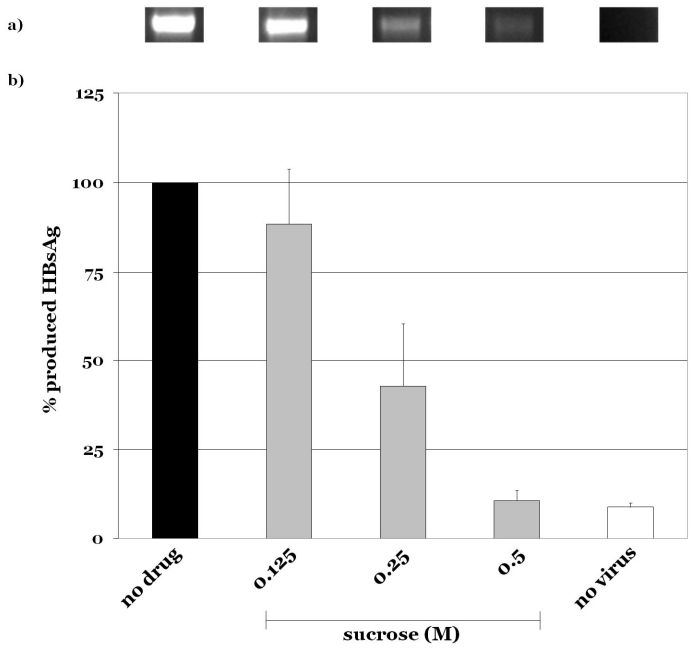

Figure 17: Effect of sucrose on HBV infection of PTH. The cells were preincubated with different sucrose concentrations (15 min, 37°C) and afterwards infected with purified plasma-derived HBV virions (2,00E+07 GE). cccDNA-formation of incoming HBV particles was determined 20 h p.i. by PCR and detected by gel electrophoresis (a). Newly secreted HBsAg was measured 14 days p.i. (b). Data in b) represent the average ± SD of three independent experiments. Cellular viability was checked via measurement of secreted urea (the positive control without sucrose was set as 100% viability) and revealed smaller effects than on infectivity: 0.125 M (77%), 0.25 M (68%) and 0.5 M (59%).

4.3 Dynamin-dependent endocytosis

4.3.1 Clathrin-mediated endocytosis

CME is a very important endocytic mechanism with an absolute requirement for dynamin (Doherty and McMahon 2009). Since 2007, a novel specific inhibitor of dynamin is available: Dynasore interferes with the GTPase activity of dynamin and was shown to block dynamin-dependent internalization of transferrin, a known cargo of CME (Macia et al. 2006). Fig. 18 illustrates that SFV infection was completely abolished when BHK cells were preincubated with Dynasore (b). The same was true for PTH (Fig. 19b) showing that also in these cells the GTPase activity of dynamin was completely inhibited with this drug.

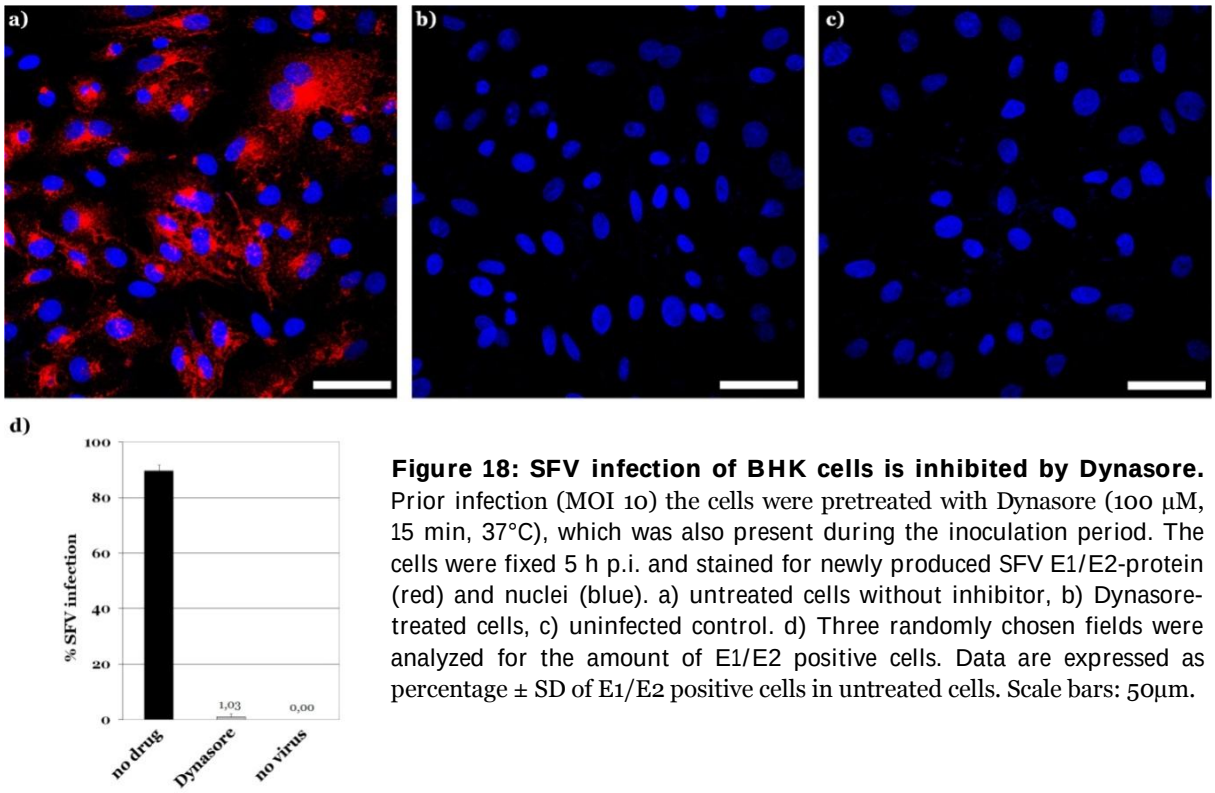

Figure 18: SFV infection of BHK cells is inhibited by Dynasore. Prior infection (MOI 10) the cells were pretreated with Dynasore (100 µM, 15 min, 37°C), which was also present during the inoculation period. The cells were fixed 5 h p.i. and stained for newly produced SFV E1/E2-protein (red) and nuclei (blue). a) untreated cells without inhibitor, b) Dynasore-treated cells, c) uninfected control. d) Three randomly chosen fields were analyzed for the amount of E1/E2 positive cells. Data are expressed as percentage ± SD of E1/E2 positive cells in untreated cells. Scale bars: 50µm.

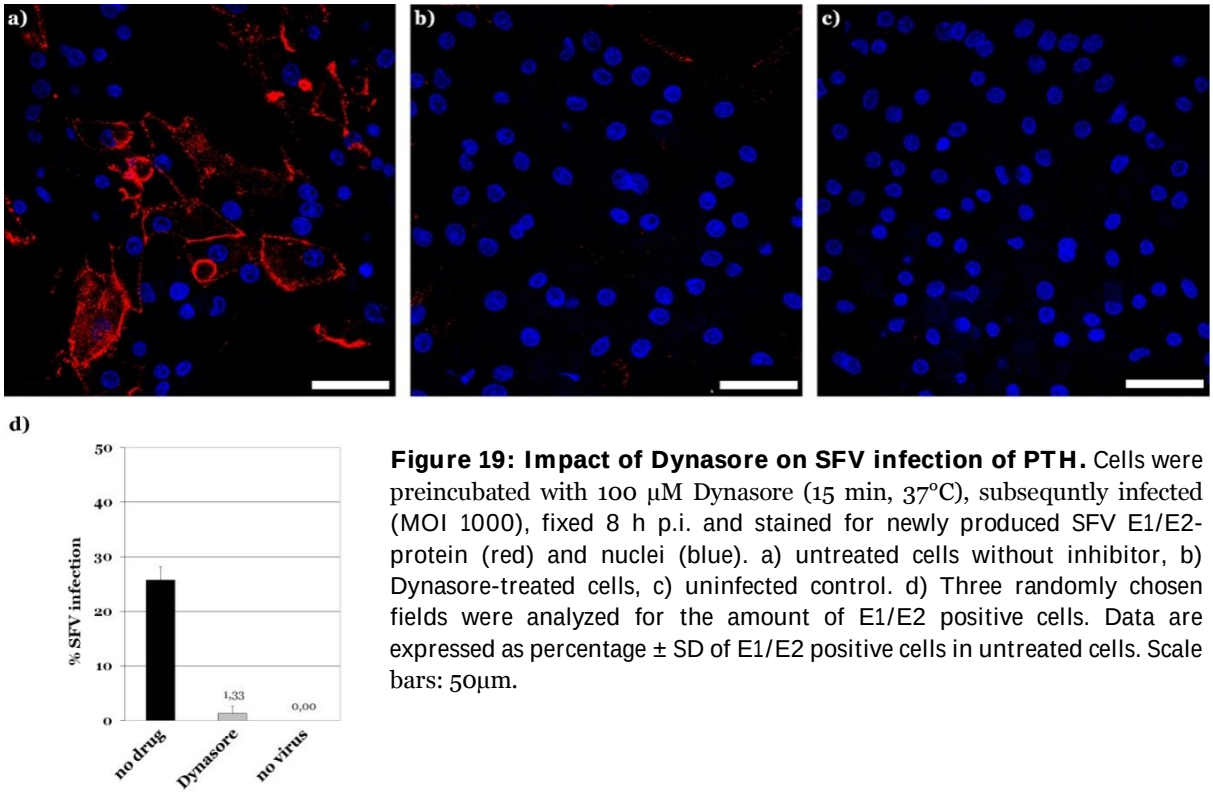

Figure 19: Impact of Dynasore on SFV infection of PTH. Cells were preincubated with 100 µM Dynasore (15 min, 37°C), subsequntly infected (MOI 1000), fixed 8 h p.i. and stained for newly produced SFV E1/E2-protein (red) and nuclei (blue). a) untreated cells without inhibitor, b) Dynasore-treated cells, c) uninfected control. d) Three randomly chosen fields were analyzed for the amount of E1/E2 positive cells. Data are expressed as percentage ± SD of E1/E2 positive cells in untreated cells. Scale bars: 50µm.

SV40 infection is dependent on dynamin when using the caveolae-mediated endocytosis into target cells. Using Dynasore to inhibit the GTPase activity of dynamin in CV-1 cells, SV40 infection was drastically reduced (Fig. 20) confirming earlier results with dominant negative-dynamin II (Pelkmans et al. 2002). In contrast to this, the direct fusion of SeV with the plasma membrane was shown to be independent of the activity of dynamin since the infection was not impaired by Dynasore (Fig. 21 and 22).

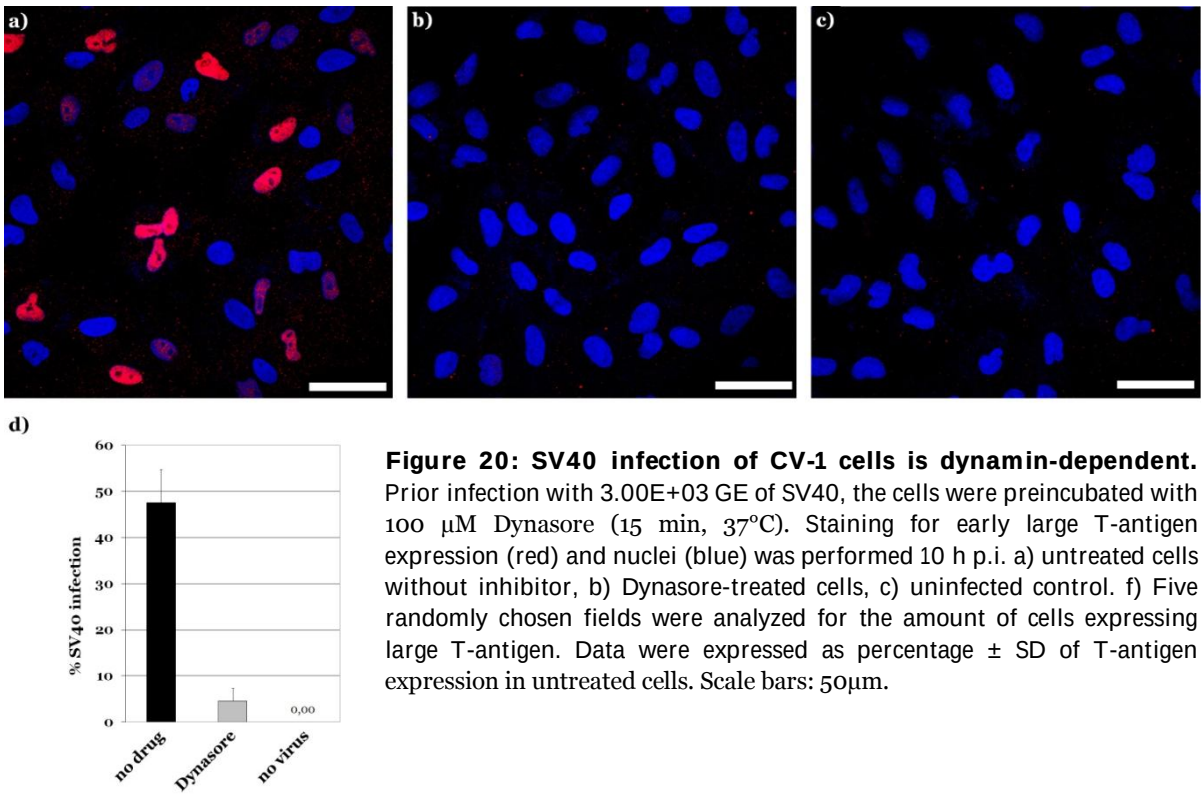

Figure 20: SV40 infection of CV-1 cells is dynamin-dependent. Prior infection with 3.00E+03 GE of SV40, the cells were preincubated with 100 µM Dynasore (15 min, 37°C). Staining for early large T-antigen expression (red) and nuclei (blue) was performed 10 h p.i. a) untreated cells without inhibitor, b) Dynasore-treated cells, c) uninfected control. f) Five randomly chosen fields were analyzed for the amount of cells expressing large T-antigen. Data were expressed as percentage ± SD of T-antigen expression in untreated cells. Scale bars: 50µm.

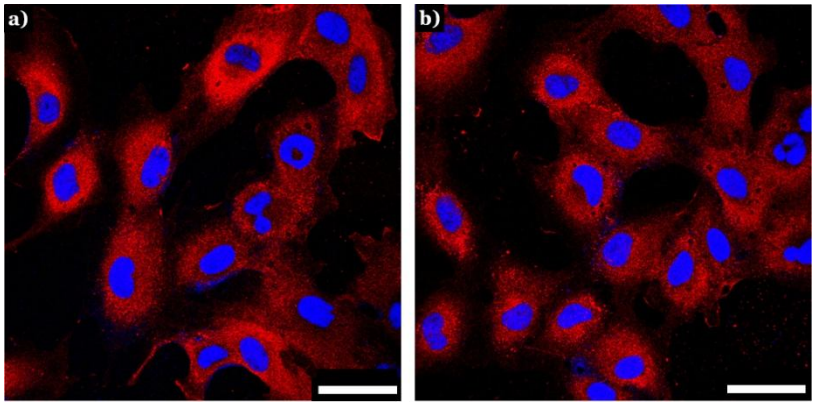

Figure 21: Dynamin-independent SeV infection of CV-1 cells. The cells were preincubated with Dynasore (100 µM) before being inoculated with 10^7 virions and stained for newly produced SeV proteins (red) and nuclei (blue) 10 h p.i. a) untreated CV-1 cells without inhibitor, b) Dynasore-treated CV-1 cells. Scale bars: 50 µm.

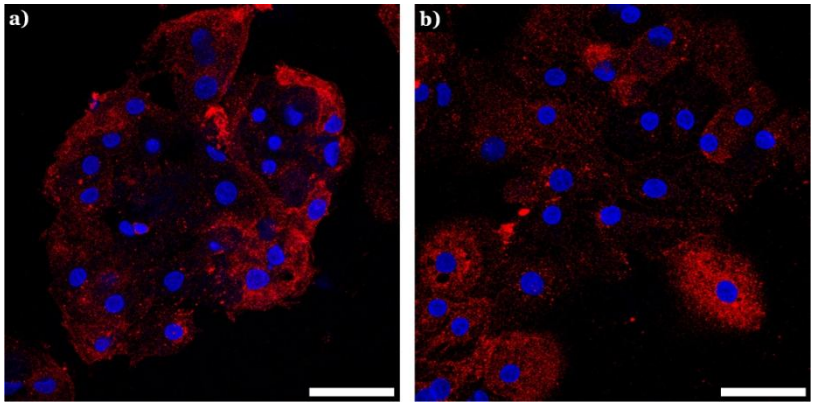

Figure 22: Dynamin-independent SeV infection of PTH. PTH were preincubated with Dynasore (100 µM) before being inoculated with 10^7 virions and stained for newly produced SeV proteins (red) and nuclei (blue) 10 h p.i. a) untreated PTH without inhibitor, b) Dynasore-treated PTH. Scale bars: 50 µm.

Both, the direct uptake of HBsAg and HBV infection in PTH were not affected by Dynasore as vesicular accumulations were visible inside the cytoplasm (Fig. 23b, full arrowheads) and the markers of HBV infection (secreted HBsAg and cccDNA) showed no difference in comparison with the positive control (Fig. 24).

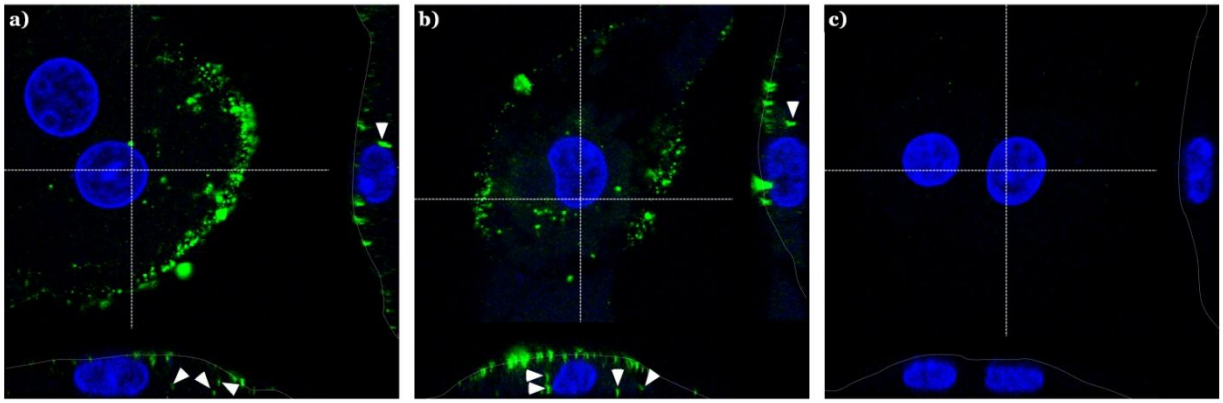

Figure 23: HBsAg uptake in presence of Dynasore. PTH were preincubated with 8 ngHBsAg (4°C, 2 h) before 100 µM Dynasore was added and the cells were shifted to 37°C for 2 h. The cells were stained for SHBs (green) and nuclei (blue). a) untreated cells without inhibitor, b) Dynasore-treated cells, c) negative control without HBsAg. Confocal images show a cut view through z-stack- images of single cells.

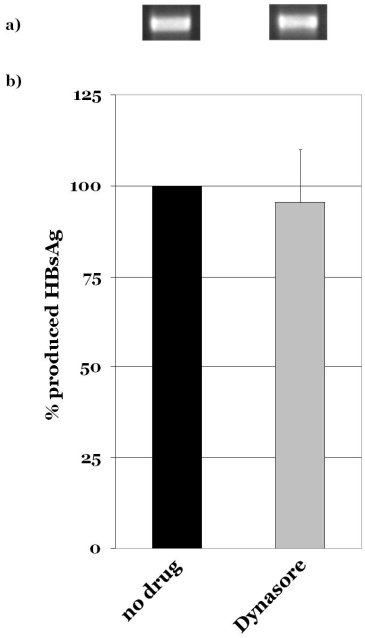

Figure 24: HBV infection of PTH in presence of Dynasore. The cells were preincubated with Dynasore (100 µM, 15 min, 37°C) and afterwards infected with purified plasma-derived HBV virions (2,00E+07GE). cccDNA-formation of incoming viral particles was determined 20 h p.i. by PCR and detected by gel electrophoresis (a). Newly secreted HBsAg was measured 14 days p.i. (b). Data in b) are means of triplicate experiments ± SD.

4.3.2 Caveolin-mediated uptake

An endocytotic uptake route independent of clathrin but dependent on dynamin is displayed by caveolae-mediated endocytosis. Caveolae are enriched in caveolins, esp. caveolin-1 (cav-1), sphingolipids and cholesterol and are present on many cell types (Mayor and Pagano 2007). Sterol-binding drugs, e.g. Nystatin or Methyl-beta-cyclodextrin (MßCD), that sequester cholesterol are probably the most effective way to disrupt caveolar function (Sieczkarski and Whittaker 2002).

Since SV40 leaves the plasma membrane in cav-1-containing vesicles before entering larger non-acidic organelles, called caveosomes (Pelkmans et al. 2001), therefore the infection process can be blocked by preincubating the host cells with MßCD (Fig. 25). In contrast, cholesterol depletion from PTH membranes using MßCD did not affect HBV infection, suggesting a lipid raft independent uptake mechanism (Fig. 26, see also Bremer et al. 2009). Similar results were obtained in the DHBV model system (Funk et al. 2008).

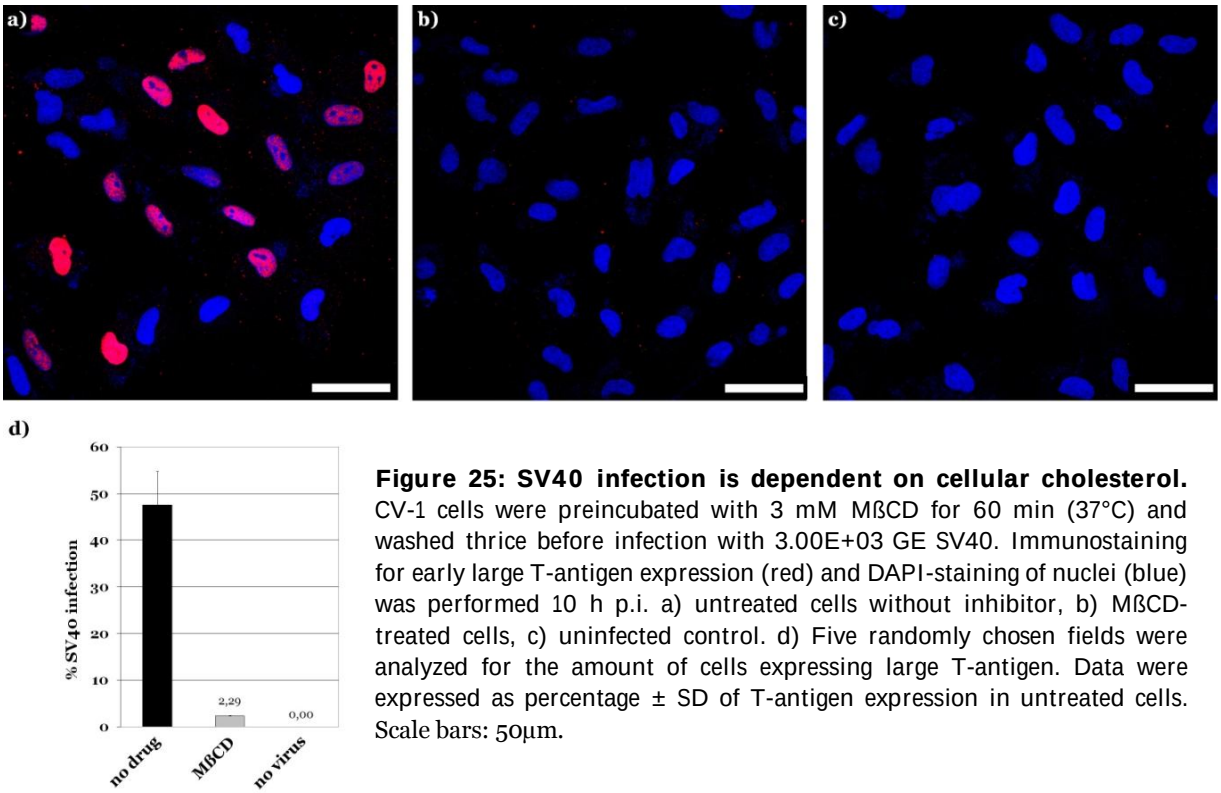

Figure 25: SV40 infection is dependent on cellular cholesterol. CV-1 cells were preincubated with 3 mM MßCD for 60 min (37°C) and washed thrice before infection with 3.00E+03 GE SV40. Immunostaining for early large T-antigen expression (red) and DAPI-staining of nuclei (blue) was performed 10 h p.i. a) untreated cells without inhibitor, b) MßCD-treated cells, c) uninfected control. d) Five randomly chosen fields were analyzed for the amount of cells expressing large T-antigen. Data were expressed as percentage ± SD of T-antigen expression in untreated cells. Scale bars: 50µm.

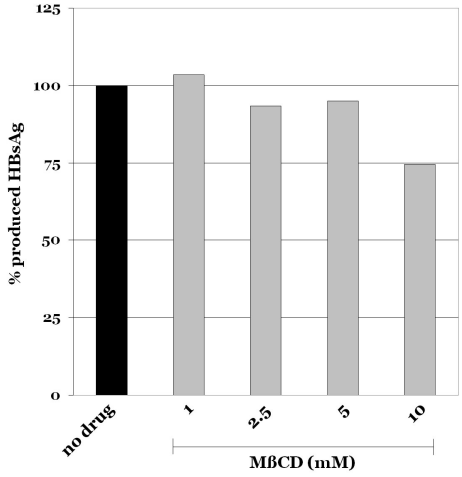

Figure 26: HBV infection is not dependent on cellular cholesterol. PTH were preincubated with the indicated concentrations of MßCD for 60 min (37°C) and washed thrice before infection with HBV (2.00E+07 GE) for 16h (37°C). Newly secreted HBsAg was measured 14 days p.i.

In contrast to that, Macovei et al. hypothesized that HBV requires cav-1-mediated entry for productive infection of HepaRG cells (Macovei et al. 2010). To follow this up, the cav-1-content of PTH should be compared with other cell types and especially with HepaRG cells which become permissive for HBV infection after several weeks of differentiation with DMSO (Gripon et al. 2002). The resulting immunostaining, depicted in Fig. 27, shows that PTH obviously do not express cav-1 as judged by the absence of protein staining (a). In contrast, HepaRG cells showed a strong cav-1-expression in undifferentiated condition (b) which was even more increased in differentiated cells (c). Other hepatic cell lines such as HepG2 (d) and Huh7 (e) lacked the cav-1-signal, and only the fibroblast cells CV-1 showed small amounts of cav-1 (f).

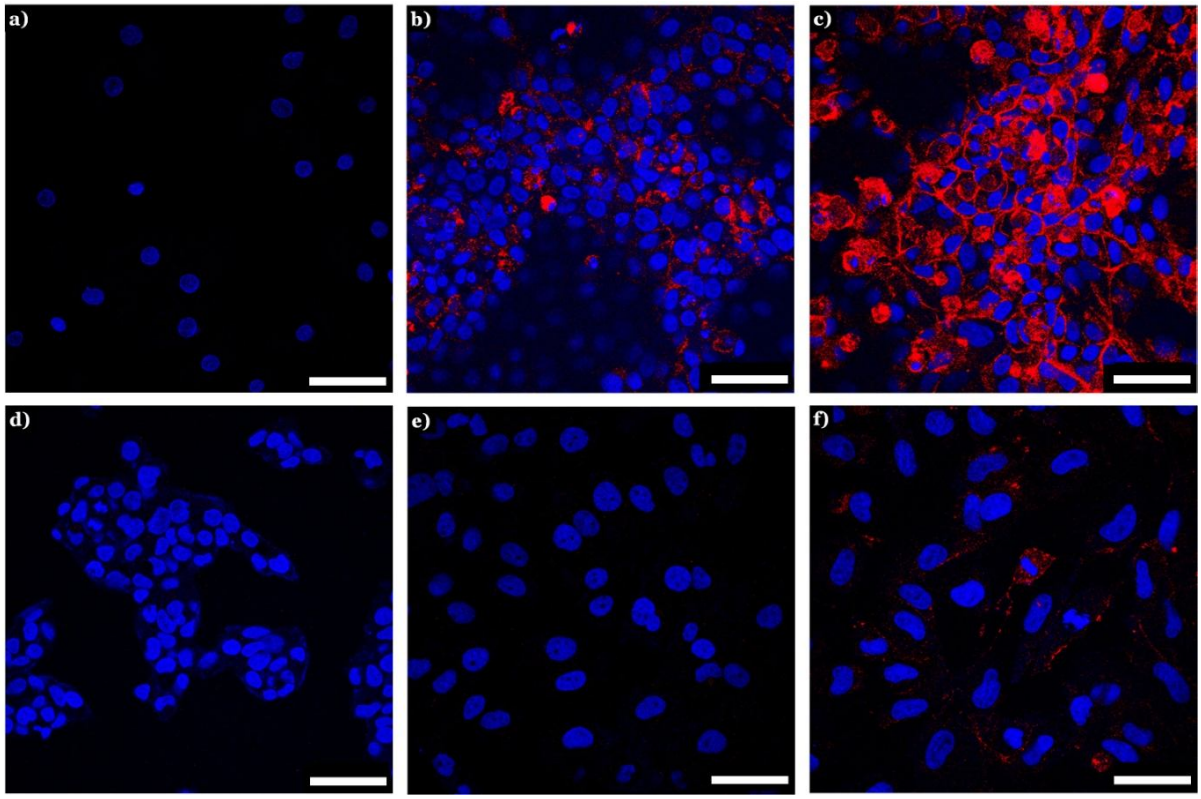

Figure 27: Cav-1 expression in different cell types. PTH were fixed three days after isolation. All other cell lines were cultivated over several weeks before being fixed the day after splitting. Cav-1 (red), nuclei (blue). a) PTH, b) HepaRG (undifferentiated), c) HepaRG (differentiated for 14 days), d) HepG2 cells, e) Huh7 cells, f) CV-1 cells. Scale bars: 50 μm.

Depletion of cholesterol from the HBV envelope using MßCD had no influence on viral binding to PTH as shown in confocal microscopy (Fig. 28): MßCD-treated HBV virions (a) bound to a similar extent to PTH as untreated HBV particles (b) and were detected in distinct areas of the PM (open arrowheads). However, cholesterol-depletion led to a reduced infectivity of HBV virions (Fig. 29) indicating that cholesterol in the viral envelope is essential during early steps of HBV infection (see also Bremer et al. 2009).

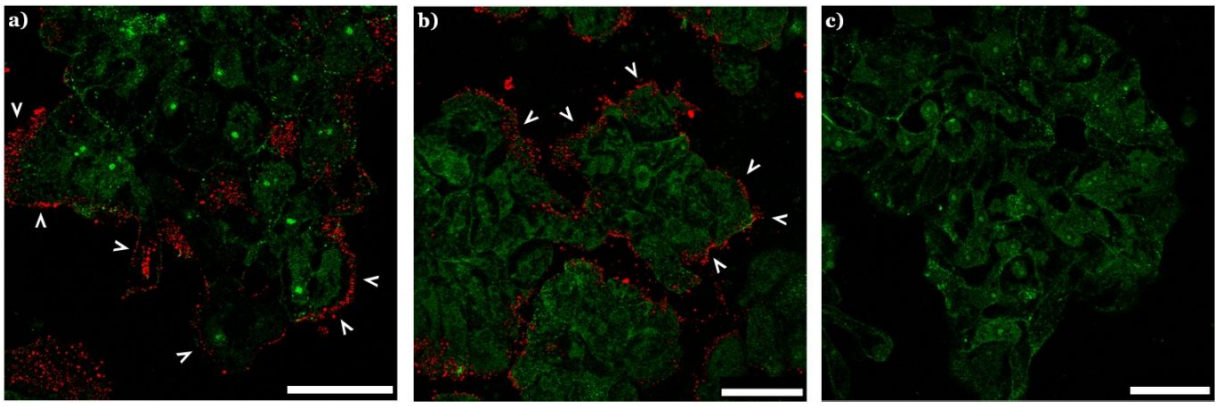

Figure 28: Influence of MßCD on HBV binding to PTH. Highly purified plasma-derived HBV virions were incubated with 10 mM MßCD for 1 h at 37°C. The cells were incubated for 1 h at 4°C with MßCD-treated HBV (a) or with untreated HBV (b); c) negative control, followed by immunostaining for SHBs (red) and asialoglycoprotein receptor (green). Scale bars: 50 µm. (published in: C. M. Bremer, C. Bung, N. Kott, M. Hardt and Dieter Glebe (2009). "Hepatitis B virus infection is dependent on cholesterol in the viral envelope." Cellular Microbiololgy 11(2), 249-60. modified)

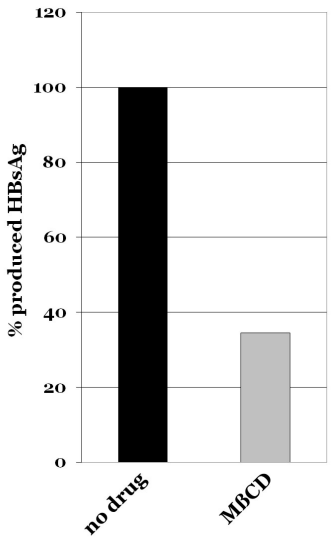

Figure 29: Effect of MßCD treatment on HBV infectivity. Highly purified plasma-derived HBV virions were incubated with 10 mM MßCD for 1 h at 37°C and the cells were infected for 16 h (37°C) with untreated or MßCD-treated virions. Newly secreted HBsAg was measured 14 days p.i.

4.4 Dynamin-independent endocytosis

4.4.1 Phagocytosis

Phagocytosis is a specific form of endocytosis and is carried out primarily by specialized cells, such as macrophages, monocytes and neutrophils (Conner and Schmid 2003). It is critical for the uptake and degradation of pathogens, e.g. bacteria and parasites (Aderem and Underhill 1999) and has recently been shown to be an infection route of the large Mimivirus in amoebal macrophages (Ghigo et al. 2008). Since most cells have at least some phagocytic capacitiy (Aderem and Underhill 1999) it was tested whether phagocytosis occurs in PTH and if it displays a potential entry mechanism for HBV. The cells were incubated with purified HBsAg and labeled E.coli (pHrodo) BioParticles and checked for possible colocalization. E.coli conjugated with pHrodo showed no fluorescence inside acidic compartments of PTH, which showed staining of bound and internalized HBsAg (Fig. 30, white arrowheads). However, in smaller, non-parenchymal cells adjacent to hepatocytes a red staining of the E.coli particles was detectable, indicating phagocytosis (grey arrowheads) whereas a specific HBsAg signal was absent in these cells.

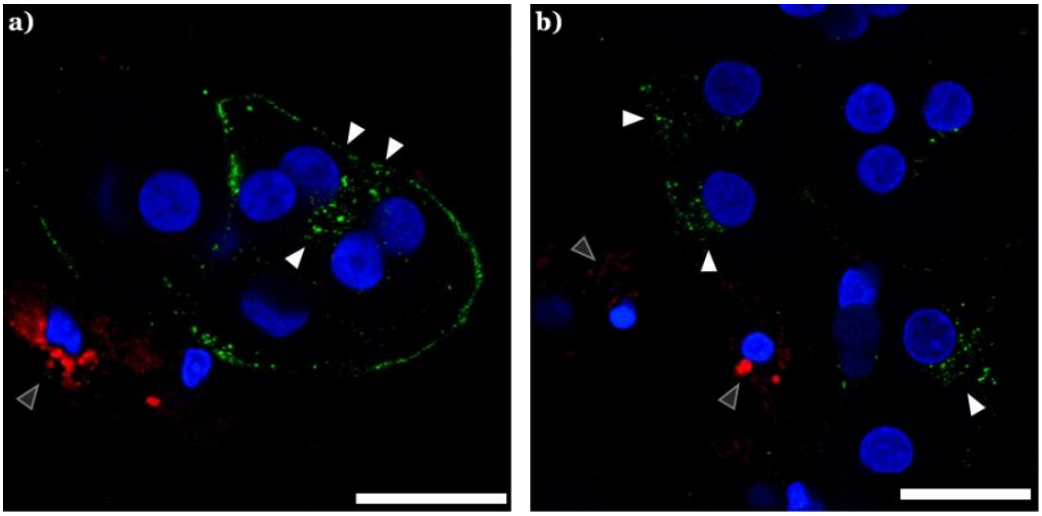

Figure 30: Role of phagocytosis in PTH. PTH were incubated with 8 ng HBsAg and pHrodo E.coli particles for 2 h at 37°C, then extensively washed, fixed and stained for SHBs (green) and nuclei (blue). pHrodo labeled E.coli (red). a) and b) show representative images of two independent experiments. Scale bars: 25 μm.

4.4.2 Macropinocytosis

Macropinocytosis is an actin-driven endocytic process that is used to internalize large amounts of fluids and solutes. In the majority of cases it is transient, growth-factor induced and involves protrusions of the plasma membrane in form of lamellipodia, circular ruffles and blebs (Doherty and McMahon 2009; Mercer and Helenius 2009). Na^+/H^+ exchangers play an important role in the process of ruffling (Mercer and Helenius 2009) and therefore EIPA (5-[N-ethyl-N-isopropyl] amiloride), a selective blocker of the Na^+/H^+-antiport, was used to study the effect on the fluid phase uptake. Furthermore, Blebbistatin (which inhibits bleb formation), Dynasore, sucrose, the actin-stabilizing/-depolymerizing drugs, Jasplakinolide (Jas) and Cytochalasin D (CytoD), as well as Brefeldin A (BFA) were used to check a possible impact on the process of fluid phase uptake in PTH. BFA has been shown to enhance macropinocytosis in CHO cells (Kumari and Mayor 2008), therefore a potential influence in PTH should be tested. Horseradish peroxidase (HRP) served as fluid phase marker (Haigler et al. 1979).

Fig. 31a shows that preincubation with EIPA lead to a 60% reduction of HRP uptake whereas treatment with Blebbistatin and Dynasore had no effect on the internalization. Sucrose blocked the uptake in a dose-dependent manner (b) and also Jas and CytoD (see also chapter 4.6) reduced the HRP uptake similar to EIPA (c). Preincubation with the fungal metabolite BFA lead to an enhancement of fluid phase endocytosis (d).

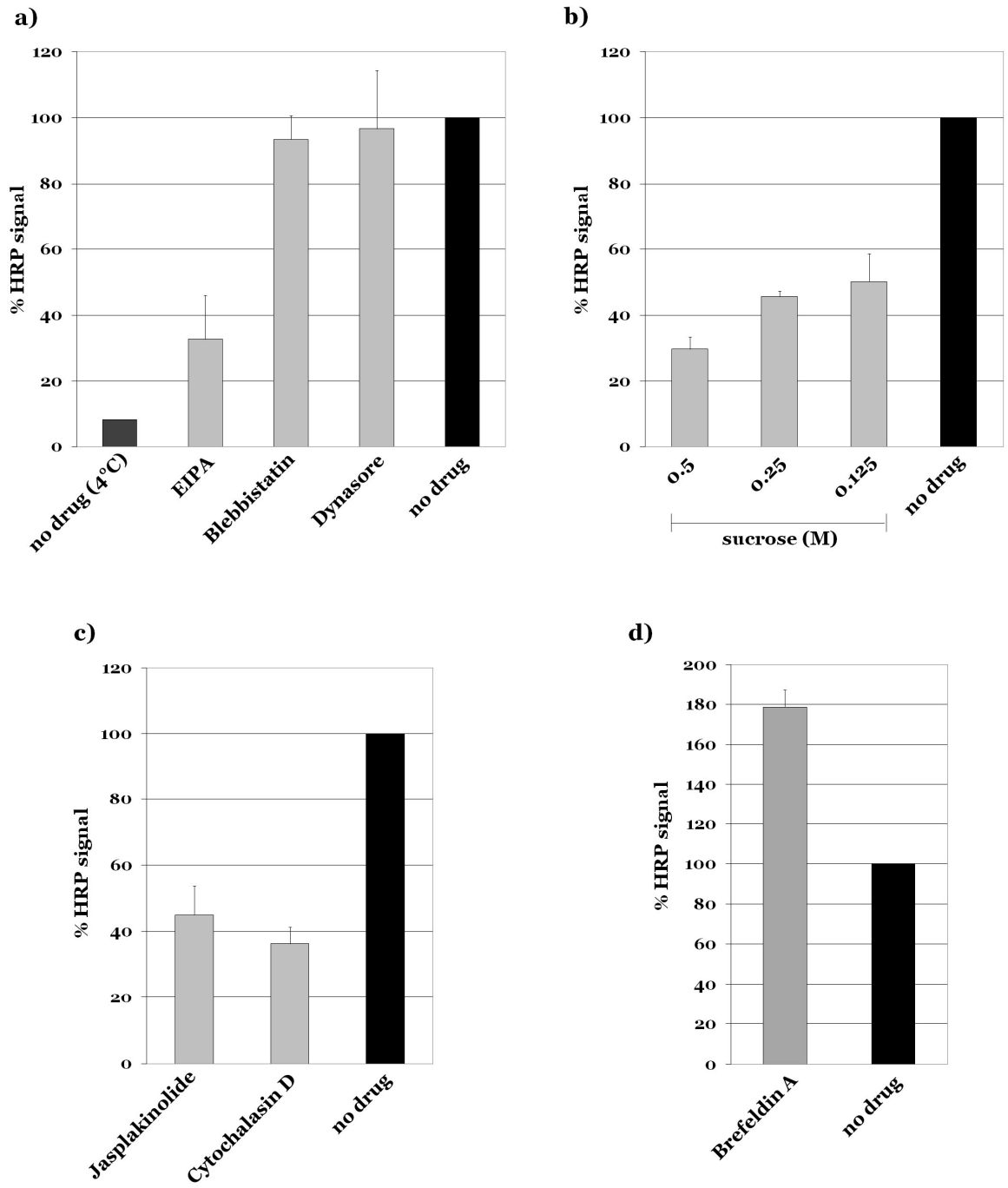

Figure 31: Impact of different chemical inhibitors on fluid phase uptake of HRP in PTH. Cells were preincubated with the indicated inhibitors (EIPA: 100 µM, Blebbistatin: 100 µM, Dynasore: 100 µM, Jasplakinolide: 1 µM, Cytochalasin D: 50 µM, Brefeldin A: 0.1 mg/ml, sucrose: as indicated) for 30 min at 37°C. HRP (0.025 mg/ml) was added and incubated for 3 h at 37°C or 4°C. After extensive washing on ice the cells were lysed and cytosolic HRP-signal was measured. a+b) The values are means ± SD of two independent experiments (four values in total), c+d) represent single experiments (three values in total).

Since Adenovirus type 2 (Ad2) transiently stimulates macropinocytosis (Meier et al. 2002) it was tested whether HBV has the same capability. Preincubation of the cells with purified virions does not have a stimulating effect on fluid phase uptake regardless of whether the incubation lasted 0.5 or 1 h (Fig. 32a).

Several pathogens do not only trigger macropinocytosis but also exploit this pathway to invade their host cells, e.g. Vaccinia Virus and Ad2/Ad5 (Meier and Greber 2004; Mercer and Helenius 2008). Endocytotic uptake and infection of those viruses can be blocked by EIPA (Kälin et al. 2010; Mercer and Helenius 2008). In contrast, HBV infection was not impaired by this inhibitor (Fig. 32 b+c).

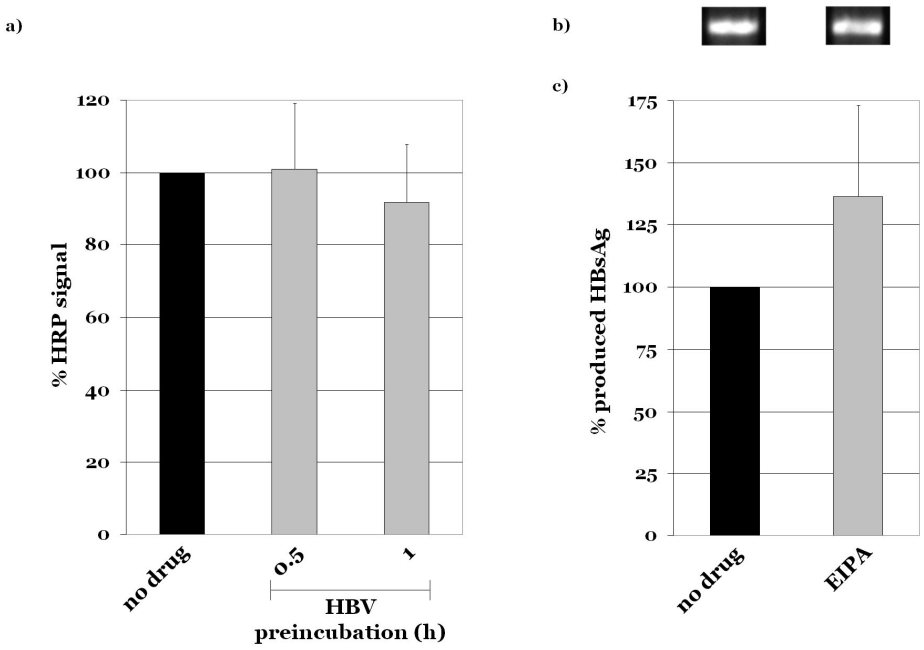

Figure 32: Effect of HBV on fluid phase uptake and impact of EIPA on HBV infection of PTH. a) Cells were incubated with purified plasma-derived HBV virions (2.00E+07 GE) for the indicated times in the cold, washed three times on ice and warmed with HGM medium containing 0.025mg/ml HRP for 3 h at 37°C. After extensive washing on ice the cells were lysed and cytosolic HRP-signal was measured. b+c) Cells were preincubated with 100 µM EIPA (30 min, 37°C) and afterwards infected with purified plasma-derived HBV virions (2.00E+07 GE). cccDNA-formation of incoming viral particles was determined 20 h p.i. by PCR and detected by gel electrophoresis (a). Newly secreted HBsAg was measured 14 days p.i. (b). Data represent the average ± SD of two (a) and three (c) independent experiments respectively.

4.5 pH-dependence of viral infection

Penetration of enveloped viruses occurs by fusion of the viral with the host cell membrane which can take place at the PM or at intracellular membranes (Kielian and Rey 2006). This fusion can be triggered either by receptor binding at neutral pH, e.g. SeV and HSV-1, or by mildly acidic pH within endosomal compartments (Smith and Helenius 2004; Marsh and Helenius 2006) which is established by the action of vacuolar-type ATPases (v-ATPases) (Jefferies et al. 2008; Huss and Wieczorek 2009). Lysosomotropic agents such as Bafilomycin A1 (BafA1), a specific inhibitor of v-ATPases, the weak base NH_4Cl or the ionophore Monensin raise the pH in early endosomes by different mechanisms and have been shown to inhibit SFV infection (Helenius et al. 1980; Rigg and Schaller 1992; Glomb-Reinmund and Kielian 1998). When used in BHK and PTH cells (Fig. 33 and 34), these drugs could completely abolish SFV infection in both cell types.

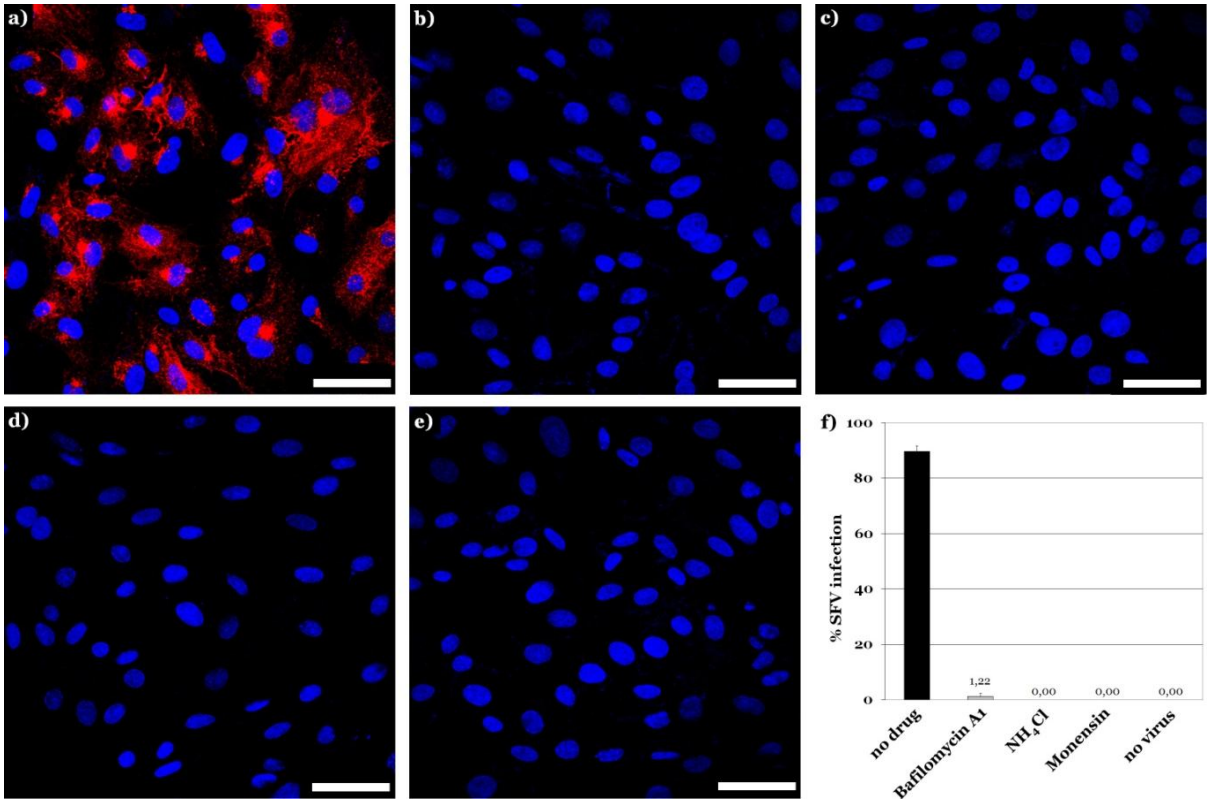

Figure 33: SFV infection of BHK cells is dependent on low endosomal pH. Cells were preincubated with 100 nM Bafilomycin A1, 20 mM NH_4Cl or 10 µM Monensin (30 min, 37°C) and subsequently infected (MOI 10). Immunostainig for newly produced SFV E1/E2-protein (red) and nuclei (blue) was performed 5 h p.i. a) untreated cells without inhibitor, b) Bafilomycin A1-treated cells, c) NH_4Cl-treated cells, d) Monensin-treated cells, e) uninfected control. f) Three randomly chosen fields were analyzed for the amount of E1/E2 positive cells. Data are expressed as percentage ± SD of E1/E2 positive cells in untreated cells. Scale bars: 50µm.

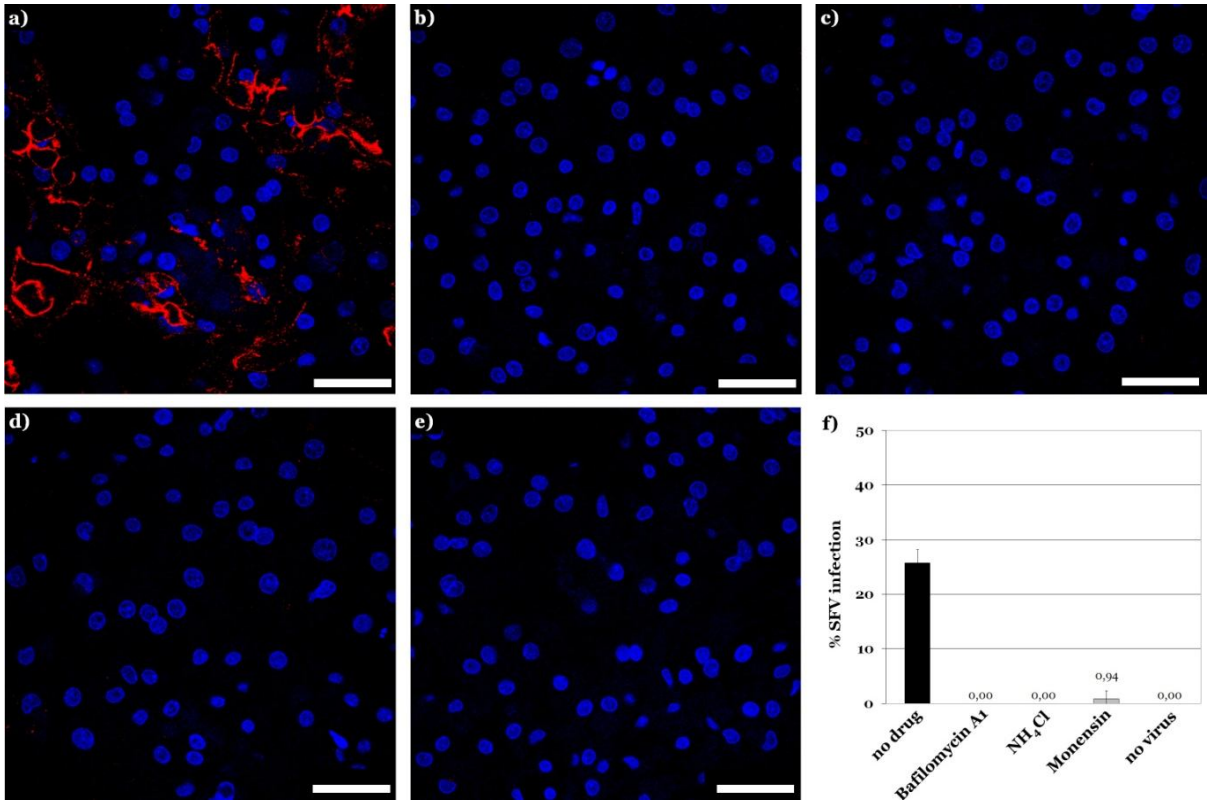

Figure 34: SFV infection of PTH is dependent on low endosomal pH. Prior infection (MOI 1000) the cells were pretreated with 100 nM Bafilomycin A1, 20 mM NH_4Cl or 10 µM Monensin (30 min, 37°C), fixed 8 h p.i. and stained for newly produced SFV E1/E2-protein (red) and nuclei (blue). a) untreated cells without inhibitor, b) Bafilomycin A1-treated cells, c) NH_4Cl-treated cells, d) Monensin-treated cells, e) uninfected control. f) Three randomly chosen fields were analyzed for the amount of E1/E2 positive cells. Data are expressed as percentage ± SD of E1/E2 positive cells in untreated cells. Scale bars: 50µm.

Treatment with BafA1 or NH_4Cl had no effect on HBsAg uptake (Fig. 35) and HBV infection (Fig. 36). Interestingly, infection in the presence of NH_4Cl showed an increase in secreted HBsAg signal 14 days after infection, suggesting an increased infection rate (b). There was also no sign of inhibition of infection when Monensin was used (c and d).

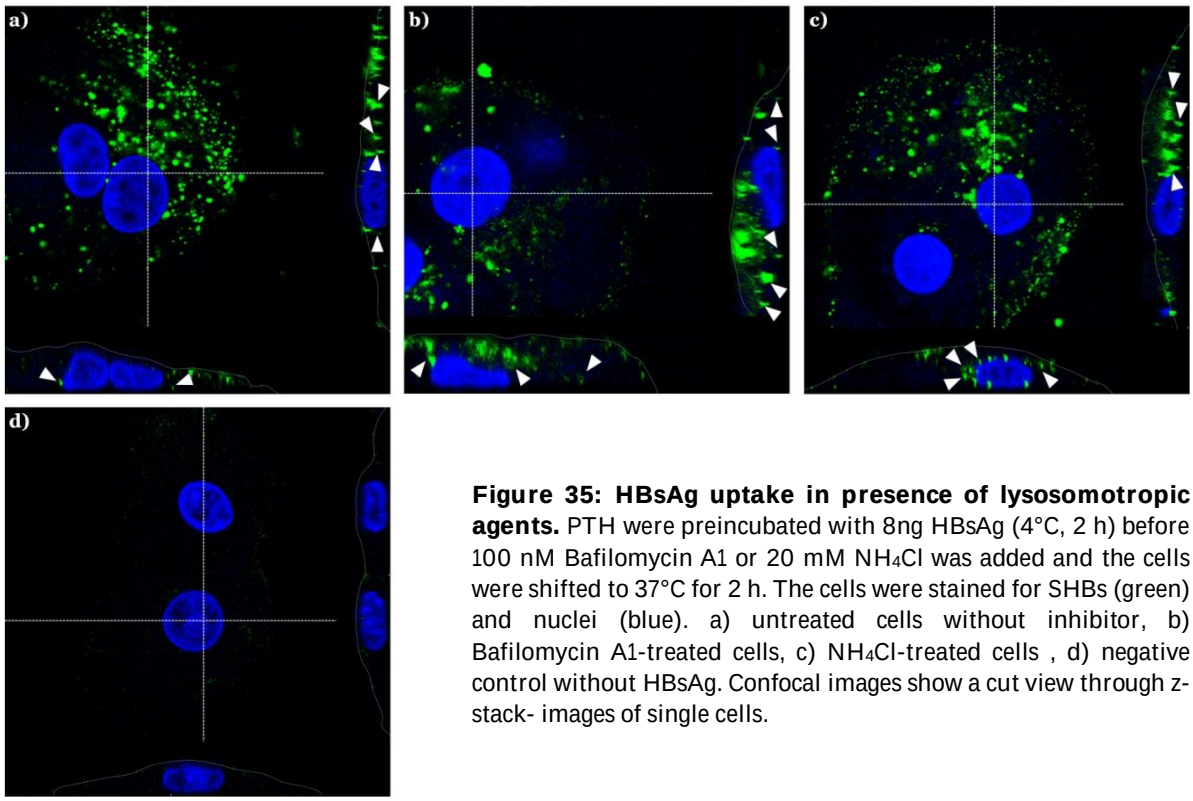

Figure 35: HBsAg uptake in presence of lysosomotropic agents. PTH were preincubated with 8ng HBsAg (4°C, 2 h) before 100 nM Bafilomycin A1 or 20 mM NH_4Cl was added and the cells were shifted to 37°C for 2 h. The cells were stained for SHBs (green) and nuclei (blue). a) untreated cells without inhibitor, b) Bafilomycin A1-treated cells, c) NH_4Cl-treated cells , d) negative control without HBsAg. Confocal images show a cut view through z-stack- images of single cells.

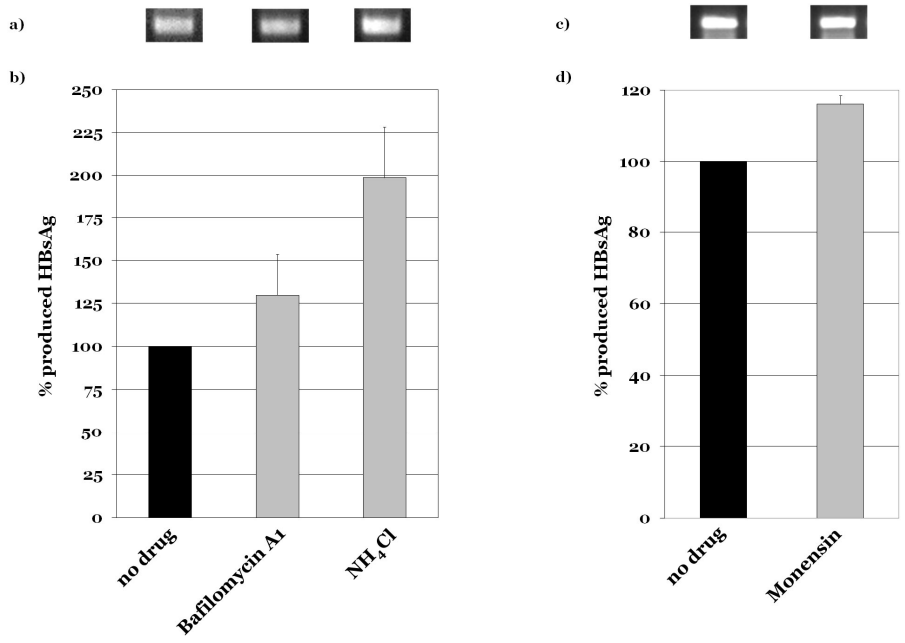

Figure 36: HBV infection of PTH in presence of lysosomotropic agents. The cells were preincubated with Bafilomycin A1 (100 nM), NH_4Cl (20 mM) or Monensin (10 µM) for 30 min at 37°C and afterwards infected with purified plasma-derived HBV virions (2.00E+07 GE). cccDNA-formation of incoming viral particles was determined 20 h p.i. by PCR and detected by gel electrophoresis (a). Newly secreted HBsAg was measured 14 days p.i. (b). Data in b) and d) are means of triplicate experiments ± SD.

4.6 Cytoskeleton

The cytoskeleton is a network made from filamentous proteins such as actin, tubulin and intermediate filaments in the cytoplasm of eukaryotic as well as prokaryotic cells (Graumann 2007; Pollard and Cooper 2009). It stabilizes the cell and its intracellular organelles and is also responsible for the motility of organelles and the cell itself (Doherty and McMahon 2008). Fig. 37 shows the cytoskeletal organization in PTH after immunostaining of actin and microtubules:

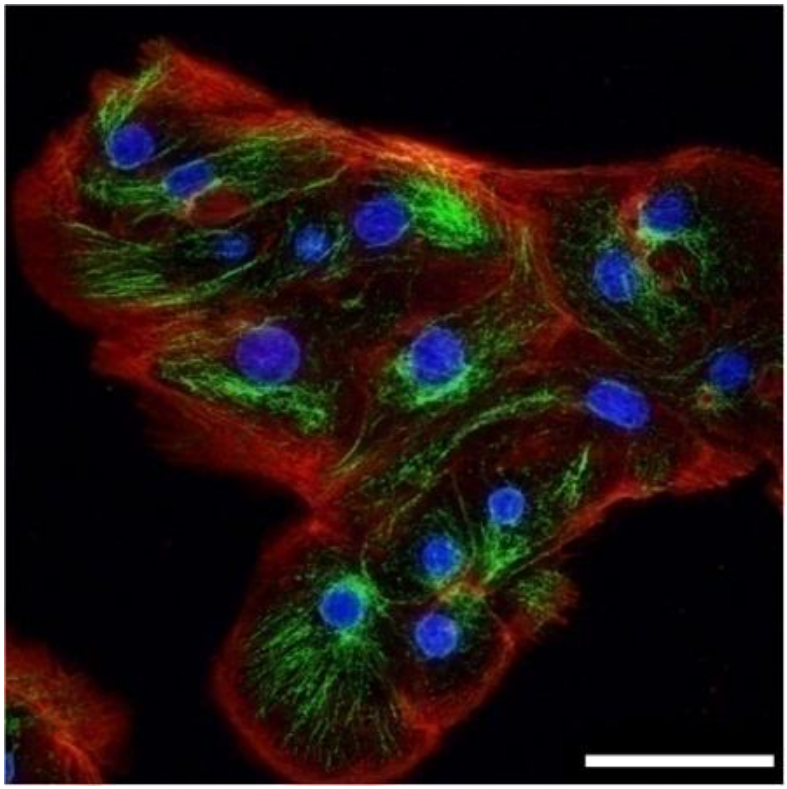

Figure 37: Cytoskeletal organization in PTH. Cells were fixed three days after isolation and stained for actin (using Alexa Fluor®647 phalloidin; red) and microtubules (using an anti-tubulin antibody; green). Nuclei (blue). Scale bar: 50 µm.

There are different types of actin-structures in the cell ranging from the dense cortex at the cytoplasmic site of the plasma membrane, actin-rich formations associated with endocytic or phagocytic structures, long filaments in filopodia etc. (Doherty and McMahon 2008). Actin is required for various types of endocytic processes (Mercer et al. 2010) in which both actin depolymerization and polymerization have been proposed to allow vesicle formation (Doherty and McMahon 2008). Intracellular microtubule-based transport, generally used for routing cellular cargoes, such as endosomes or secretory vesicles, is commonly exploited by viruses to reach their replication site inside the host cell (Greber and Way 2006). Whether functioning actin filaments and microtubules are needed for cytoplasmic trafficking of SFV, SV40 and HBV upon entry should be determined by using the following

pharmacological inhibitors: Jas which stabilizes F-actin or CytoD which causes actin depolymerization (Burckhardt and Greber 2009) and Nocodazole (Noco) which depolymerizes microtubules (Vasquez et al. 1997).

Preincubation with the above-mentioned cytoskeleton disrupting agents had no effect on SFV infection in BHK cells and PTH since there was virtually no difference in the number of infected cells compared to the untreated control (Fig. 38 and 39). The relatively high inhibitor concentrations (see also Figs. 43, 45, 47) were tolerated by PTH and also by the BHK cells with the exception of Jas (Fig. 38b). These cells showed a shrinked morphology but were nevertheless clearly infected.

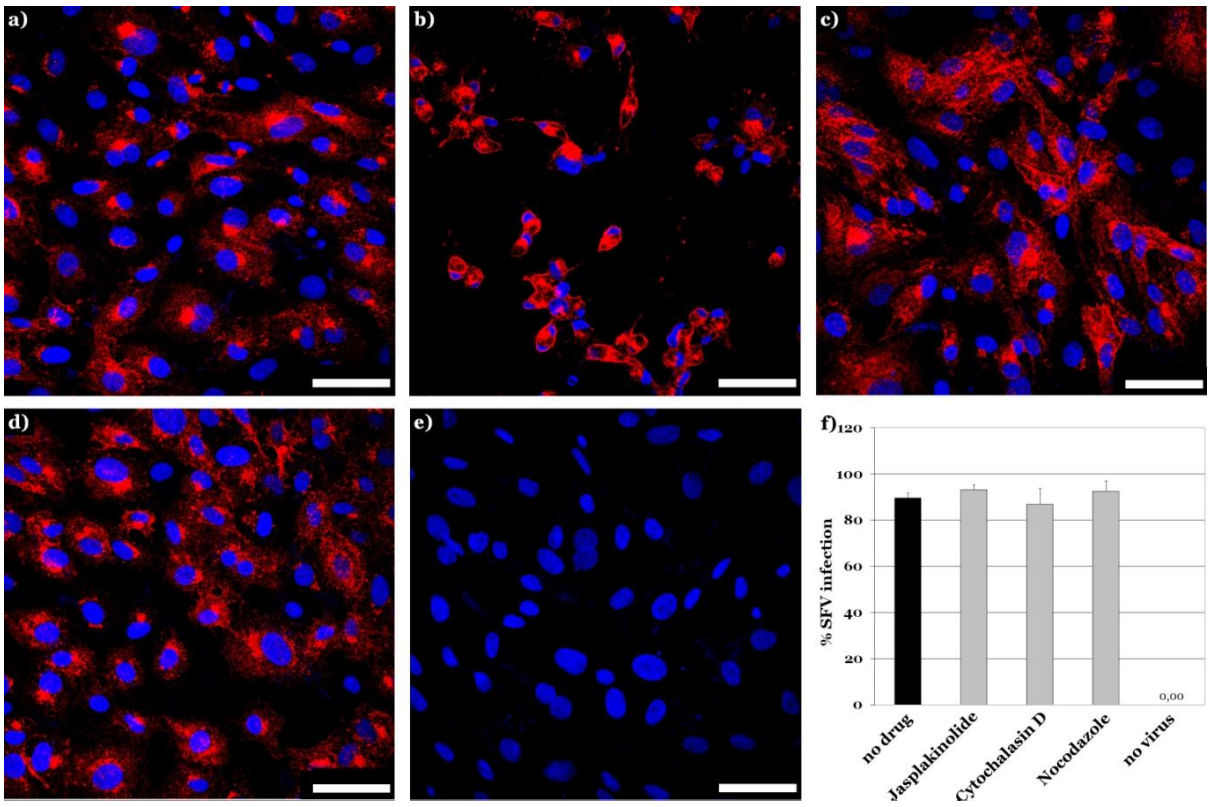

Figure 38: Impact of cytoskeleton destroying agents on SFV infection of BHK. Prior infection (MOI 10) the cells were left untreated (a) or preincubated with 1 µM Jasplakinolide (b), 50 µM Cytochalasin D (c) or 50 µM Nocodazole (d) for 30 min at 37°C. The cells were fixed 5 h p.i. and newly synthesized SFV E1/E2-protein (red) and nuclei (blue) were stained. e) uninfected control. f) Three randomly chosen fields were analyzed for the amount of E1/E2 positive cells. Data are expressed as percentage ± SD of E1/E2 positive cells in untreated cells. Scale bars: 50µm.

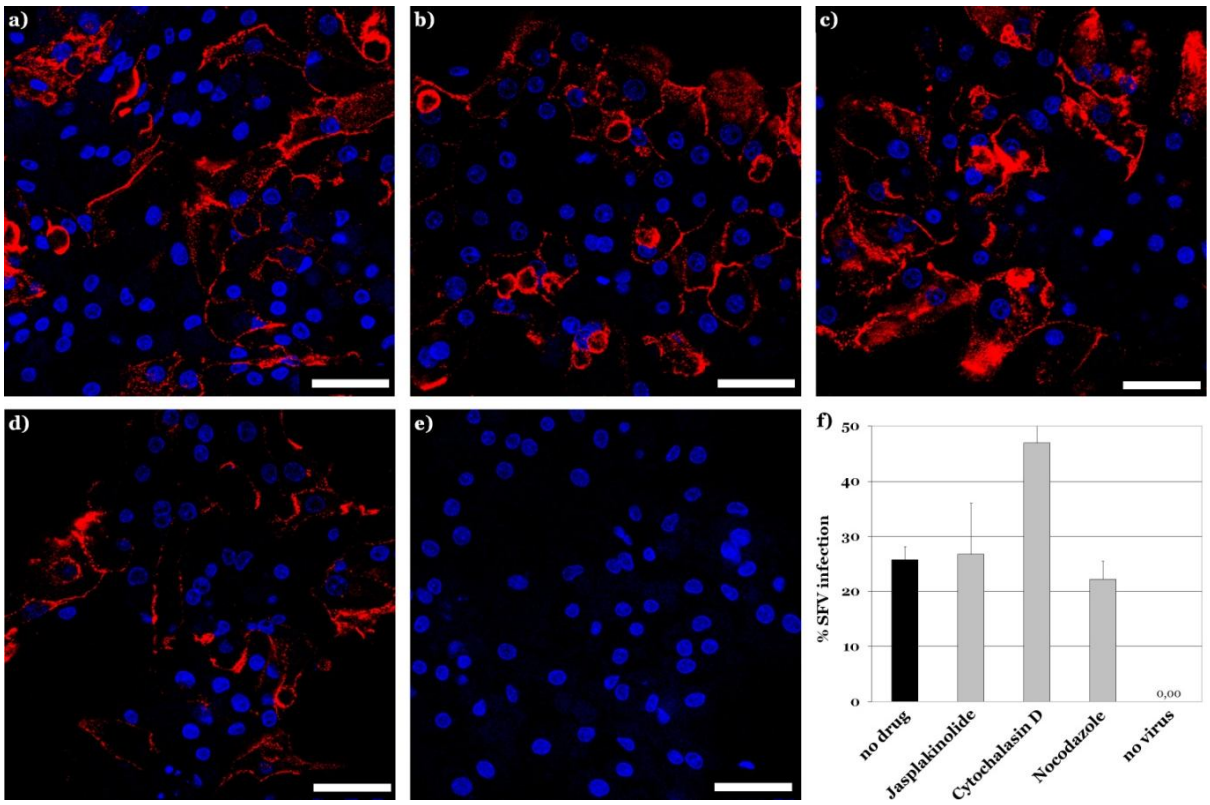

Figure 39: SFV infection of PTH in presence of actin-and microtubule disrupting agents. Cells were were left untreated (a) or preincubated with 1 µM Jasplakinolide (b), 50 µM Cytochalasin D (c) or 50 µM Nocodazole (d) for 30 min at 37°C, subsequently infected (MOI 1000), fixed 8 h p.i. and stained for newly produced SFV E1/E2-protein (red) and nuclei (blue). e) uninfected control. f) Three randomly chosen fields were analyzed for the amount of E1/E2 positive cells. Data are expressed as percentage ± SD of E1/E2 positive cells in untreated cells. Scale bars: 50µm.

Next, the effect of treatment of cells with Jas, CytoD and Noco on SV40 infection was studied. SV40 is dependent on caveolae-mediated endocytosis and microtubule-based transport (Kartenbeck, Stukenbrok et al. 1989). SV40 infection was completely abolished in Noco-treated cells (Fig. 40d) but was unaffected when the actin-stabilizing drug Jas was used (b). However, an approx. twofold reduction in infection was observed in the CytoD-treated cells which probably results from the fact that the cells showed already signs of apoptosis (c).

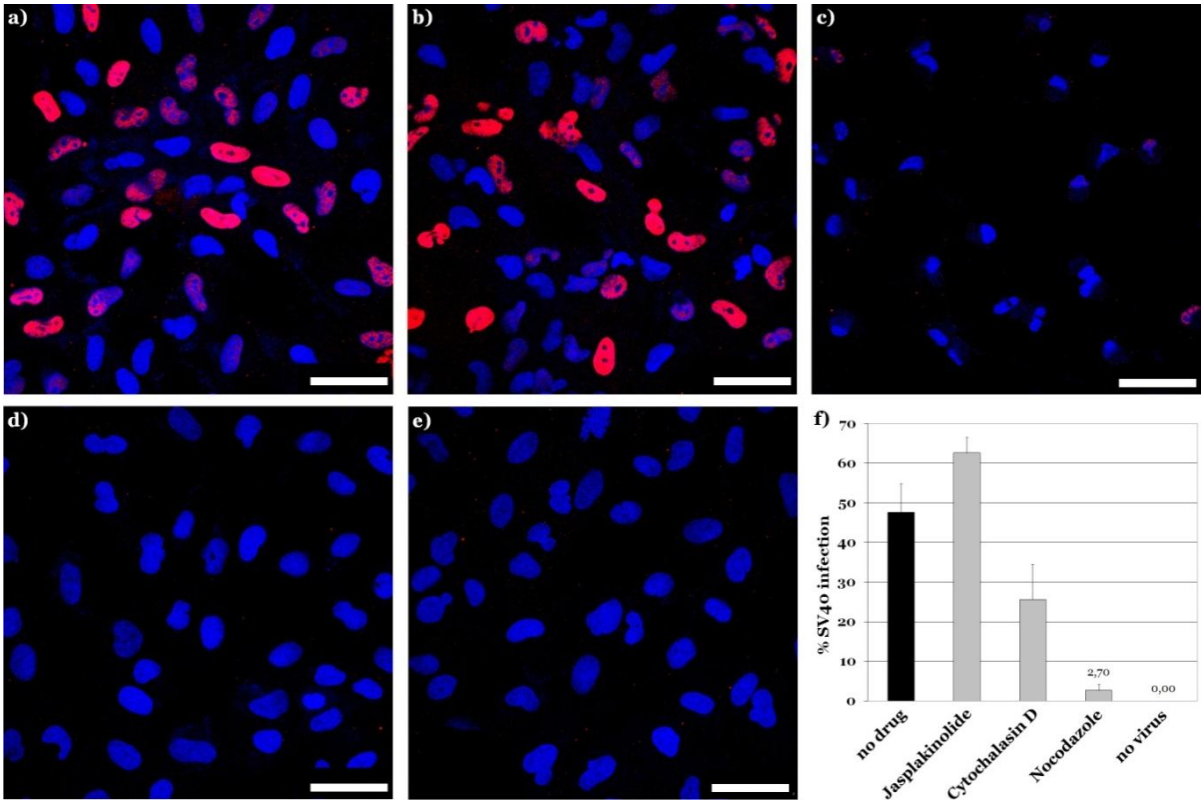

Figure 40: Effect of cytoskeleton disrupting agents on SV40 infection of CV-1 cells. Prior infection with 3.00E+03 GE the cells were preincubated with 1 µM Jasplakinolide (b), 50 µM Cytochalasin D (c) or 50 µM Nocodazole (d) for 30 min at 37°C. Immunostaining for early large T-antigen expression (red) and nuclei (blue) was performed 10 h p.i. e) uninfected control. f) Five randomly chosen fields were analyzed for the amount of cells expressing large T-antigen. Data were expressed as percentage ± SD of T-antigen expression in untreated cells. Scale bars: 50µm.

Jas, CytoD and Noco were also used to test a possible requirement of a functional cytoskeleton for HBsAg uptake and HBV infection, respectively. The inhibitors were utilized in the same concentrations as in the previous experiments. Fig. 41 demonstrates that the uptake of HBsAg into PTH was reduced by all chemicals to a certain degree. Similarly, all drugs affected HBV infection (Fig. 42) which showed a decrease in secreted HBsAg levels to 30-50% (b) and only very limited cccDNA formation from incoming viral particles after 20 h of infection (a).

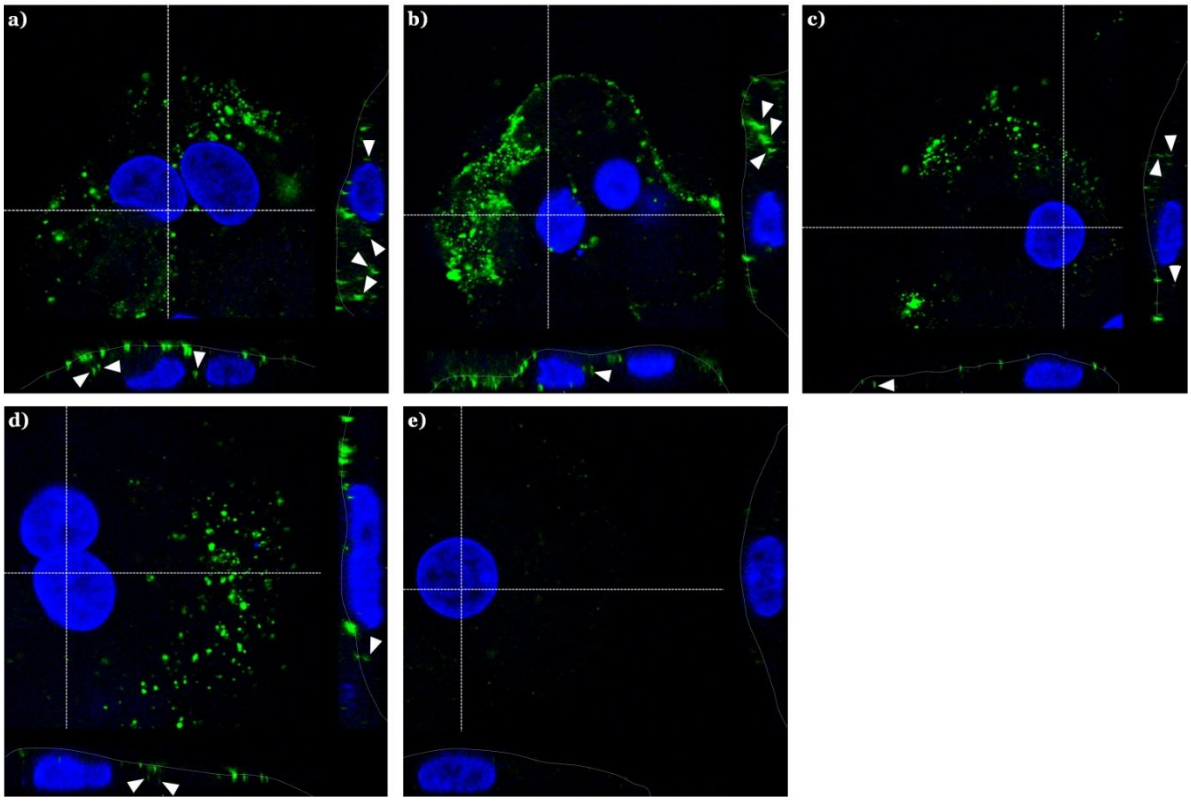

Figure 41: Impact of Jasplakinolide, Cytochalasin D and Nocodazole on HBsAg uptake. After preincubation with 8ng HBsAg (4°C, 2 h), the chemicals were added to the cells which were then shifted to 37°C for 2 h. Staining for SHBs (green) and nuclei (blue) was performed 2 h later. a) untreated cells without inhibitor, b) Jasplakinolide (1 µM), c) Cytochalasin D (50 µM), d) Nocodazole (50 µM), e) negative control without HBsAg. Confocal images show a cut view through z-stack-images of single cells.

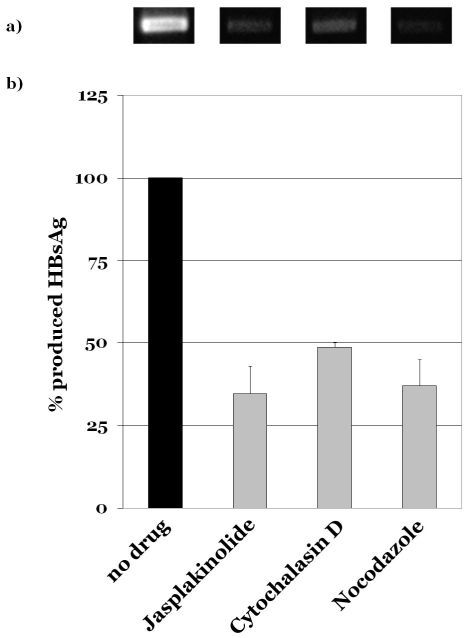

Figure 42: HBV infection of PTH in presence of cytoskeleton altering agents. The cells were preincubated with 1 µM Jasplakinolide, 50 µM Cytochalasin D or 50 µM Nocodazole (30 min at 37°C) and subsequently infected with purified plasma-derived HBV (5,48E+09 GE). cccDNA-formation of incoming viral particles was determined 20 h p.i. by PCR and detected by gel electrophoresis (a). Newly secreted HBsAg was measured 14 days p.i. (b). Data in b) are means of triplicate experiments ± SD.

To analyze whether this inhibitory effect of these agents also takes place with lower concentrations, PTH were incubated with serial dilutions of Jas, CytoD and Noco and either fixed for immunostaining or infected with purified HBV virions. Fig. 43a-e illustrates the appearance of PTH after a 4 h-treatment with Jas. The actin staining dissolves with increasing drug concentration which can be explained by the fact that Jas occupies the phalloidin binding sites on actin. Hence, the more drug is used the less dye can bind to actin. Preincubation of PTH with different Jas concentrations prior HBV infection lead to a dose-dependent reduction of up to approx. 75% (Fig. 44).

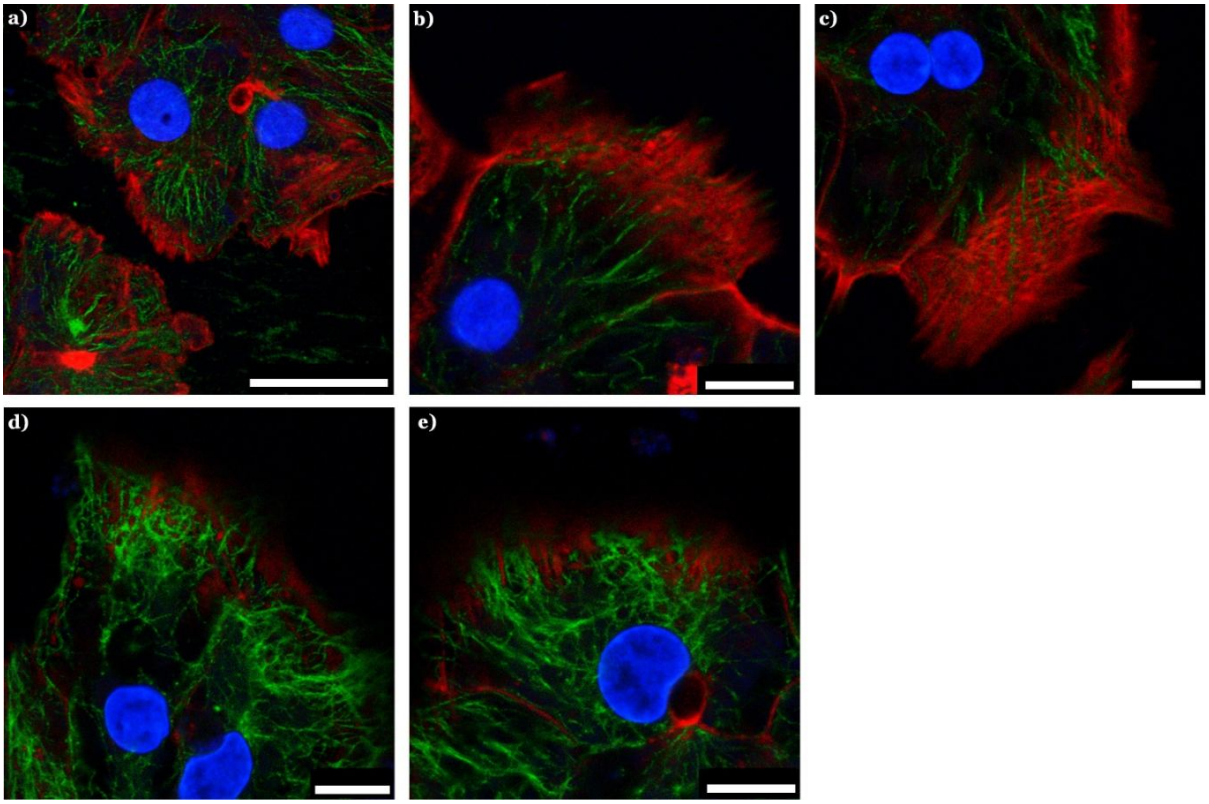

Figure 43: Effect of Jasplakinolide on the cytoskeleton of PTH. The cells were either left untreated (a) or incubated with different concentrations of Jasplakinolide: b) 0.25 µM, c) 0.5 µM, d) 1 µM, e) 2 µM for 4 h. The cells were washed, fixed and subsequently stained for actin (red), microtubules (green) and nuclei (blue). Representative images are shown. Scale bars: a) 25 µm, b-e) 10 µm.

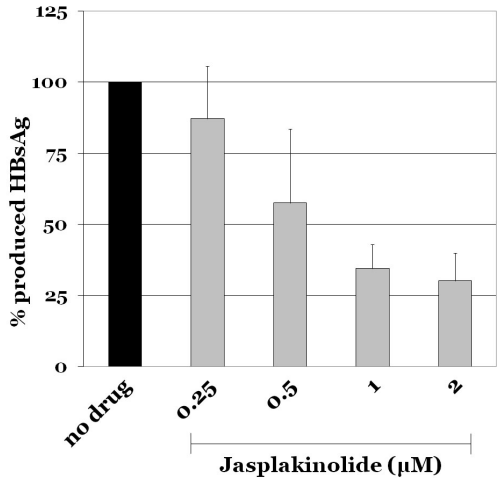

Figure 44: Effect of Jasplakinolide on HBV infection of PTH. PTH were incubated with the indicated Jasplakinolide concentrations (30 min, 37°C) and subsequently infected with purified plasma-derived HBV virions (5,48E+09 GE). Newly secreted HBsAg was measured 14 days p.i. Data represent the average of three independent experiments ± SD.

The impact of CytoD on the cytoskeletal architecture of PTH is depicted in Fig. 45. Since this inhibitor blocks actin polymerization by binding to the growing plus-end of the filaments whereas the minus-end is constantly degraded, only knob-like structures are left over and can be stained by phalloidin (b-e). Regarding HBV infection, 5-25 µM had a slightly enhancing effect whereas higher concentrations of 50 and 100 µM inhibited infection down to 25% of control infection (Fig. 46).

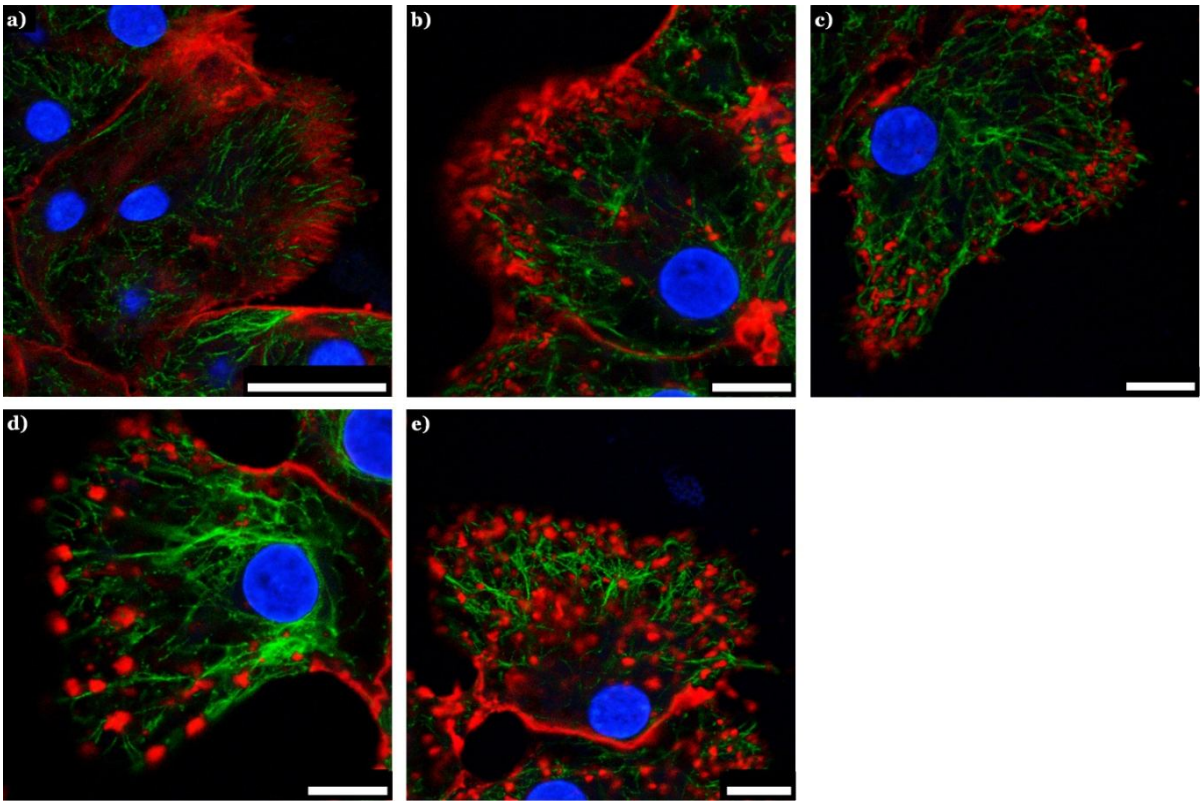

Figure 45: Impact of Cytochalasin D on the cytoskeleton of PTH. The cells were either left untreated (a) or incubated for 4 h with different concentrations of Cytochalasin D: b) 5 µM, c) 10 µM, d) 25 µM, e) 50 µM. The cells were washed, fixed and subsequently stained for actin (red), microtubules (green) and nuclei (blue). Representative images are shown. Scale bars: a) 25 µm, b-e) 10 µm.

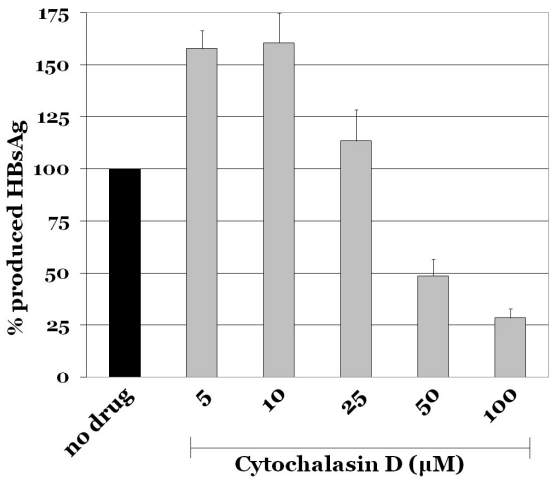

Figure 46: Impact of Cytochalasin D on HBV infection of PTH. PTH were incubated with the indicated Cytochalasin D concentrations (30 min, 37°C) and subsequently infected with purified plasma-derived HBV virions (5,48E+09 GE). Newly secreted HBsAg was measured 14 days p.i. Data are means of triplicate experiments ± SD.

The microtubule pattern in untreated PTH shows a filamentous staining that is occasionally concentrated near the nuclei presumably presenting the microtubule-organizing center (MTOC) (Fig. 47a, arrowheads). Treatment with Noco leads to a disruption of the microtubule network with apparently twisted tubules (b-e).

Furthermore, a dose-dependent inhibition of HBV was observed in the Nocodazole-approaches (Fig. 48).

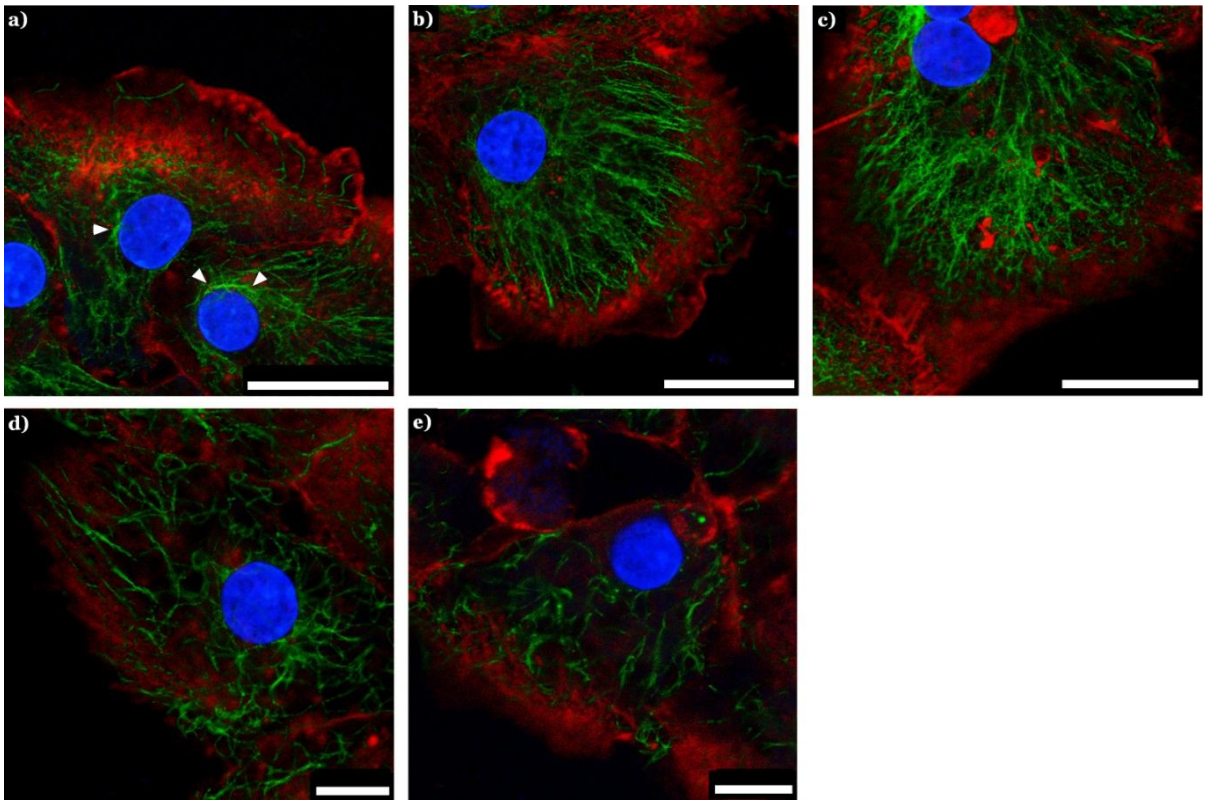

Figure 47: Impact of Nocodazole on the cytoskeleton of PTH. The cells were either left untreated (a) or incubated for with different concentrations of Nocodazole: b) 5 µM, c) 10 µM, d) 25 µM, e) 50 µM. The cells were washed, fixed and subsequently stained for actin (red), microtubules (green) and nuclei (blue). Representative images are shown. Scale bars: a-c) 25 µm, d+e) 10 µm.

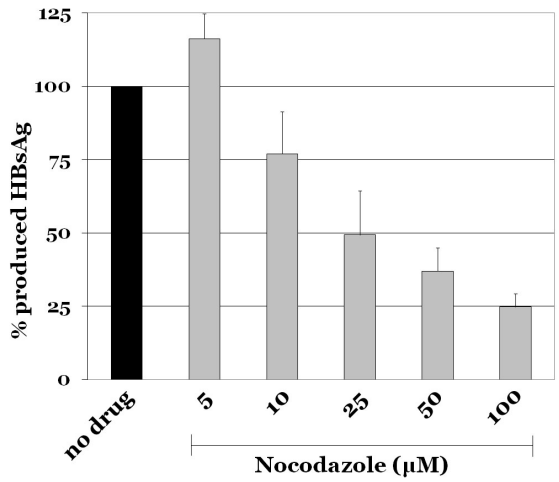

Figure 48: Impact of Nocodazole on HBV infection of PTH. PTH were incubated with the indicated Nocodazole concentrations (30 min, 37°C) and subsequently infected with purified plasma-derived HBV virions (5,48E+09 GE). Newly secreted HBsAg was measured 14 days p.i. Data represent the average of three independent experiments ± SD.

4.7 Retrograde pathway

Retrograde transport describes the trafficking of endosomes to the biosynthetic/secretory compartments, e.g. the Golgi apparatus or the ER, and is important for certain cellular functions such as receptor trafficking and cell signaling (Johannes and Popoff 2008). Some bacterial toxins use the endosome-to-ER trafficking (Lord and Roberts 1998) and also viruses rely on this entry route: SV40 enters its host cells through caveolin-mediated endocytosis (Pelkmans et al. 2001). The next step is microtubule-dependent transport to the ER (Kartenbeck et al. 1989) from which it translocates into the cytosol and is thought to enter the nucleus via nuclear pore complexes (Schelhaas et al. 2007). The SV40 infection process can therefore be blocked by drugs that depolymerize the microtubule-based transport (e.g. Noco, see above), BFA affecting GTPase Arf1-activation (Damm et al. 2005), inhibitors of proteasomal degradation, e.g. MG-132, and ER Ca^{2+}-homeostasis, e.g. Thapsigargin (Schelhaas et al. 2007) which could be reproduced in this work (Fig. 49).

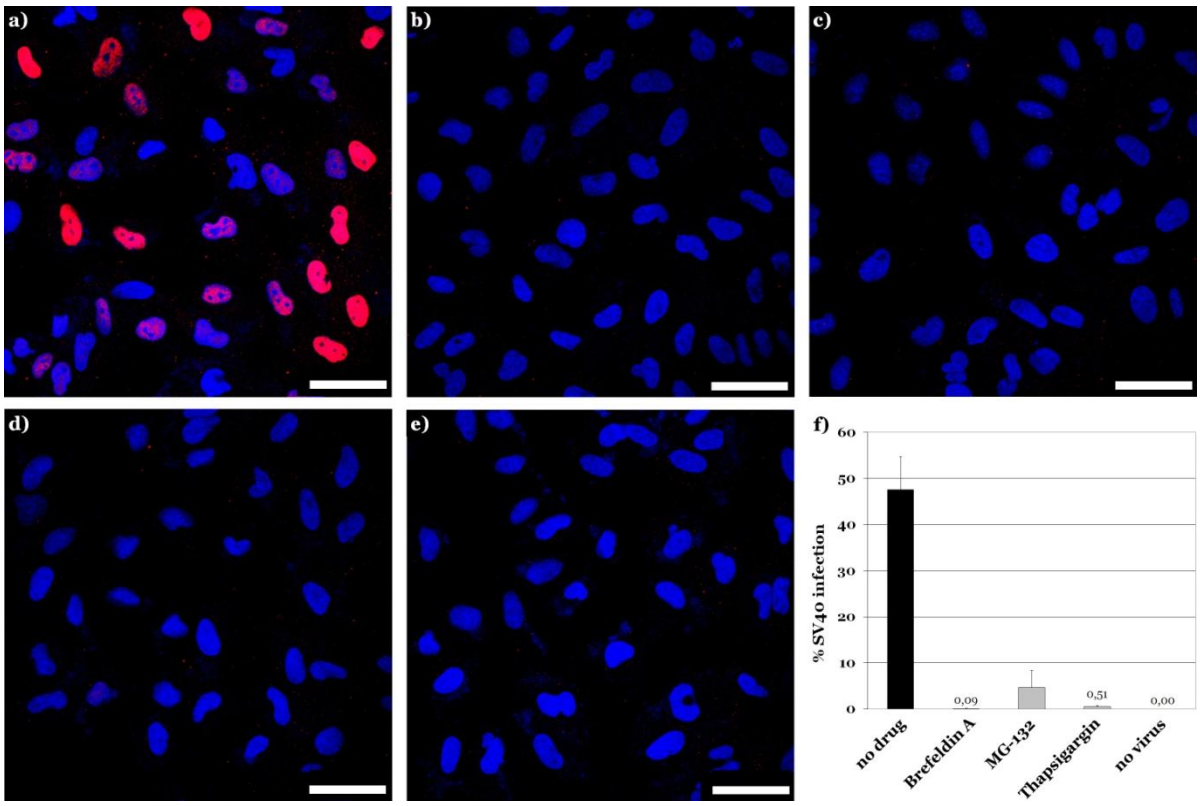

Figure 49: SV40 infection in CV-1 cells relies on functional GTPase Arf1-activity and ER-associated processes. Cells were left untreated (a) or preincubated with 0.1 µg/ml Brefeldin A (b), 1 µM Thapsigargin (c) and 20 µM MG-132 (d) for 30 min at 37°C and subsequently infected with 3.00E+03 GE. Immunostaining for early large T-antigen expression (red) and nuclei (blue) was performed 10 h p.i. e) uninfected control. f) Five randomly chosen fields were analyzed for the amount of cells expressing large T-antigen. Data were expressed as percentage ± SD of T-antigen expression in untreated cells. Scale bars: 50µm.

The HBV infection could not be blocked by Dynasore (Fig. 24) and was shown to be independent of low endosomal pH (Fig. 36). Additionally, PTH did not show cav-1-expression (Fig. 27), therefore the entry mechanism might resemble the uptake of SV40 in cav-1 deficient cells (see above). Furthermore, the disulfide bond-containing S-domains of HBV which are important for infection (Abou-Jaude et al. 2007; Grün-Bernhard 2008) perhaps need to be reduced during the entry process. This could take place in the ER and therefore resemble the SV40 infection mechanism (see above). To test this, the same concentrations of BFA, Thapsigargin and MG-132 as in the SV40-approach were used during HBV infection. Inhibition of Arf1-GTPase activation with BFA caused a minor reduction in secreted HBsAg-signal (Fig. 50b) but hardly no difference in cccDNA-formation of incoming viruses was observed (a). Pertubation of ER-associated processes using MG-132 or Thapsigargin had no influence on HBV infection (c and d).

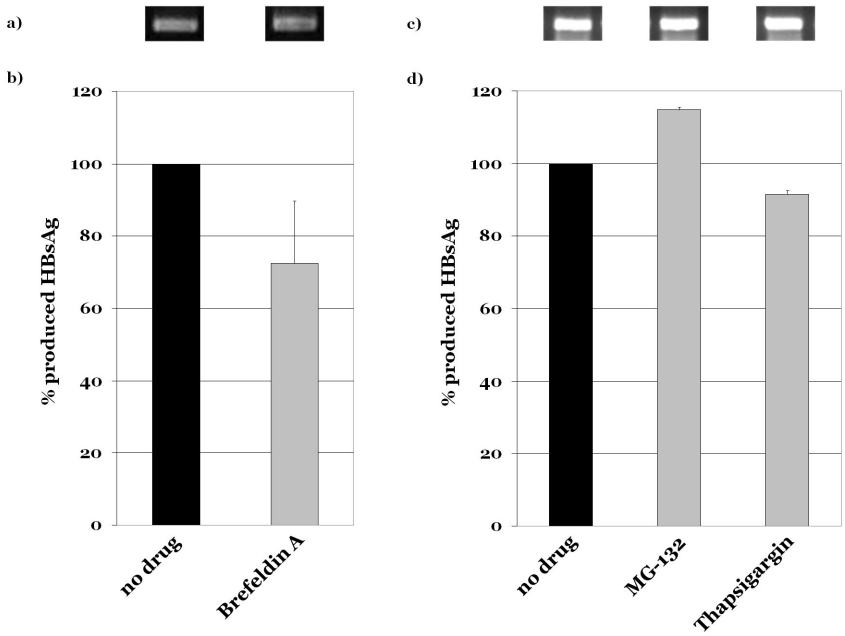

Figure 50: Effect of Brefeldin A and inhibitors of ER-processes on HBV infection of PTH. Prior infection with purified plasma-derived HBV virions (5,48E+09 GE) the cells were preincubated with Brefeldin A (1 µg/ml), MG-132 (20 µM) or Thapsigargin (1 µM) for 30 min at 37°C. cccDNA-formation of incoming viral particles was determined 20 h p.i. by PCR and detected by gel electrophoresis (a+c). Newly secreted HBsAg was measured 14 days p.i. (b+d). Data in b) and d) represent two independent experiments ± SD.

Table 4 summarizes the previously shown results gained with the different markers and pharmaceutical inhibitors.

Table 4: Summarized results

Virus/ marker		**HBV**	**SFV**	**SV40**	**Sendai**	**HRP**
Entry mechanism		?	CME	Caveolae/rafts	Direct fusion with PM	Fluid phase
Mechanisms, conditions or markers implicated:						
Endocytosis	Sucrose	+	+	+	-	+
Dynamin	Dynasore	-	+	+	-	-
Cholesterol-rich rafts	MßCD	- *)	n.d.	+	n.d.	n.d.
Na^+/H^+-exchangers	EIPA	-	n.d.	n.d.	n.d.	+
pH	Bafilomycin A1	-	+	n.d.	n.d.	n.d.
	NH_4Cl	-	+	n.d.	n.d.	n.d.
	Monensin	-	+	n.d.	n.d.	n.d.
Cytoskeleton	Jasplakinolide	+	-	-	n.d.	+
	Cytochalasin D	+	-	+	n.d.	+
	Nocodazole	+	-	+	n.d.	n.d.
Retrograde pathway	Brefeldin A	-	n.d.	+	n.d.	n.d.
	MG-132	-	n.d.	+	n.d.	n.d.
	Thapsigargin	-	n.d.	+	n.d.	n.d.

+ = inhibition; - = no inhibition

*) present work and Bremer et al. 2009

Abbreviations: CME, Clathrin-mediated endocytosis; EIPA, 5-[N-ethyl-N-isopropyl] amiloride; HRP, horseradish peroxidase; MßCD, Methyl-ß-Cyclodextrin; n.d., not determined; PM, plasma membrane

4.8 Transfection of PTH

4.8.1 Lipofection vs. electroporation

Besides using pharmaceutical inhibitors to study different internalization pathways it is possible to target key proteins of particular cellular endocytic pathways by introducing dominant-negative (dn) mutant versions of those into the cells. One way to accomplish that is transfection of the cells with expression vectors encoding dn-mutant proteins. Unfortunately, the transfection of primary cells is challenging since most methods working effectively for cell lines in culture fail to yield satisfying results in primary cells. The Amaxa®Nucleofector technology (Amaxa) provides a technique designed for primary cells and hard-to-transfect cell lines based on the method of electroporation and was compared with the lipofection agent FuGene® (Roche). PTH were transfected with low endotoxin pmaxGFP-plasmid DNA either two days after isolation (FuGene®; adherent cells) or directly after isolation (Amaxa®; suspension cells). Fig. 51 shows representative images of GFP-expression 48 h post-transfection. In the FuGene®-approach only the smaller epithelial-like cells in the space between the hepatocytes showed GFP-expression (a, arrowheads). The Amaxa®Nucleofection indeed allowed the transfection of hepatocytes although only very few cells showed GFP-expression (b, arrowheads).

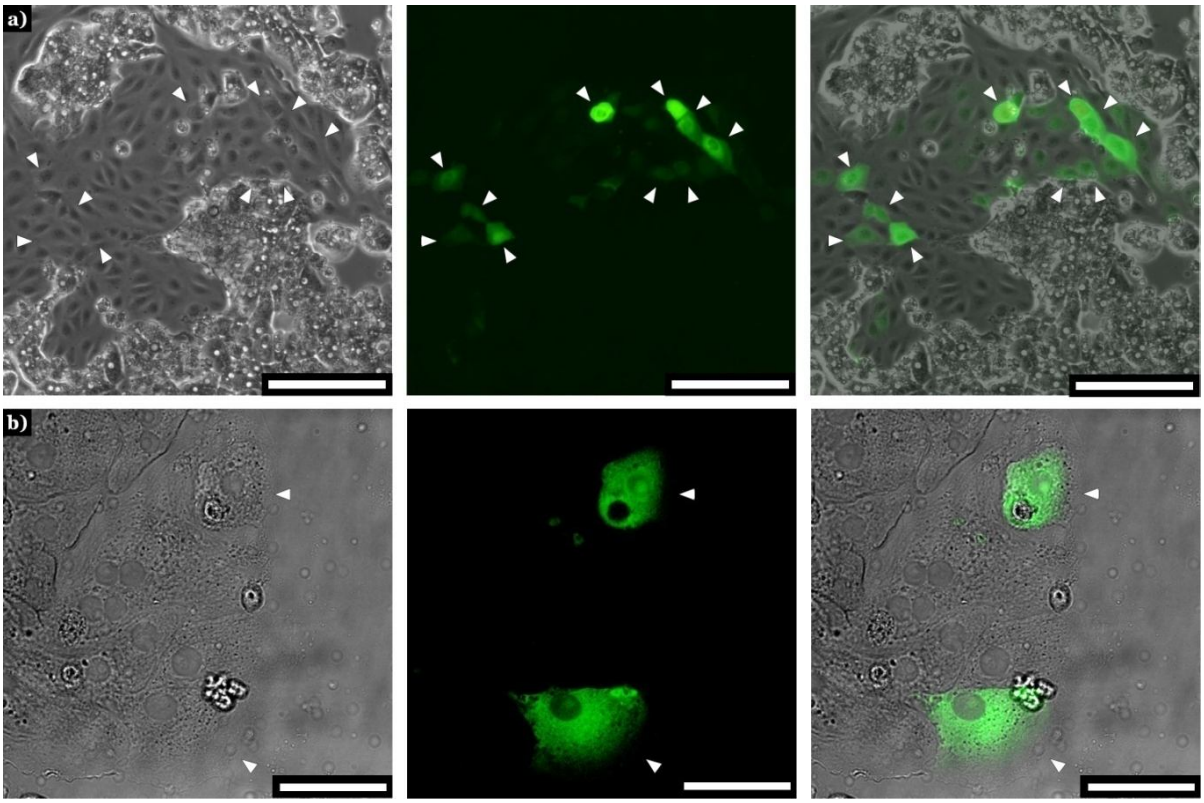

Figure 51: Transfection of PTH. PTH were transfected with endofree pmaxGFP-plasmid DNA and GFP-expression was checked after 48 h. a) FuGene-transfected cells, b) Amaxa-transfected cells. Representative pictures are shown. Scale bars: a) 200 µm, b) 50 µm.

4.8.2 Transduction by Baculoviruses

Gene delivery via “BacMam-viruses”, recombinant baculoviruses containing mammalian cell-active expression cassettes, was first demonstrated in primary human hepatocytes (Kost et al. 2005). Besides insect cells, baculoviruses can also enter mammalian cells and direct the expression of e.g. autofluorescent cellular proteins localized to specific intracellular compartments. PTH were transduced the day after plating with the commercial available “Organelle Lights™” reagent (Invitrogen) encoding for the endosomal Rab5-protein fused to RFP (red fluorescent protein). Expression is illustrated in Fig. 52 showing only few cells expressing the recombinant protein (arrowheads).

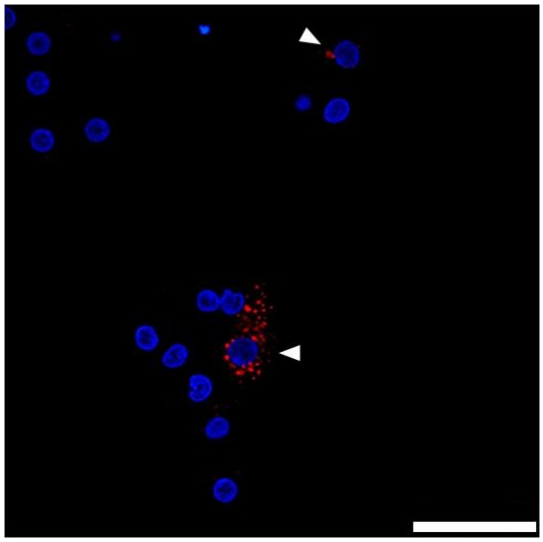

Figure 52: Transduction of PTH. PTH were transduced with Organelle Lights™ BacMam reagent (Invitrogen) encoding autofluorescent Rab5-RFP (red fluorescent protein) which localizes to endosomes. Rab5-expression was checked 48h post-transduction (red); DAPI-staining of nuclei (blue). Representative picture is shown. Scale bar: 50 µm.

5. Discussion

5.1 Binding and uptake of HBsAg

Attachment of viral particles to cell surface structures of the host is a prerequisite for entry and subsequent infection. Previous work has shown that attachment of HBV to susceptible hepatocyte cultures and subsequent infection depends on the preS1 domains in the viral envelope. Since HBV particles are difficult to obtain in large amounts, many experiments in this work were done with preS1-rich HBsAg subviral particles which are comparable to the viral envelope. It was shown that these particles bound to PTH with an uneven distribution within the hepatocyte population. This heterogeneity supposedly arises from different phenotypic states of the cells and their activities and thus determines cell-to-cell variability in viral infection (Snijder et al. 2009). On the single-cell level, the confinement of HBsAg in distinct patches could argue for an association with specific membrane areas, e.g. raft microdomains, and display endocytic spots but this has to be verified in the future. The strongest binding was observed at surface protrusions, probably microvilli or lamellipodia. A similar staining pattern of HBsAg to PTH was observed by Glebe et al. (2003) using conventional immunohistochemistry. Perhaps, these protrusions are enriched in HBV receptor(s) that are still not defined. Binding to those structures may also facilitate the entry of viruses by inducing retrograde movement on the host membrane towards the cellular body (Lehmann et al. 2005). Such actin- and myosin-dependent “surfing” on cellular membranes has already been described for different viruses, such as retroviral Murine Leukemia Virus (MLV), Ad2, HPV-16 or Vaccinia Virus, and seems particularly important for viral transmission (Lehmann et al. 2005; Mercer and Helenius 2008; Schelhaas et al. 2008; Burckhardt and Greber 2009). Furthermore, PTH supported, in contrast to non-susceptible cells, the uptake of HBsAg into a not yet known compartment.

5.2 Difficulties in studying endocytic processes

By now, it is evident that mammalian cells have multiple endocytic pathways with an ever increasing number of novel mechanisms being discovered. Furthermore, the knowledge about distinct pathways is still growing and the increasing quantity of alternative cofactors, adaptors and accessory proteins reveal an unexpected complexity of endocytic mechanisms (Marsh and Helenius 2006). However, one has to take great care when comparing results that have been made in distinct cell types, since specialized cells may have individual pathways occuring in varying proportions in some types but may be completely absent in others (Doherty and McMahon 2009). In addition, it is possible that modes of immortalization of cell lines or their repeated passage during cultivation could have consequences on how endocytic events are configured (Doherty and McMahon 2009; Kumari et al. 2010). Also varying conditions in a same cell type, e.g. cell density or adhesion, as well as differences in the experimental procedures, can lead to a switch to

another uptake route of the same endocytic cargo (Mayor and Pagano 2007; Sandvig et al. 2008). Finally it should be considered, that not all endocytic mechanisms identified *in vitro* need to reflect the situation *in vivo* since viruses also adapt to growth conditions in tissue culture (Marsh and Helenius 2006).

5.2.1 Methods for the classification of endocytic mechanisms

Several tools and approaches can be used to classify the different endocytic mechanisms and are discussed in the following. Identification of the ultrastructural morphology by EM provides the simplest way to define pathways. Until now, four different structures have been determined: the electron-dense coat of CCPs, flask-shaped invaginations (i.e. caveolae or similar structures containing flotilins), larger vesicles originating from macropinocytic or phagocytic uptake and polymorphous tubular structures (Hansen and Nichols 2009). This method, however, requires fixed samples. Thus, it is possible that certain structures which are sensitive to the fixation procedure, cannot be visualized at all (Doherty and McMahon 2009). In addition, one cannot be sure that the observed invaginations always represent nascent pits and really would have undergone scission from the PM before fixation (Hansen and Nichols 2009). Also, tubular structures may appear spherical in a cross section leading to misinterpretations (Doherty and McMahon 2009).

Another classification criterion for defining different endocytic mechanisms can be utilization of certain cargoes, such as fluorescently labeled analogues of lipids, labeled or clustered GPI-APs, toxins and viruses (Mayor and Pagano 2007). It is noteworthy, that although some cargoes enter exclusively by one pathway, most ligands can be taken up by different processes depending on the cell type or, in the same cell type, sometimes simultaneously (Nichols and Lippincott-Schwartz 2001; Sieczkarski and Whittaker 2002; Rust et al. 2004; Mayor and Pagano 2007; Doherty and McMahon 2009). However, those internalization pathways do not always lead to a productive infection or toxicity and therefore not necessarily reflect the *in vivo*-situation (Nichols and Lippincott-Schwartz 2001; Sieczkarski and Whittaker 2002). Furthermore, labeling with fluorescent dyes/proteins or clustering into distinct microdomains might alter the internalization route (Doherty and McMahon 2009). Finally, also the amount of virions or particles used in the experimental setup can affect the uptake pathway.

In addition to the above-mentioned approaches to classify certain pathways, extensive studies have been carried out to examine their sensitivity to certain drugs or to identify their dependencies on specific molecular markers, such as certain lipids, proteins and kinases (Doherty and McMahon 2009). However, one should keep in mind that some regulatory factors, such as GTPases, are true key players that may influence more than one individual uptake mechanism (Mayor and Pagano 2007). There are various tools to interfere with cellular markers ranging from RNA interference (RNAi) techniques, microinjection,

dominant-negative mutant proteins to pharmacological inhibitors (Graessmann and Graessmann 1983; Tuschl 2001; Sieczkarski and Whittaker 2002; Doherty and McMahon 2009). Microinjection is a technique for transferring exogenous material, such as RNA molecules, inhibitory antibodies or peptides, into cultured cells. The protein-of-interest is then either not produced (upon post-transcriptional silencing by small RNAs) or directly inhibited by bound antibodies/peptides and thus not functional. However, this displays a rather complex method in which special equipment is needed. Since only individual cells are targeted, this method is applicable for analysis on the single-cell level but not for cell-culture-wide approaches.

Dominant-negative (dn) mutant variants of cellular proteins provide a specific way to analyse their relevance for defined pathways within the cell (Sieczkarski and Whittaker 2002). The dn-mutant version, when expressed, results in an inhibitory phenotype by suppression of the endogenous wild-type protein (Mayor and Pagano 2007). The insertion of those mutants is usually accomplished by transfection. Unfortunately, primary cells cannot be efficiently transfected by the commonly used protocols (Glebe and Urban 2007). Transfection of differentiated PTH failed indeed when the conventional lipofection agent FuGene® was used. Only the proliferating non-hepatic cells, with an epithelial-like morphology, displayed GFP-expression. Therefore specialized methods were tested in the present work. The Nucleofector technology permits transfection of particularly primary cells and hard-to-transfect cell lines which divide more slowly or are completely mitotically inactive (Gresch et al. 2004). Transfection efficiencies obtained with this technology using different primary cells of human origin (hepatocytes were not included) ranged from 30-60% with varying mortality rates depending on the cell type (Hamm et al. 2002; Gresch et al. 2004). Using this method, transfection of PTH was possible, though the efficiency of <10% was very low. Also transduction with baculoviruses failed to achieve higher efficiencies. Since only one in several thousand HBV particles is infectious in the PTH system and not all cells seem to have similar binding capacities, only a portion of about 10-20% hepatocytes can be infected at all (Glebe et al. 2003). A potential inhibitory effect of distinct dn-mutant proteins would probably remain undetected if an infection of non-transfected cells leads to compensation in measured HBsAg levels. Therefore, these methods were considered to be inappropriate for the cell-culture-wide analysis of HBV entry into PTH. Furthermore, a general drawback of this method is highlighted by the fact that cells, expressing dn-mutant proteins, can completely compensate for the loss of this particular route by upregulation of an alternative pathway (Damke et al. 1995). This physiological regulation of uptake mechanisms may even induce pathways that are nonexistent before (Marsh and Helenius 2006; Doherty and McMahon 2009).

Another tool for direct probing of endocytic mechanisms in living cells is the use of pharmacological/chemical inhibitors (Ivanov 2008). These provide several advantages over

previously described methods: The application is very easy since the cell culture medium simply has to be replaced by drug-containing medium. Pharmacological inhibitors are supposed to equally affect all cells in a population and the effects can be easily titrated. Finally, the cells are usually exposed to the drugs over a short period which is thought to exclude compensatory uptake mechanisms and reduces the likelihood of delayed side effects (Ivanov 2008). However, one has to keep in mind that a distinct marker can contribute to various pathways and therefore inhibitory drugs might affect more than one pathway (Mayor and Pagano 2007; Sandvig et al. 2008). The current information about hepadnaviral entry mainly derived from the DHBV model system in which chemical drugs were used to reveal early events of infection (Glebe and Urban 2007). However, one has to be aware of the differences between HBV and DHBV and the possibility that various uptake strategies might have evolved in the two virus genera (Funk et al. 2007; Glebe and Urban 2007). To elucidate the entry mechanism of HBV into PTH pharmacological inhibitors were used as well. Possible nonspecific effects of the drugs (Ivanov 2008) should be uncovered by employing several control viruses and substrates with established uptake routes.

5.3 Endocytosis vs. plasma membrane fusion of HBV

In this study, a dose-dependent inhibition of HBsAg uptake and HBV infection was achieved by increasing hypertonic sucrose concentrations. An explanation for this observation might be that high sucrose concentrations were shown to cause dispersion and, with time, disappearance of cellular clathrin lattices at the inner leaflet of the PM and were therefore thought to impair CME exclusively (Daukas and Zigmond 1985; Heuser and Anderson 1989). This is in line with the sucrose-dependent inhibition of SFV infection, known to enter via CME, both in BHK and PTH. More recently, it has been postulated that extracellular hypertonicity interferes with endocytic processes in general by inducing cell shrinkage thereby remodeling the actin cytoskeleton (Ivanov 2008). This could also explain the effect that the infection of the second control virus, namely SV40 known to enter via caveolae/raft-dependent endocytosis, was also blocked by hypertonic sucrose dose-dependently. In contrast, hypertonic sucrose treatment did not inhibit SeV infection which starts with direct fusion with the PM thus bypassing endocytic uptake. Combining these results, it can be postulated for the first time that HBV enters susceptible cells (here: PTH) by an endocytic step rather than by direct fusion with the PM. One might argue that this displays a special situation in hepatocytes from *Tupaias* since these animals are not a natural host for HBV and therefore the “real” infection pathway in human hepatocytes is different. However, similar experiments with the HBV-susceptible human hepatoma cell line HepaRG and identical viral HBV inocula have led to comparable results (König 2010), indicating that the postulated HBV entry mechanism by endocytosis is similar for human and *Tupaia* hepatocytes. Since infection experiments with the HepaRG cell line always

showed a low infection rate and strong heterogeneity in susceptibility (due to a difficult re-differentiation process in cell culture necessary for susceptibility; König 2010; Gripon et al. 2002), all HBV infection experiments in the present study were done with PTH. Due to the lack of a suitable HBV-infection model, Köck et al. used the related duck hepatitis B virus (DHBV) and primary duck hepatocytes (PDH) to study DHBV uptake and infection. By inducing energy depletion of the cells, they observed prevention of DHBV uptake and concluded that DHBV enters its host cells by endocytosis (Köck et al. 1996).

Concerns that the inhibition of HBV infectivity by sucrose may be caused by an altered interaction of the viral lipids with the PM can be excluded since the uptake of the non-enveloped SV40 was affected to a similar extent as the internalization of enveloped viruses (SFV). Moreover, the used HBV viral- and subviral particle-fractions have been purified by a sucrose gradient and the remaining sucrose amounts (43% for the virion fraction) neither altered particle integrity nor infectivity (Glebe et al. 2003; Glebe et al. 2005). This argues for an impairement of endocytotic events by sucrose rather than effects on the viruses themselves.

After showing that an endocytic step is necessary for HBV entry, the next task was to identify the cellular endocytic pathway(s) which mediate(s) HBV entry. This was done with the use of specific chemical inhibitors of key enzymes or proteins of the respective pathways.

5.4 Dynamin-dependent endocytosis

5.4.1 Clathrin-mediated endocytosis

CME is an extremely important endocytic mechanism and the most commonly used route for viruses to enter their host cells (Marsh and Helenius 2006). CME is a constitutive and fast pathway that delivers its cargo within a few minutes from the surface to intracellular organelles. SFV was the first virus shown taking CME as productive infectious route and many other viruses, such as VSV, Ad2 and 5, as well as Influenza Virus followed (Helenius et al. 1980; Cureton et al. 2009; Mercer et al. 2010). Regarding the just mentioned examples, the versatile nature of CME becomes apparent: not only small or medium-sized viruses, like SFV (60-70 nm) and Influenza (90-120 nm) use this pathway, but also larger particles, such as the bullet-shaped VSV (180 x 70 nm) and even bacteria (Cossart and Veiga 2008).

Former HBV infection studies in PTH showed that chlorpromazine, which prevents the assembly of CCPs at the PM (Wang et al. 1993), did not block HBV infection (Grün-Bernhard 2008). Since this inhibitor is considered to have unspecific effects on other intracellular enzymes (Sieczkarski and Whittaker 2002; Ivanov 2008) utilization of Dynasore, a specific inhibitor of dynamin (Macia et al. 2006), was preferred. Given the fact that CME strictly relies on functional dynamin, preincubation with the drug Dynasore

completely abolished CME-dependent SFV infection in both cell types, BHK and PTH. As expected, direct fusion of SeV with the PM was not impaired, neither in CV-1 cells nor in PTH. Preincubation with Dynasore did not affect HBsAg uptake or HBV infection, indicating that dynamin-activity is not needed for these processes. Therefore, it is likely that HBV does not use CME or any other dynamin-dependent pathway as endocytic route.
Cooper and Shaul proposed CME to be the uptake mechanism used by recombinant HBV core particles in HepG2 and Cos7 cells (Cooper and Shaul 2006). Neither HepG2 cells nor Cos7 cells, an immortalized kidney cell line, are susceptible for HBV infection (Glebe and Urban 2007) and free HBV core particles do not occur in the plasma of infected individuals. Furthermore, the authors used a huge and unphysiological amount of HBV core particles for their studies (Cooper and Shaul 2006). Therefore, those results are not relevant for the natural HBV infection process, but represent more likely an example for the utilization of CME as a constitutive and efficient uptake mechanism.

5.4.2 Caveolin-mediated endocytosis

Lipid raft-mediated endocytosis has increasingly been brought in connection with clathrin-independent entry pathways. These microdomains are rich in sphingolipids and cholesterol and are thought to occur in different manifestations (Parton and Richards 2003). One subtype of lipid rafts are caveolae which are formed principally by the assembly of caveolins, especially cav-1 (Simons and Toomre 2000; Kumari et al. 2010). Cav-1 can form higher-ordered oligomers and directly binds membrane cholesterol (Murata et al. 1995), therefore caveolae represent structures particularly enriched in this component (Doherty and McMahon 2009). Inhibition of this pathway can be achieved by several drugs with sterol-binding ones, such as Nystatin or MßCD, being the most effective (Sieczkarski and Whittaker 2002). Cholesterol depletion leads to flattening and disassembly of caveolae and has been shown to block endocytosis of different caveolin-dependent cargoes (Doherty and McMahon 2009; Kumari et al. 2010). Our group is the first to show that HBV infection of PTH is not dependent on cholesterol within the cellular PM, since an extraction of cholesterol by MßCD (up to 10 mM) did not affect the HBV infection (present work and Bremer et al. 2009). In the present study, the caveolae-dependent SV40 infection of CV-1 cells was completely abolished even at low concentrations (3 mM MßCD). Also, treatment of PTH with genistein, a Src-family kinase inhibitor known to block the caveolae-dependent entry pathway (Nichols 2003), had no effect on HBV infection (Bremer et al. 2009). However, the most important results came from the treatment of the cells with Dynasore, inhibiting besides CME also dynamin-dependent caveolae-mediated endocytosis. While abrogating SV40 infection as expected, it had no impact on HBV binding, uptake and infection.

Recently, it was hypothesized that HBV infection of the HepaRG cell line depends on caveolin-mediated endocytosis (Macovei et al. 2010). As already mentioned, this human hepatoma cell line is permissive for HBV infection only after an unknown differentiation process induced by treatment with DMSO and hydrocortisone (Gripon et al. 2002). The authors used the HepaRG cell line to stably express dn-mutant variants of cav-1 and dynamin-2 to investigate the implication of caveolae in HBV internalization (Macovei et al. 2010). Unfortunately, it was not convincingly shown that in dn-mutant expressing cells, a complete inhibition of HBV infection has taken place. Moreover, treatment of the original HepaRG cell line with pharmacological inhibitors, like MßCD or genistein, did also not impair infection significantly which is consistent with our previously published data using PTH (Bremer et al. 2009). In our hands, cholesterol depletion of re-differentiated HepaRG cells with MßCD had also no effect on HBV infection (König 2010). Interestingly, the experiments to compare the cav-1 content of PTH with that of other cell types revealed that PTH did not express cav-1, which is consistent with other reports stating that hepatocytes per se have only few or no caveolae (Fielding and Fielding 2000; Vainio et al. 2002; Ikonen et al. 2004; Woundenberg et al. 2010). In contrast, HepaRG cells showed a very strong expression of cav-1 particularly in their differentiated and HBV-susceptible state. Since overexpression of cav-1 strongly increases the number of caveolae in a given cell type, it simultaneously reduces overall membrane fluidity and therefore even inhibits caveolin-mediated endocytosis (Doherty and McMahon 2009). For that reason, it will be important to elucidate the specific function and regulation of caveolar assembly and budding in the HepaRG cell line to find out whether HBV uses this pathway as entry portal in that particular cell type. In addition, caution is advised since there is always the possibility that signaling pathways responsible for controlling caveolar events are somehow misregulated in long term cultured cell lines (Hansen and Nichols 2009).

5.5 Dynamin-independent endocytosis

5.5.1 Phagocytosis

Phagocytosis occurs mainly in specialized cells of the immune system and beside its function of internalizing and destroying opsonised material, this process turned out to be an entry portal for certain bacteria (Kinchen and Ravichandran 2008). Interestingly, although not commonly used for entry, also large viruses, such as HSV-1 or Mimivirus, exploit this pathway (Clement et al. 2006; Ghigo et al. 2008). One reason for this may simply be their size which probably makes it more difficult to use standard-sized endocytic vesicles (Schelhaas 2010). In contrast to macropinocytosis, phagocytosis depends on specific ligand-receptor interactions and could therefore offer a cell type-specific entry pathway. Since HBV infection is dependent on the interaction of its preS1-domain with a yet uncharacterized receptor (Glebe and Urban 2007) the possibility of a receptor-induced phagocytic entry was

examined using HBsAg and fluorescently labeled bacteria as a marker for phagocytosis. The bacteria were observed exclusively in smaller non-hepatic cells whereas HBsAg particles were found in PTH only. This suggests that PTH are not capable of phagocytosis. Moreover, since this mechanism seems to be dependent on dynamin in some cell types (Doherty and McMahon 2009) it apparently does not display the endocytic pathway used by HBV.

5.5.2 Macropinocytosis

In contrast to the above-mentioned processes, macropinocytosis describes a rather unspecific endocytic mechanism used for internalization of large amounts of extracellular compounds, such as fluids and solutes, and does not rely on a defined ligand-receptor-binding (Doherty and McMahon 2009). However, macropinocytosis can be transiently induced by external stimulation, some pathogens themselves trigger this process by binding to cell surface proteins which has been shown for Ad2 (Meier et al. 2002). Experiments in the PTH system showed that, in contrast to the results obtained with Ad2, prebinding of HBV did not lead to transient stimulation of fluid phase uptake. Neither Dynasore nor Blebbistatin had an effect on the uptake of HRP, a known fluid phase marker (Haigler et al. 1979). This shows, that dynamin, which has been reported to be required for this process in some systems (Mercer and Helenius 2009), is not needed for macropinocytic endocytosis in PTH. Induction of large membrane extrusions, so-called blebs, during macropinocytic entry of Vaccinia Virus (Mercer and Helenius 2008) as well as virus “surfing” along filopodia (Lehmann et al. 2005), is reduced upon treatment with Blebbistatin (Straight et al. 2003; Mercer and Helenius 2008). Blebbistatin is a specific inhibitor of class II myosins (Straight et al. 2003) which are anchored in the actin mesh at the cell body/cortex and act as molecular motors fulfilling essential functions, such as muscle contraction, cytokinesis, neurite outgrow and retraction, in most eukaryotic cells (Kovacs et al. 2004; Burckhardt and Greber 2009). Inhibition of myosin II by Blebbistatin prevents retrograde actin flow, virus drifts and infection (Burckhardt and Greber 2009). Bleb formation in PTH seems either not to exist or does not contribute to macropinocytosis, since no inhibition of HRP internalization in the presence of Blebbistatin was observed. In contrast to that, impairment of the cytoskeleton function by Jas or CytoD, brought a reduction in HRP uptake reflecting the expectation that actin modulation is definetely required for macropinocytosis regardless in which cell types (Doherty and McMahon 2009). Further cellular factors required for macropinocytosis are numerous, interconnected with other endocytic mechanisms and depend, to a certain extent, on the cell type (Sieczkarski and Whittaker 2002; Doherty and McMahon 2009; Mercer et al. 2010). However, Na^+/H^+exchangers have been implicated to be crucial for this mechanism which distinguishes it from other types of endocytosis (Koivusalo et al. 2010). The exact mechanism of action of this drug remains largely unknown, but recently it has been postulated that amilorides inhibit the macropinocytic

process by lowering submembranous pH and prevent signaling of distinct GTPases (Koivusalo et al. 2010). Specific inhibition of macropinocytosis using EIPA, a blocker of Na^+/H^+exchangers (Ghigo 2010), reduced the uptake of the fluid phase marker HRP, confirming the susceptibility of this process towards this drug. However, it had no impact on the internalization of HBsAg and HBV infection. Based on the observations that binding of HBV did not stimulate macropinocytic activity of PTH and neither HBsAg internalization nor HBV infection was blocked by EIPA, one can postulate that HBV does not enter PTH via macropinocytosis.

5.5.3 CLIC/GEEC, flotilin and TEM pathways

Besides macropinocytosis, another mechanism for fluid phase uptake has been discovered a few years ago: the CLIC/GEEC pathway describes, contrary to macropinocytosis, a constitutive route which is dependent on the small GTPase cdc42 (Sabharanjak et al. 2002). Cargo delivery through this route does not occur in classical small spherical vesicles but involves larger, polymorphous structures appearing almost tubular in ultrastructural analysis. CLIC/GEEC membranes can either fuse with early endosomes or traffic directly to compartments such as the Golgi (Doherty and Lundmark 2009) possibly providing a direct route to perinuclear regions. Cells may have evolved this mechanism especially for the efficient uptake of large amounts of cargo and/or fluid within one single budding event (Mayor and Pagano 2001; Polishchuk et al. 2009). Treatment with Brefeldin A (BFA), a fungal metabolite known to affect Arf1-activation, lead to an enhanced fluid phase uptake of HRP which has been already described (Kumari and Mayor 2008). In contrast to that, HBV infection was slightly reduced when this drug was used, suggesting this pathway to be irrelevant for HBV entry. More detailed information about the molecular machineries involved in this endocytic event is still lacking, but it has been suggested that it is sensitive to cholesterol depletion and is, at least in some cells, dynamin-dependent (Mayor and Pagano 2007; Hansen and Nichols 2009). If this also proves true for PTH, it would ultimately exclude this pathway for HBV uptake, since neither MßCD (see above and Bremer et al. 2009) nor Dynasore (see above) have an impact on infection. More data on the roles of different cellular marker proteins will resolve this issue in the future.

Another specific clathrin-independent endocytic pathway is suggested to rely on flotilins which assemble into microdomains similar to those formed by caveolins (Hansen and Nichols 2009). The uptake of proteoglycan-binding ligands has been reported to be flotilin-dependent (Payne et al. 2007) and hence could be a possible route for HBV which binds to heparan-sulfate proteoglycans (HSPGs) as described by our group (Leistner et al. 2008) and others (Schulze et al. 2007). However, Payne et al. found this pathway to be dependent on dynamin and, based on their observations, they finally suggested that this mechanism may be used by proteoglycan-binding ligands that lack secondary receptors (Payne et al.

2007). This would exclude HBV, whose infection is not dependent on dynamin action (present work) but on (a) specific receptor(s) (Glebe and Urban 2007).
Whether the recently discovered invasion mechanism for HPV-16, which is clathrin-, caveolin-, flotilin-, lipid raft-, dynamin-independent and involves tetraspanin-enriched microdomains (TEMs) (Spoden et al. 2008; Mercer et al. 2010) could also come into question for HBV entry needs to be tested in the future.

5.6 pH-dependence of HBV infection

The pH regulation within endosomal compartments is mainly modulated by v-ATPases, which are ATP-driven multisubunit proton pumps, ubiquitously expressed in all eukaryotic cells (Jefferies et al. 2008). The establishment of a low pH within cellular organelles can be prevented by several lysosomotropic agents, such as BafA1, which specifically inhibits the v-ATPases, the ionophore Monensin or the weak base NH_4Cl (Bowman et al. 1988; Glomb-Reinmund and Kielian 1998). These drugs raise the pH of endocytic organelles and prevented the establishment of the SFV infection in BHK cells and PTH in the present work, but did not impair HBsAg uptake or cccDNA formation in the PTH system. The amount of newly secreted particles after 14 days was also not reduced, but rather showed increased HBsAg amounts. The reason for this enhanced infection or production can currently not be explained, however, a similar phenomenon was observed in HepaRG cells (König 2010) and has also been described in the DHBV system (Rigg and Schaller 1992). Other studies that investigated the requirement of acidification during DHBV infection came to contradictory results: Offensperger et al. observed inhibition of infection by using NH_4Cl (Offensberger et al. 1991). Since the authors used long incubation times of up to several days, it is likely that not only the initiation of infection, but also late steps of the viral life cycle were affected, which has already been reported (Carillo et al. 1984; Cassell et al. 1984; Marsh and Helenius 1989). In other studies where the NH_4Cl-treatment lasted only a few hours, no inhibition was observed (Rigg and Schaller 1992; Funk et al. 2006). Although the results obtained with NH_4Cl indicated that a low pH is indispensable for the establishment of a productive DHBV infection, further experiments showed, that virions are transported from early to late endosomes and can thereby be blocked by BafA1 (Chojnacki et al. 2005). Funk et al. observed the same in PDH and could partially rescue the inhibited phenotype with the ionophore Monensin (Funk et al. 2006). BafA1 not only destroys the proton gradient generated by the v-ATPases but also the formation of ion motive force across the endosomal membrane (Sun-Wada and Wada 2010) which can be partially overcome by the presence of Monensin (Malecki et al. 2002). Therefore, Funk et al. concluded that the endosomal transmembrane potential generated by the v-ATPases is at least partially necessary for DHBV infection (Funk et al. 2006). In contrast to that, HBV infection of PTH (present

work) as well as HepaRG cells (König 2010; Glebe and Urban 2007) is not influenced by BafA1, indicating, that HBV and DHBV might use different endocytic pathways.

5.7 Role of the cytoskeleton for HBV infection

Actin polymerization is certainly required for some CME (Doherty and McMahon 2008) noting, for example the internalization of VSV (Cureton et al. 2009). In contrast to that, the uptake of SFV, known to be taken up via CME, was shown to be unaffected by drugs that interfere with the actin cytoskeleton in BHK cells and PTH in the present study. This suggests that the decision whether actin provides assistance or not, may in part depend on the cargo (here, e.g. its size). Pelkmans et al. showed that the actin-stabilizing drug Jas reduced SV40 internalization into CV-1 suspension cells and also blocked infection (Pelkmans et al. 2002). However, although Jas is thought to stabilize actin, including the submembranous filaments at the PM, some virus-containing vesicles were endocytosed in the presence of Jas and remained just below the PM (Pelkmans et al. 2002). In the present work, no inhibition of SV40 infection was observed using the same cell line (adherent cells). Since actin disrupting drugs were found to have variable effects in a distinct cell type under different conditions (Fujimoto et al. 2000), given in the present case (with respect to the state of the cells, inhibitor concentrations, incubation period and medium) might explain the conflicting results.

Treatment of PTH with relatively high concentrations of Jas and CytoD, which has led to actin disassembly, reduced HBsAg uptake as well as HBV infection by 50-60% rather than blocking it completely. This seems to be a specific feature of those kind of actin-targeting drugs (Smythe and Ayscough 2006). However, the importance of actin could depend on the physiological state in which the cells find themselves: when cells exhibit abundant filopodia, e.g. CytoD has greater inhibitory effects on viral infection (Lehmann et al. 2005). This could mean that hepatocytes which possess increased amounts of F-actin-rich microvilli on their surface are more drug-sensitive, whereas cells without those special membrane structures are still able to internalize the virus. Funk et al. argued that the actin cytoskeleton is completely dispensable for a productive DHBV infection of PDH (Funk et al. 2004). However, the CytoD concentration used in their study (20 μM) was noneffective on HBV infection in the present work as well; only higher concentrations lead to a reduced HBsAg signal after 14 days and a lower cccDNA content respectively.

Intracellular trafficking of HBV capsids and incoming DHBV particles was shown to be dependent on active microtubule (MT)-based transport since MT-disruption with Noco prevented capsid transfer towards the nucleus and also DHBV infection (Funk et al. 2004; Rabe et al. 2006). However, the inhibition of DHBV infection in PDH was strong but not complete (Funk et al. 2004) which was also observed for HBV infection in the present work. This is perhaps due to the fact that not all MTs are completely inactivated by the drug and a

few particles are able to reach the nucleus despite the presence of the drug. Furthermore, it has been reported that the different membrane sides of polarized cells are not equally affected by treatment with drugs that interfere with the cytoskeleton (Doherty and McMahon 2008) therefore, the internalization could take place at drug-insensitive spots. An alternative explanation could be that in PTH probably MT independent transport mechanisms exist, e.g. polymorphous structures similar to those observed in the CLIC/GEEC pathway (see chapter 5.5.3) that may provide a direct route to the perinuclear region. However, this needs to be tested in the future.

5.8 Retrograde pathway involved in viral uptake

The retrograde transport pathway, i.e. the endosomal trafficking to the Golgi or ER, is a specialized route taken by some surface glycoproteins and is also hijacked by certain pathogens or pathogenic products (Johannes and Popoff 2008; Pfeffer 2009). Also, in trafficking of SV40 from the PM to the ER this route is crucial for its infectivity (Schelhaas et al. 2007). SV40 enters cells via caveolin-or raft-mediated endocytosis which delivers the virus into the pH-neutral caveosomes (Pelkmans et al. 2001; Damm et al. 2005). From there, SV40 moves along microtubules to the ER (Kartenbeck et al. 1989). Afterwards, the virus benefits from the protein folding and quality control factors present in the ER, which support initial uncoating, i.e. disulfide bond shuffling within the capsid (Schelhaas et al. 2007). As demonstrated in the present work, HBV does not rely on dynamin action for endocytic uptake and does not need a low pH within endosomal compartments for infection. Furthermore, the HBV S-domain contains 8 Cysteine residues, forming inter- and intramolecular disulfide bonds within the antigenic loop that are important during the entry of the virus (Abou-Jaoude et al. 2007; Grün-Bernhard 2008). Those disulfide bonds are essential for infection and possibly have to be reduced during this process so that the core particles can be released. This could possibly take place in the ER and show similarities to the infection mechanism of SV40. Therefore, the sensitivity of HBV infection towards certain drugs, interfering with the SV40 infection of CV-1 cells, was tested. SV40 infection was completely abolished when BFA was present (Richards et al. 2002; Damm et al. 2005). The inhibitory potential of the drug is based on its effects on Arf1, which belongs to a family of regulatory GTPases important for membrane traffic at the ER/Golgi (Richards et al. 2002; Damm et al. 2005; Kahn 2009). In contrast to that, HBV infection was only slightly reduced. The reason for this could be, that BFA has several effects on different membrane sides of polarized cells (Klausner et al. 1992) and internalization of HBV at multiple sides, if occuring at all, would therefore be differentially impaired. Moreover, the effects of Arf-family members may be, at least in some instances, cell type specific (Mayor and Pagano 2007). Therefore, further work needs to be done to characterize the Arf-function in PTH.

In order to infect its host cells, SV40 exploits the ERAD (ER-associated protein degradation)-machinery that is normally used to eliminate misfolded or unassembled proteins by proteasomal degradation (Meusser et al. 2005; Schelhaas et al. 2007). Furthermore, the final dissociation of SV40 capsids seem to occur in the cytosol and relies on the Ca^{2+}-gradient present during ER-release (Schelhaas et al. 2007). Pertubation of these processes by MG-132, which inhibits proteasomal degradation or Thapsigargin, an inhibitor of the ubiquitous ER Ca^{2+}-ATPases (Treiman et al. 1998), impairs the ER-escape of SV40 and blocks infection (Schelhaas et al. 2007). However, neither of those drugs had any effect on HBV infection which indicates that it does not rely on this specialized mechanism for initiation of infection. Since the ER redox system contains many different enzymes which can assist other viruses during their infection (Burckhardt and Greber 2008) it is nevertheless possible that HBV may use a similar entry pathway perhaps by engaging other isomerases or chaperones.

5.9 Future issues

With the *Tupaia* hepatocyte *in vitro* model system, it will be possible to characterize further viral and cellular interactions important for elucidation of the HBV entry mechanism. Several approaches, ranging from EM, single virus particle tracking via confocal microscopy to RNAi screens etc., will allow a better understanding of the behavior of HBV during entry and possibly uncover definite requirements, such as the high-specific receptor(s) and perhaps other accessory proteins and distinct lipid compositions that might play a role in the early events of infection. Identification of the molecular machineries needed may also lead to development of inhibitors that specifically target key proteins or enzymes of the HBV entry process and thereby specifically inhibit infection. HBV is a highly variable DNA virus especially under immunity or antiviral therapy, e.g. due to treatment with reverse transcriptase inhibitors, resulting in escape mutants and drug resistance (Glebe and Urban 2007). The emergence of such mutants would be unlikely if entry inhibitors that target conserved intermediates of the process (e.g. receptor structures), were used, since mutations within the essential preS1-region result in reduction or loss of infectivity. Myrcludex B, an acylated HBV preS1-derived lipopeptide, is such an inhibitor: It was shown to block virus entry *in vitro* and *in vivo* and possibly represents a novel antiviral approach of acute and chronic hepatitis B, similar to the HIV-peptide entry-inhibitor *Fuzeon*/*Enfuvirtide* (Kilby and Eron 2003; Glebe et al. 2005; Gripon et al. 2005; Petersen et al. 2008). Potential application areas of this and future viral entry blockers are: post exposure prophylaxis (e.g. after needle stick injuries), prophylaxis of re-infection in liver transplanted HBV-positive patients and perhaps also during treatment of chronic HBV infections (Glebe and Urban 2007).

6. References

Abou-Jaude D. and C. Sureau (2007). "Entry of hepatitis delta virus requires the conserved cysteine residues of the hepatitis B virus envelope protein antigenic loop and is blocked by inhibitors of thiol-disulfide exchange." J Virol **81**(23): 13057-66.

Aden, D. P., A. Fogel, et al. (1979). "Controlled synthesis of HBsAg in a differentiated human liver carcinoma-derived cell line." Nature **282**(5739): 615-6.

Aderem, A. and D. M. Underhill (1999). "Mechanisms of phagocytosis in macrophages." Annu Rev Immunol **17**: 593-623.

Allen, C. L., D. Goulding, et al. (2003). "Clathrin-mediated endocytosis is essential in Trypanosoma brucei." Embo J **22**(19): 4991-5002.

Almeida, J. D., D. Rubenstein, et al. (1971). "New antigen-antibody system in Australia-antigen-positive hepatitis." Lancet **2**(7736): 1225-7.

Anderson, H. A., Y. Chen, et al. (1996). "Bound simian virus 40 translocates to caveolin-enriched membrane domains, and its entry is inhibited by drugs that selectively disrupt caveolae." Mol Biol Cell **7**(11): 1825-34.

Barker, L. F., F. V. Chisari, et al. (1973). "Transmission of type B viral hepatitis to chimpanzees." J Infect Dis **127**(6): 648-62.

Bartenschlager, R. and H. Schaller (1988). "The amino-terminal domain of the hepadnaviral P-gene encodes the terminal protein (genome-linked protein) believed to prime reverse transcription." Embo J **7**(13): 4185-92.

Bartenschlager, R. and H. Schaller (1992). "Hepadnaviral assembly is initiated by polymerase binding to the encapsidation signal in the viral RNA genome." Embo J **11**(9): 3413-20.

Bartholomeusz, A. and S. Schaefer (2004). "Hepatitis B virus genotypes: comparison of genotyping methods." Rev Med Virol **14**(1): 3-16.

Baumert, T. F., R. Thimme, et al. (2007). "Pathogenesis of hepatitis B virus infection." World J Gastroenterol **13**(1): 82-90.

Beck, J. and M. Nassal (2007). "Hepatitis B virus replication." World J Gastroenterol **13**(1): 48-64.

Benmerah, A. and C. Lamaze (2007). "Clathrin-coated pits: vive la difference?" Traffic **8**(8): 970-82.

Bitzer, M., U. Lauer, et al. (1997). "Sendai virus efficiently infects cells via the asialoglycoprotein receptor and requires the presence of cleaved F0 precursor proteins for this alternative route of cell entry." J Virol **71**(7): 5481-6.

Bock, C. T., P. Schranz, et al. (1994). "Hepatitis B virus genome is organized into nucleosomes in the nucleus of the infected cell." Virus Genes **8**(3): 215-29.

Bossart, K. N. and C. C. Broder (2010). Viral Entry into Host Cells, Landes Biosciences. Announced publication date at submission of this work: December 1, 2010.

Bowman, E. J., A. Siebers, et al. (1988). "Bafilomycins: a class of inhibitors of membrane ATPases from microorganisms, animal cells, and plant cells." Proc Natl Acad Sci U S A **85**(21): 7972-6.

Bremer, C. M., C. Bung, et al. (2009). "Hepatitis B virus infection is dependent on cholesterol in the viral envelope." Cell Microbiol **11**(2): 249-60.

Bremer, C. M., I. Sominskaya, et al. (2010).“ N-terminal myristoylation-dependent masking of neutralizing epitopes in the preS1 attachment site of hepatitis B virus.” J Hepatol. In press

Briz, V., E. Poveda, et al. (2006). "HIV entry inhibitors: mechanisms of action and resistance pathways." J Antimicrob Chemother **57**(4): 619-27.

Bruss, V., X. Lu, et al. (1994). "Post-translational alterations in transmembrane topology of the hepatitis B virus large envelope protein." Embo J **13**(10): 2273-9.

Burckhardt, C. J. and U. F. Greber (2008). "Redox rescues virus from ER trap." Nat Cell Biol **10**(1): 9-11.

Burckhardt, C. J. and U. F. Greber (2009). "Virus movements on the plasma membrane support infection and transmission between cells." PLoS Pathog **5**(11): e1000621.

Cao, H., F. Garcia, et al. (1998). "Differential distribution of dynamin isoforms in mammalian cells." Mol Biol Cell **9**(9): 2595-609.

Carrillo, E. C., C. Giachetti, et al. (1984). "Effect of lysosomotropic agents on the foot-and-mouth disease virus replication." Virology **135**(2): 542-5.

Carman, W.F. et al. (1990). "Vaccine-induced escape mutant of hepatitis B virus." Lancet **336**(8711): 325-9.

Cassell, S., J. Edwards, et al. (1984). "Effects of lysosomotropic weak bases on infection of BHK-21 cells by Sindbis virus." J Virol **52**(3): 857-64.

Chisari, F. V. (1997). "Cytotoxic T cells and viral hepatitis." J Clin Invest **99**(7): 1472-7.

Chisari, F. V. and C. Ferrari (1995). "Hepatitis B virus immunopathogenesis." Annu Rev Immunol **13**: 29-60.

Chojnacki, J., D. A. Anderson, et al. (2005). "A hydrophobic domain in the large envelope protein is essential for fusion of duck hepatitis B virus at the late endosome." J Virol **79**(23): 14945-55.

Clement, C., V. Tiwari, et al. (2006). "A novel role for phagocytosis-like uptake in herpes simplex virus entry." J Cell Biol **174**(7): 1009-21.

Conner, S. D. and S. L. Schmid (2003). "Regulated portals of entry into the cell." Nature **422**(6927): 37-44.

Cooper, A. and Y. Shaul (2006). "Clathrin-mediated endocytosis and lysosomal cleavage of hepatitis B virus capsid-like core particles." J Biol Chem.

Cossart, P. and E. Veiga (2008). "Non-classical use of clathrin during bacterial infections." J Microsc **231**(3): 524-8.

Crowther, R. A., N. A. Kiselev, et al. (1994). "Three-dimensional structure of hepatitis B virus core particles determined by electron cryomicroscopy." Cell **77**(6): 943-50.

Cureton, D. K., R. H. Massol, et al. (2009). "Vesicular stomatitis virus enters cells through vesicles incompletely coated with clathrin that depend upon actin for internalization." PLoS Pathog **5**(4): e1000394.

Dacks, J. B. and M. C. Field (2007). "Evolution of the eukaryotic membrane-trafficking system: origin, tempo and mode." J Cell Sci **120**(Pt 17): 2977-85.

Damke, H., T. Baba, et al. (1995). "Clathrin-independent pinocytosis is induced in cells overexpressing a temperature-sensitive mutant of dynamin." J Cell Biol **131**(1): 69-80.

Damm, E. M., L. Pelkmans, et al. (2005). "Clathrin- and caveolin-1-independent endocytosis: entry of simian virus 40 into cells devoid of caveolae." J Cell Biol **168**(3): 477-88.

Dane, D. S., C. H. Cameron, et al. (1970). "Virus-like particles in serum of patients with Australia-antigen-associated hepatitis." Lancet **1**(649): 695-8.

Daukas, G. and S. H. Zigmond (1985). "Inhibition of receptor-mediated but not fluid-phase endocytosis in polymorphonuclear leukocytes." J Cell Biol **101**(5 Pt 1): 1673-9.

De Falco, S., M. G. Ruvoletto, et al. (2001). "Cloning and expression of a novel hepatitis B virus-binding protein from HepG2 cells." J Biol Chem **276**(39): 36613-23.

Doherty, G. J. and R. Lundmark (2009). "GRAF1-dependent endocytosis." Biochem Soc Trans **37**(Pt 5): 1061-5.

Doherty, G. J. and H. T. McMahon (2008). "Mediation, modulation, and consequences of membrane-cytoskeleton interactions." Annu Rev Biophys **37**: 65-95.

Doherty, G. J. and H. T. McMahon (2009). "Mechanisms of endocytosis." Annu Rev Biochem **78**: 857-902.

Doherty, G. J. and R. Lundmark (2009). "GRAF1-dependent endocytosis." Biochem Soc Trans **37**(Pt 5): 1061-5.

Dohner, K. and B. Sodeik (2005). "The role of the cytoskeleton during viral infection." Curr Top Microbiol Immunol **285**: 67-108.

Donald, H. B. and A. Isaacs (1954). "Counts of influenza virus particles." J Gen Microbiol **10**(3): 457-64.

Dryden, K. A., S. F. Wieland, et al. (2006). "Native hepatitis B virions and capsids visualized by electron cryomicroscopy." Mol Cell **22**(6): 843-50.

Engelke, M., K. Mills, et al. (2006). "Characterization of a hepatitis B and hepatitis delta virus receptor binding site." Hepatology **43**(4): 750-60.

Faisca, P. and D. Desmecht (2007). "Sendai virus, the mouse parainfluenza type 1: a longstanding pathogen that remains up-to-date." Res Vet Sci **82**(1): 115-25.

Fielding, C. J. and P. E. Fielding (2000). "Cholesterol and caveolae: structural and functional relationships." Biochim Biophys Acta **1529**(1-3): 210-22.

Fujimoto, L. M., R. Roth, et al. (2000). "Actin assembly plays a variable, but not obligatory role in receptor-mediated endocytosis in mammalian cells." Traffic **1**(2): 161-71.

Funk, A., M. Mhamdi, et al. (2004). "Itinerary of hepatitis B viruses: delineation of restriction points critical for infectious entry." J Virol **78**(15): 8289-300.

Funk, A., M. Mhamdi, et al. (2006). "pH-independent entry and sequential endosomal sorting are major determinants of hepadnaviral infection in primary hepatocytes." Hepatology **44**(3): 685-93.

Funk, A., M. Mhamdi, et al. (2008). "Duck hepatitis B virus requires cholesterol for endosomal escape during virus entry." J Virol **82**(21): 10532-42.

Ganem, D. and A. M. Prince (2004). "Hepatitis B virus infection--natural history and clinical consequences." N Engl J Med **350**(11): 1118-29.

Ganem, D. and H. E. Varmus (1987). "The molecular biology of the hepatitis B viruses." Annu Rev Biochem **56**: 651-93.

Gerlich, W. H. and W. S. Robinson (1980). "Hepatitis B virus contains protein attached to the 5' terminus of its complete DNA strand." Cell **21**(3): 801-9.

Gerlich, W. H. u. S. Schaefer (2002). Hepadnaviren: Hepatitis B Virus., Thieme.

Gey, G. O., Coffman, W. D., and M.T. Kubicek (1952). "Tissue culture studies of the proliferative capacity of cervical carcinoma and normal epithelium." Cancer Res. 12: 264-265.

Ghigo, E. (2010). "A dilemma for viruses and giant viruses: which endocytic pathway to use to enter cells?" Intervirology **53**(5): 274-83.

Ghigo, E., J. Kartenbeck, et al. (2008). "Ameobal pathogen mimivirus infects macrophages through phagocytosis." PLoS Pathog **4**(6): e1000087.

Glebe, D. (2006). "Attachment sites and neutralising epitopes of hepatitis B virus." Minerva Gastroenterol Dietol **52**(1): 3-21.

Glebe, D., M. Aliakbari, et al. (2003). "Pre-S1 antigen-dependent infection of Tupaia hepatocyte cultures with human hepatitis B virus." J Virol **77**(17): 9511-21.

Glebe, D. and S. Urban (2007). "Viral and cellular determinants involved in hepadnaviral entry." World J Gastroenterol **13**(1): 22-38.

Glebe, D., S. Urban, et al. (2005). "Mapping of the hepatitis B virus attachment site by use of infection-inhibiting preS1 lipopeptides and tupaia hepatocytes." Gastroenterology **129**(1): 234-45.

Glomb-Reinmund, S. and M. Kielian (1998). "The role of low pH and disulfide shuffling in the entry and fusion of Semliki Forest virus and Sindbis virus." Virology **248**(2): 372-81.

Graessmann, M. and A. Graessmann (1983). "Microinjection of tissue culture cells." Methods Enzymol **101**: 482-92.

Graumann, P. L. (2007). "Cytoskeletal elements in bacteria." Annu Rev Microbiol **61**: 589-618.

Greber, U. F. and M. Way (2006). "A superhighway to virus infection." Cell **124**(4): 741-54.

Gresch, O., F. B. Engel, et al. (2004). "New non-viral method for gene transfer into primary cells." Methods **33**(2): 151-63.

Grethe, S., J. O. Heckel, et al. (2000). "Molecular epidemiology of hepatitis B virus variants in nonhuman primates." J Virol **74**(11): 5377-81.

Gripon, P., I. Cannie, et al. (2005). "Efficient inhibition of hepatitis B virus infection by acylated peptides derived from the large viral surface protein." J Virol **79**(3): 1613-22.

Gripon, P., S. Rumin, et al. (2002). "Infection of a human hepatoma cell line by hepatitis B virus." Proc Natl Acad Sci U S A **99**(24): 15655-60.

Grün-Bernhard, S. (2008). Inaugural-Dissertation, Fachbereich 08-Biologie und Chemie, Justus-Liebig-Universität, Giessen. "Molekulare Determinanten der Infektiosität von Hepatitis B Virus Partikeln".

Haigler, H. T., J. A. McKanna, et al. (1979). "Rapid stimulation of pinocytosis in human carcinoma cells A-431 by epidermal growth factor." J Cell Biol **83**(1): 82-90.

Hamm, A., N. Krott, et al. (2002). "Efficient transfection method for primary cells." Tissue Eng **8**(2): 235-45.

Hansen, C. G. and B. J. Nichols (2009). "Molecular mechanisms of clathrin-independent endocytosis." J Cell Sci **122**(Pt 11): 1713-21.

Heermann, K. H., U. Goldmann, et al. (1984). "Large surface proteins of hepatitis B virus containing the pre-s sequence." J Virol **52**(2): 396-402.

Helenius, A., J. Kartenbeck, et al. (1980). "On the entry of Semliki forest virus into BHK-21 cells." J Cell Biol **84**(2): 404-20.

Heuser, J. E. and R. G. Anderson (1989). "Hypertonic media inhibit receptor-mediated endocytosis by blocking clathrin-coated pit formation." J Cell Biol **108**(2): 389-400.

Hewlett, L. J., A. R. Prescott, et al. (1994). "The coated pit and macropinocytic pathways serve distinct endosome populations." J Cell Biol **124**(5): 689-703.

Hinshaw, J. E. (2000). "Dynamin and its role in membrane fission." Annu Rev Cell Dev Biol **16**: 483-519.

Hruska, J. F., D. A. Clayton, et al. (1977). "Structure of hepatitis B Dane particle DNA before and after the Dane particle DNA polymerase reaction." J Virol **21**(2): 666-72.

Hu, J. and C. Seeger (1996). "Hsp90 is required for the activity of a hepatitis B virus reverse transcriptase." Proc Natl Acad Sci U S A **93**(3): 1060-4.

Huang, J. and T. J. Liang (1993). "A novel hepatitis B virus (HBV) genetic element with Rev response element-like properties that is essential for expression of HBV gene products." Mol Cell Biol **13**(12): 7476-86.

Huang, Z. M. and T. S. Yen (1995). "Role of the hepatitis B virus posttranscriptional regulatory element in export of intronless transcripts." Mol Cell Biol **15**(7): 3864-9.

Huss, M. and H. Wieczorek (2009). "Inhibitors of V-ATPases: old and new players." J Exp Biol **212**(Pt 3): 341-6.

Ikonen, E., S. Heino, et al. (2004). "Caveolins and membrane cholesterol." Biochem Soc Trans **32**(Pt 1): 121-3.

Inoue, Y., N. Tanaka, et al. (2007). "Clathrin-dependent entry of severe acute respiratory syndrome coronavirus into target cells expressing ACE2 with the cytoplasmic tail deleted." J Virol **81**(16): 8722-9.

Ito, Y., F. Yamamoto, et al. (1983). "Detection of cellular receptors for Sendai virus in mouse tissue sections." Arch Virol **75**(1-2): 103-13.

Ivanov, A. I. (2008). "Pharmacological inhibition of endocytic pathways: is it specific enough to be useful?" Methods Mol Biol **440**: 15-33.

Jaoude, G. A. and C. Sureau (2005). "Role of the antigenic loop of the hepatitis B virus envelope proteins in infectivity of hepatitis delta virus." J Virol **79**(16): 10460-6.

Jefferies, K. C., D. J. Cipriano, et al. (2008). "Function, structure and regulation of the vacuolar (H+)-ATPases." Arch Biochem Biophys **476**(1): 33-42.

Jensen, F. C., A. J. Girardi, et al. (1964). "Infection of Human and Simian Tissue Cultures with Rous Sarcoma Virus." Proc Natl Acad Sci U S A 52: 53-9.

Johannes, L. and V. Popoff (2008). "Tracing the retrograde route in protein trafficking." Cell **135**(7): 1175-87.

Junker Niepmann, M., R. Bartenschlager, et al. (1990). "A short cis-acting sequence is required for hepatitis B virus pregenome encapsidation and sufficient for packaging of foreign RNA." Embo J **9**(10): 3389-96.

Jursch, C. A., W. H. Gerlich, et al. (2002). "Molecular approaches to validate disinfectants against human hepatitis B virus." Med Microbiol Immunol (Berl) **190**(4): 189-97.

Kahn, R. A. (2009). "Toward a model for Arf GTPases as regulators of traffic at the Golgi." FEBS Lett **583**(23): 3872-9.

Kalia, M., S. Kumari, et al. (2006). "Arf6-independent GPI-anchored protein-enriched early endosomal compartments fuse with sorting endosomes via a Rab5/phosphatidylinositol-3'-kinase-dependent machinery." Mol Biol Cell **17**(8): 3689-704.

Kälin, S., B. Amstutz, et al. (2010). "Macropinocytotic uptake and infection of human epithelial cells with species B2 adenovirus type 35." J Virol **84**(10): 5336-50.

Kann, M. and W. H. Gerlich (2005). Hepatitis B virus and other hepadnaviridae. Structure and Molecular Virology. Edinburgh, London, Madrid, Melbourne, New York, Tokyo, Churchill Livingston.

Kann, M., B. Sodeik, et al. (1999). "Phosphorylation-dependent binding of hepatitis B virus core particles to the nuclear pore complex." J Cell Biol **145**(1): 45-55.

Kartenbeck, J., H. Stukenbrok, et al. (1989). "Endocytosis of simian virus 40 into the endoplasmic reticulum." J Cell Biol **109**(6 Pt 1): 2721-9.

Kenney, J. M., C. H. von Bonsdorff, et al. (1995). "Evolutionary conservation in the hepatitis B virus core structure: comparison of human and duck cores." Structure **3**(10): 1009-19.

Kielian, M. and F. A. Rey (2006). "Virus membrane-fusion proteins: more than one way to make a hairpin." Nat Rev Microbiol **4**(1): 67-76.

Kilby, J. M. and J. J. Eron (2003). "Novel therapies based on mechanisms of HIV-1 cell entry." N Engl J Med **348**(22): 2228-38.

Kinchen, J. M. and K. S. Ravichandran (2008). "Phagosome maturation: going through the acid test." Nat Rev Mol Cell Biol **9**(10): 781-95.

Kirchhausen, T. (1999). "Adaptors for clathrin-mediated traffic." Annu Rev Cell Dev Biol **15**: 705-32.

Kirkham, M., A. Fujita, et al. (2005). "Ultrastructural identification of uncoated caveolin-independent early endocytic vehicles." J Cell Biol **168**(3): 465-76.

Klausner, R. D., J. G. Donaldson, et al. (1992). "Brefeldin A: insights into the control of membrane traffic and organelle structure." J Cell Biol **116**(5): 1071-80.

Köck, J., E. M. Borst, et al. (1996). "Uptake of duck hepatitis B virus into hepatocytes occurs by endocytosis but does not require passage of the virus through an acidic intracellular compartment." J Virol **70**(9): 5827-31.

Köck, J. and H. J. Schlicht (1993). "Analysis of the earliest steps of hepadnavirus replication: genome repair after infectious entry into hepatocytes does not depend on viral polymerase activity." J Virol **67**(8): 4867-74.

Koivusalo, M., C. Welch, et al. (2010). "Amiloride inhibits macropinocytosis by lowering submembranous pH and preventing Rac1 and Cdc42 signaling." J Cell Biol **188**(4): 547-63.

König, A. (2010). Diplomarbeit, Fachbereich 08-Biologie und Chemie, Justus-Liebig-Universität, Giessen. "Infektionssysteme und Methoden zur Untersuchung der frühen Infektionsschritte des Hepatitis B Virus".

Kost, T. A., J. P. Condreay, et al. (2005). "Baculovirus as versatile vectors for protein expression in insect and mammalian cells." Nat Biotechnol **23**(5): 567-75.

Kovacs, M., J. Toth, et al. (2004). "Mechanism of blebbistatin inhibition of myosin II." J Biol Chem **279**(34): 35557-63.

Kumari, S. and S. Mayor (2008). "ARF1 is directly involved in dynamin-independent endocytosis." Nat Cell Biol **10**(1): 30-41.

Kumari, S., Swetha, M.G. and S. Mayor (2010). "Endocytosis unplugged: multiple ways to enter the cell." Cell Res **20**(3): 256-75.

Lafourcade, C., K. Sobo, et al. (2008). "Regulation of the V-ATPase along the endocytic pathway occurs through reversible subunit association and membrane localization." PLoS One **3**(7): e2758.

Lambert, C., T. Doring, et al. (2007). "Hepatitis B virus maturation is sensitive to functional inhibition of ESCRT-III, Vps4, and gamma 2-adaptin." J Virol **81**(17): 9050-60.

Lambert, C. and R. Prange (2001). "Dual topology of the hepatitis B virus large envelope protein: determinants influencing post-translational pre-S translocation." J Biol Chem **276**(25): 22265-72.

Lanford, R. E., D. Chavez, et al. (1998). "Isolation of a hepadnavirus from the woolly monkey, a New World primate." Proc Natl Acad Sci U S A **95**(10): 5757-61.

Larkin, J. M., M. S. Brown, et al. (1983). "Depletion of intracellular potassium arrests coated pit formation and receptor-mediated endocytosis in fibroblasts." Cell **33**(1): 273-85.

Lavanchy, D. (2004). "Hepatitis B virus epidemiology, disease burden, treatment, and current and emerging prevention and control measures." J Viral Hepat **11**(2): 97-107.

Lavanchy, D. (2005). "Worldwide epidemiology of HBV infection, disease burden, and vaccine prevention." J Clin Virol **34 Suppl 1**: S1-3.

Le Seyec, J., P. Chouteau, et al. (1999). "Infection process of the hepatitis B virus depends on the presence of a defined sequence in the pre-S1 domain." J Virol **73**(3): 2052-7.

Lehmann, M. J., N. M. Sherer, et al. (2005). "Actin- and myosin-driven movement of viruses along filopodia precedes their entry into cells." J Cell Biol **170**(2): 317-25.

Leistner, C. M., S. Gruen-Bernhard, et al. (2008). "Role of glycosaminoglycans for binding and infection of hepatitis B virus." Cell Microbiol **10**(1): 122-33.

Lord, J. M. and L. M. Roberts (1998). "Toxin entry: retrograde transport through the secretory pathway." J Cell Biol **140**(4): 733-6.

Lucey, B. P., W. A. Nelson-Rees, et al. (2009). "Henrietta Lacks, HeLa cells, and cell culture contamination." Arch Pathol Lab Med 133(9): 1463-7.

Lundmark, R., G. J. Doherty, et al. (2008). "The GTPase-activating protein GRAF1 regulates the CLIC/GEEC endocytic pathway." Curr Biol **18**(22): 1802-8.

Macia, E., M. Ehrlich, et al. (2006). "Dynasore, a cell-permeable inhibitor of dynamin." Dev Cell **10**(6): 839-50.

Macovei, A., C. Radulescu, et al. (2010). "Hepatitis B virus requires intact caveolin-1 function for productive infection in HepaRG cells." J Virol **84**(1): 243-53.

Malecki, J., A. Wiedlocha, et al. (2002). "Vesicle transmembrane potential is required for translocation to the cytosol of externally added FGF-1." Embo J **21**(17): 4480-90.

Marion, P. L., L. S. Oshiro, et al. (1980). "A virus in Beechey ground squirrels that is related to hepatitis B virus of humans." Proc Natl Acad Sci U S A **77**(5): 2941-5.

Marsh, M. and A. Helenius (1989). "Virus entry into animal cells." Adv Virus Res **36**: 107-51.

Marsh, M. and A. Helenius (2006). "Virus entry: open sesame." Cell **124**(4): 729-40.

Marsh, M. and H. T. McMahon (1999). "The structural era of endocytosis." Science **285**(5425): 215-20.

Mason, W. S., G. Seal, et al. (1980). "Virus of Pekin ducks with structural and biological relatedness to human hepatitis B virus." J Virol **36**(3): 829-36.

Mayor, S. and R. E. Pagano (2007). "Pathways of clathrin-independent endocytosis." Nat Rev Mol Cell Biol **8**(8): 603-12.

Meier, O., K. Boucke, et al. (2002). "Adenovirus triggers macropinocytosis and endosomal leakage together with its clathrin-mediated uptake." J Cell Biol **158**(6): 1119-31.

Meier, O. and U. F. Greber (2004). "Adenovirus endocytosis." J Gene Med **6 Suppl 1**: S152-63.

Mercer, J. and A. Helenius (2008). "Vaccinia virus uses macropinocytosis and apoptotic mimicry to enter host cells." Science **320**(5875): 531-5.

Mercer, J. and A. Helenius (2009). "Virus entry by macropinocytosis." Nat Cell Biol **11**(5): 510-20.

Mercer, J., M. Schelhaas, et al. (2010). "Virus entry by endocytosis." Annu Rev Biochem **79**: 803-33.

Mettlen, M., T. Pucadyil, et al. (2009). "Dissecting dynamin's role in clathrin-mediated endocytosis." Biochem Soc Trans **37**(Pt 5): 1022-6.

Meusser, B., C. Hirsch, et al. (2005). "ERAD: the long road to destruction." Nat Cell Biol **7**(8): 766-72.

Murata, M., J. Peranen, et al. (1995). "VIP21/caveolin is a cholesterol-binding protein." Proc Natl Acad Sci U S A **92**(22): 10339-43.

Nakabayashi, H., K. Taketa, et al. (1982). "Growth of human hepatoma cells lines with differentiated functions in chemically defined medium." Cancer Res 42(9): 3858-63.

Neurath, A. R., S. B. Kent, et al. (1986). "Identification and chemical synthesis of a host cell receptor binding site on hepatitis B virus." Cell **46**(3): 429-36.

Neurath, A. R., B. Seto, et al. (1989). "Antibodies to synthetic peptides from the preS1 region of the hepatitis B virus (HBV) envelope (env) protein are virus-neutralizing and protective." Vaccine **7**(3): 234-6.

Newbold, J. E., H. Xin, et al. (1995). "The covalently closed duplex form of the hepadnavirus genome exists in situ as a heterogeneous population of viral minichromosomes." J Virol **69**(6): 3350-7.

Nichols, B. (2003). "Caveosomes and endocytosis of lipid rafts." J Cell Sci **116**(Pt 23): 4707-14.

Nichols, B. J. and J. Lippincott-Schwartz (2001). "Endocytosis without clathrin coats." Trends Cell Biol **11**(10): 406-12.

Nieland, T. J., M. Ehrlich, et al. (2005). "Endocytosis is not required for the selective lipid uptake mediated by murine SR-BI." Biochim Biophys Acta **1734**(1): 44-51.

Norder, H., A. M. Couroucé, et al. (2004). "Genetic diversity of hepatitis B virus strains derived worldwide: Genotypes, subgenotypes, and HBsAg subtypes." Intervirology **47**: 286-309.

Norder, H., J. W. Ebert, et al. (1996). "Complete sequencing of a gibbon hepatitis B virus genome reveals a unique genotype distantly related to the chimpanzee hepatitis B virus." Virology **218**(1): 214-23.

Norkin, L. C. (1999). "Simian virus 40 infection via MHC class I molecules and caveolae." Immunol Rev **168**: 13-22.

Offensperger, W. B., S. Offensperger, et al. (1991). "Inhibition of duck hepatitis B virus infection by lysosomotropic agents." Virology **183**(1): 415-8.

Oh, P., D.P. McIntosh et al. (1998)."Dynamin at the neck of caveolae mediates their budding to form transport vesicles by GTP-driven fission from the plasma membrane of endothelium." J Cell Biol. **141**(1): 101- 14.

Palade, G. E. (1953). "The fine structure of blood capillaries." J. Appl. Phys. **24**: 1424.

Pante, N. and M. Kann (2002). "Nuclear Pore Complex Is Able to Transport Macromolecules with Diameters of ~39 nm." Mol Biol Cell **13**(2): 425-34.

Parton, R. G. and A. A. Richards (2003). "Lipid rafts and caveolae as portals for endocytosis: new insights and common mechanisms." Traffic **4**(11): 724-38.

Payne, C. K., S. A. Jones, et al. (2007). "Internalization and trafficking of cell surface proteoglycans and proteoglycan-binding ligands." Traffic **8**(4): 389-401.

Pearse, B. M. (1976). "Clathrin: a unique protein associated with intracellular transfer of membrane by coated vesicles." Proc Natl Acad Sci U S A **73**(4): 1255-9.

Pelkmans, L., J. Kartenbeck, et al. (2001). "Caveolar endocytosis of simian virus 40 reveals a new two-step vesicular-transport pathway to the ER." Nat Cell Biol **3**(5): 473-83.

Pelkmans, L., D. Puntener, et al. (2002). "Local actin polymerization and dynamin recruitment in SV40-induced internalization of caveolae." Science. **296:** 535-9.

Pfeffer, S. R. (2009). "Multiple routes of protein transport from endosomes to the trans Golgi network." FEBS Lett **583**(23): 3811-6.

Polishchuk, R. S., M. Capestrano, et al. (2009). "Shaping tubular carriers for intracellular membrane transport." FEBS Lett **583**(23): 3847-56.

Pollard, T. D. and J. A. Cooper (2009). "Actin, a central player in cell shape and movement." Science **326**(5957): 1208-12.

Pontisso, P., M. G. Ruvoletto, et al. (1989). "Identification of an attachment site for human liver plasma membranes on hepatitis B virus particles." Virology **173**(2): 522-30.

Prassolov, A., H. Hohenberg, et al. (2003). "New hepatitis B virus of cranes that has an unexpected broad host range." J Virol **77**(3): 1964-76.

Qiao, M., T. B. Macnaughton, et al. (1994). "Adsorption and penetration of hepatitis B virus in a nonpermissive cell line." Virology **201**(2): 356-63.

Rabe, B., D. Glebe, et al. (2006). "Lipid-mediated introduction of hepatitis B virus capsids into nonsusceptible cells allows highly efficient replication and facilitates the study of early infection events." J Virol **80**(11): 5465-73.

Rabe, B., A. Vlachou, et al. (2003). "Nuclear import of hepatitis B virus capsids and release of the viral genome." Proc Natl Acad Sci U S A **100**(17): 9849-54.

Radziwill, G., W. Tucker, et al. (1990). "Mutational analysis of the hepatitis B virus P gene product: domain structure and RNase H activity." J Virol **64**(2): 613-20.

Rall, L. B., D. N. Standring, et al. (1983). "Transcription of hepatitis B virus by RNA polymerase II." Mol Cell Biol **3**(10): 1766-73.

Richards, A. A., E. Stang, et al. (2002). "Inhibitors of COP-mediated transport and cholera toxin action inhibit simian virus 40 infection." Mol Biol Cell **13**(5): 1750-64.

Rigg, R. J. and H. Schaller (1992). "Duck hepatitis B virus infection of hepatocytes is not dependent on low pH." J Virol **66**(5): 2829-36.

Robinson, W. S. (1977). "The genome of hepatitis B virus." Annu Rev Microbiol **31**: 357-77.

Rust, M. J., M. Lakadamyali, et al. (2004). "Assembly of endocytic machinery around individual influenza viruses during viral entry." Nat Struct Mol Biol **11**(6): 567-73.

Sabharanjak, S., P. Sharma, et al. (2002). "GPI-anchored proteins are delivered to recycling endosomes via a distinct cdc42-regulated, clathrin-independent pinocytic pathway." Dev Cell **2**(4): 411-23.

Sandvig, K., M. L. Torgersen, et al. (2008). "Clathrin-independent endocytosis: from nonexisting to an extreme degree of complexity." Histochem Cell Biol **129**(3): 267-76.

Sattler, F. and W. S. Robinson (1979). "Hepatitis B viral DNA molecules have cohesive ends." J Virol **32**(1): 226-33.

Schaller, H. and M. Fischer (1991). "Transcriptional control of hepadnavirus gene expression." Curr Top Microbiol Immunol **168**: 21-39.

Schelhaas, M. (2010). "Come in and take your coat off - how host cells provide endocytosis for virus entry." Cell Microbiol.

Schelhaas, M., H. Ewers, et al. (2008). "Human papillomavirus type 16 entry: retrograde cell surface transport along actin-rich protrusions." PLoS Pathog **4**(9): e1000148.

Schelhaas, M., J. Malmstrom, et al. (2007). "Simian Virus 40 depends on ER protein folding and quality control factors for entry into host cells." Cell **131**(3): 516-29.

Schmitt, S., D. Glebe, et al. (1999). "Analysis of the pre-S2 N- and O-linked glycans of the M surface protein from human hepatitis B virus." J Biol Chem **274**(17): 11945-57.

Schmitz, J., M. Ohme, et al. (2000). "The complete mitochondrial genome of Tupaia belangeri and the phylogenetic affiliation of scandentia to other eutherian orders." Mol Biol Evol **17**(9): 1334-43.

Schulze, A., P. Gripon, et al. (2007). "Hepatitis B virus infection initiates with a large surface protein-dependent binding to heparan sulfate proteoglycans." Hepatology **46**(6): 1759-68.

Seeger, C., D. Ganem, et al. (1986). "Biochemical and genetic evidence for the hepatitis B virus replication strategy." Science **232**(4749): 477-84.

Seglen, P. O. (1976). "Preparation of isolated rat liver cells." Methods Cell Biol **13**: 29-83.

Seifer, M., S. Zhou, et al. (1993). "A micromolar pool of antigenically distinct precursors is required to initiate cooperative assembly of hepatitis B virus capsids in Xenopus oocytes." J Virol **67**(1): 249-57.

Seitz, S., S. Urban, et al. (2007). "Cryo-electron microscopy of hepatitis B virions reveals variability in envelope capsid interactions." Embo J **26**(18): 4160-7.

Shih, C. H., L. S. Li, et al. (1989). "In vitro propagation of human hepatitis B virus in a rat hepatoma cell line." Proc Natl Acad Sci U S A **86**(16): 6323-7.

Shouval, D. (2003). "Hepatitis B vaccines." J Hepatol **39 Suppl 1**: S70-6.

Sieczkarski, S. B. and G. R. Whittaker (2002). "Dissecting virus entry via endocytosis." J Gen Virology **83**(7): 1535-45.

Simons, K. and D. Toomre (2000). "Lipid rafts and signal transduction." Nat Rev Mol Cell Biol **1**(1): 31-9.

Smith, A. E. and A. Helenius (2004). "How viruses enter animal cells." Science **304**(5668): 237-42.

Smythe, E. and K. R. Ayscough (2006). "Actin regulation in endocytosis." J Cell Sci **119**(Pt 22): 4589-98.

Snijder, B., R. Sacher, et al. (2009). "Population context determines cell-to-cell variability in endocytosis and virus infection." Nature **461**(7263): 520-3.

Spoden, G., K. Freitag, et al. (2008). "Clathrin- and caveolin-independent entry of human papillomavirus type 16--involvement of tetraspanin-enriched microdomains (TEMs)." PLoS One **3**(10): e3313.

Sprengel, R., E. F. Kaleta, et al. (1988). "Isolation and characterization of a hepatitis B virus endemic in herons." J Virol **62**(10): 3832-9.

Stang, E., J. Kartenbeck, et al. (1997). "Major histocompatibility complex class I molecules mediate association of SV40 with caveolae." Mol Biol Cell **8**(1): 47-57.

Straight, A. F., A. Cheung, et al. (2003). "Dissecting temporal and spatial control of cytokinesis with a myosin II Inhibitor." Science **299**(5613): 1743-7.

Su, J. J. (1987). "[Experimental infection of human hepatitis B virus (HBV) in adult tree shrews]." Zhonghua Bing Li Xue Za Zhi **16**(2): 103-6, 22.

Summers, J., O. C. A, et al. (1975). "Genome of hepatitis B virus: restriction enzyme cleavage and structure of DNA extracted from Dane particles." Proc Natl Acad Sci U S A **72**(11): 4597-601.

Summers, J. and W. S. Mason (1982). "Replication of the genome of a hepatitis B--like virus by reverse transcription of an RNA intermediate." Cell **29**(2): 403-15.

Summers, J., J. M. Smolec, et al. (1978). "A virus similar to human hepatitis B virus associated with hepatitis and hepatoma in woodchucks." Proc Natl Acad Sci U S A **75**(9): 4533-7.

Sun, X., V. K. Yau, et al. (2005). "Role of clathrin-mediated endocytosis during vesicular stomatitis virus entry into host cells." Virology **338**(1): 53-60.

Sun-Wada, G. H. and Y. Wada (2010). "Vacuolar-type proton pump ATPases: roles of subunit isoforms in physiology and pathology." Histol Histopathol **25**(12): 1611-20.

Tang, H., K. E. Banks, et al. (2001). "Hepatitis B virus transcription and replication." Drug News Perspect **14**(6): 325-34.

Testut, P., C. A. Renard, et al. (1996). "A new hepadnavirus endemic in arctic ground squirrels in Alaska." J Virol **70**(7): 4210-9.

Thomsen, P., K. Roepstorff, et al. (2002). "Caveolae are highly immobile plasma membrane microdomains, which are not involved in constitutive endocytic trafficking." Mol Biol Cell **13**(1): 238-50.

Tillmann, H. L. (2007). "Antiviral therapy and resistance with hepatitis B virus infection." World J Gastroenterol **13**(1): 125-40.

Treiman, M., C. Caspersen, et al. (1998). "A tool coming of age: thapsigargin as an inhibitor of sarco-endoplasmic reticulum Ca(2+)-ATPases." Trends Pharmacol Sci **19**(4): 131-5.

Tuschl, T. (2001). "RNA interference and small interfering RNAs." Chembiochem **2**(4): 239-45.

Tuttleman, J. S., C. Pourcel, et al. (1986). "Formation of the pool of covalently closed circular viral DNA in hepadnavirus-infected cells." Cell **47**(3): 451-60.

Vainio, S., S. Heino, et al. (2002). "Dynamic association of human insulin receptor with lipid rafts in cells lacking caveolae." EMBO Rep **3**(1): 95-100.

Vasquez, R. J., B. Howell, et al. (1997). "Nanomolar concentrations of nocodazole alter microtubule dynamic instability in vivo and in vitro." Mol Biol Cell **8**(6): 973-85.

Vaudin, M., A. J. Wolstenholme, et al. (1988). "The complete nucleotide sequence of the genome of a hepatitis B virus isolated from a naturally infected chimpanzee." J Gen Virol **69 (Pt 6)**: 1383-9.

Wang, L. H., K. G. Rothberg, et al. (1993). "Mis-assembly of clathrin lattices on endosomes reveals a regulatory switch for coated pit formation." J Cell Biol **123**(5): 1107-17.

Warren, K. S., J. L. Heeney, et al. (1999). "A new group of hepadnaviruses naturally infecting orangutans (Pongo pygmaeus)." J Virol **73**(9): 7860-5.

Weber, M., V. Bronsema, et al. (1994). "Hepadnavirus P protein utilizes a tyrosine residue in the TP domain to prime reverse transcription." J Virol **68**(5): 2994-9.

Will, H., W. Reiser, et al. (1987). "Replication strategy of human hepatitis B virus." J Virol **61**(3): 904-11.

Woudenberg, J., K. P. Rembacz, et al. (2010). "Caveolin-1 is enriched in the peroxisomal membrane of rat hepatocytes." Hepatology **51**(5): 1744-53.

Wu, T. T., L. Coates, et al. (1990). "In hepatocytes infected with duck hepatitis B virus, the template for viral RNA synthesis is amplified by an intracellular pathway." Virology **175**(1): 255-61.

Yan, R. Q., J. J. Su, et al. (1996). "Human hepatitis B virus and hepatocellular carcinoma. I. Experimental infection of tree shrews with hepatitis B virus." J Cancer Res Clin Oncol **122**(5): 283-8.

7. Publications

C. M. Bremer, C. Bung, **N. Kott**, M. Hardt and Dieter Glebe (2009). "Hepatitis B virus infection is dependent on cholesterol in the viral envelope."Cellular Microbiololgy 11(2), 249-60.

Oral Presentations:

1st GGL Annual Conference
Gießen, September 30-October 1, 2008
"Hepatitis B Virus: Analysis of binding and uptake using confocal laser scanning microscopy"
Nicole Kott, Dieter Glebe and Wolfram H. Gerlich

International Meeting on "The Molecular Biology of Hepatitis B Viruses"
Tours, France, August 30- September 2, 2009
"Hepatitis B Virus infection of primary hepatocytes via a clathrin/-caveolin and dynamin-independent endocytic pathway"
Nicole Kott, Alexander König and Dieter Glebe

Fourth European Congress of Virology
Cernobbio, Italy, April 7-11, 2010
"Hepatitis B Virus infects primary hepatocytes via a clathrin/-caveolin and dynamin-independent endocytic pathway"
Nicole Kott, Alexander König and Dieter Glebe

International Meeting on "The Molecular Biology of Hepatitis B Viruses"
Taipei, Taiwan, October 9-13, 2010
"Requirement of a functional cytoskeleton for early steps of hepatitis B virus infection in primary hepatocytes"
Nicole Kott, Alexander König and Dieter Glebe

Poster Presentations:

2nd GGL Annual Conference
Gießen, September 30-October 1, 2009
"Hepatitis B Virus infects primary hepatocytes via a novel clathrin/-caveolin and dynamin-independent endocytic pathway"
Nicole Kott and Dieter Glebe

8. Acknowledgements

An dieser Stelle möchte ich allen danken, die zum Gelingen meiner Arbeit beigetragen haben:

Ganz besonderer Dank gilt **Prof. Dr. Dr. h.c. W. H. Gerlich** für sein enormes Engagement und vor allem für sein Vertrauen. Ausführliche Diskussionen brachten mir nicht nur mehr Wissen ein, sondern oftmals auch neue Blickwinkel und Denkansätze.

Prof. Dr. M. Martin danke ich herzlich für die Begutachtung meiner Dissertation sowie für die Vertretung vor dem Fachbereich 08- Biologie und Chemie.

Prof. Dr. A. Bindereif danke ich sehr für seine Bereitschaft als Prüfer meiner Disputation beizusitzen.

Mein großer Dank gilt **HDoz. Dr. Dieter Glebe** für die engagierte Betreuung sowie seine ständige Diskussionsbereitschaft. Seine Ideen und Hilfestellungen haben mich bei meiner Arbeit sehr unterstützt.

Vielen Dank an alle (auch ehemaligen) Mitarbeiter des Instituts für Medizinische Virologie besonders: **Alex K.**, **Alex S.**, **Andi**, **Christina, Corinna**, **Heidi**, **Mona**, **Siggi**, **Steffi** und **Ulli**! Danke für Eure vielfältige Hilfe (angefangen von der exzellenten technischen Unterstützung, den vielen Diskusionen und Eurem Beistand bei Vorträgen) und das tolle Arbeitsklima, was mich bei meiner Arbeit extrem unterstüzt hat und mich auch nach gescheiterten Versuchen und langen Stunden im Labor immer wieder motivierte!

Magy danke ich herzlich für die Aufmunterungen und das Mitfiebern in der letzten Phase meiner Arbeit.

Mein besonderer Dank gilt **Lucas** für seinen Rückhalt und die Motivation, die mich aufbaute wenn es mal wieder nicht so lief wie ich gern wollte.

Auch möchte ich **meinen Eltern** von ganzem Herzen danken: Ihr habt mich immer unterstützt und an mich geglaubt!

9. Declaration

Eidesstattliche Erklärung:

Hiermit versichere ich an Eides statt, die vorliegende Arbeit selbständig ausgeführt und keine anderen als die angegebenen Hilfsmittel verwendet zu haben.

_____

Nicole Kott